DOWNSTREAM EFFECTS ON DENITRIFICATION AND NITROUS OXIDE FROM AN ADVANCED WASTEWATER TREATMENT PLANT UPGRADE

A Thesis Submitted to the College of
Graduate and Postdoctoral Studies
In Partial Fulfillment of the Requirements
For the Degree of Master of Environment and Sustainability
In the School of Environment and Sustainability
University of Saskatchewan
Saskatoon

By

Nicholas P. Dylla

PERMISSION TO USE STATEMENT

In presenting this thesis in partial fulfillment of the requirements for a postgraduate degree from the University of Saskatchewan, I agree that the libraries of the University may make it freely available for inspection. I further agree that permission for copying of this thesis in any manner, in whole or in part, for scholarly purposes may be granted by the professors supervising my thesis work or, in their absence, by the head of the School of Environment and Sustainability or the dean of the College of Graduate Studies and Research. Requests should be addressed to:

Director of the School of Environment and Sustainability
University of Saskatchewan
117 Science Place, Kirk Hall
Saskatoon, Saskatchewan S7N 5C8
Canada

OR:
Dean of the College of Graduate and Postdoctoral Studies
University of Saskatchewan
107 Administration Place
Saskatoon, Saskatchewan S7N 5A2
Canada

It is understood that any copying, publication, or use of this thesis or parts thereof for financial gain shall not be allowed without my written permission. It is also understood that due recognition shall be given to me and to the University of Saskatchewan in any scholarly use which may be made of any material in my thesis. I certify that the version submitted is the same as that approved by my advisory committee.

ABSTRACT

All humans excrete waste. In developed countries, this waste is often treated at a wastewater treatment plant (WWTP). Eventually, the nutrient-rich, treated wastewater—effluent—enters a water body to be diluted or naturally processed. However, in the case of the Regina (Canada) WWTP, this dilution does not immediately occur as the effluent is released into the small, effluent-dominated system of Wascana Creek. This study capitalized on a novel opportunity to determine the effects of WWTP upgrade on: in-stream water quality, nitrogen (N) cycling measured as denitrification rates, and nitrous oxide (N_2O) concentrations and emissions. Using a before-after-control-impact (BACI) design, nutrient, sediment, and gas samples were obtained before and after the upgrade at both upstream (control) and downstream (impact) sites on both Wascana Creek and the larger, downstream Qu'Appelle River. Although nitrate (NO_3^-) concentrations did not significantly change post-upgrade, I found that the upgrade significantly reduced concentrations of ammonium (NH_4^+) and toxic un-ionized ammonia (NH_3), which declined by ~35 times from pre-upgrade values, ultimately mitigating potential toxicity (Environment Canada 1999). The WWTP significantly impacted denitrification rates at downstream sites. Denitrification rates at sites downstream of the WWTP were >1200 times the rates at the upstream site. While impacts were lesser, denitrification rates at the larger Qu'Appelle River downstream site were still >20 times the rates at the upstream site. Denitrification rates were unaffected by the upgrade. Moreover, NO_3^- saturation, a negative indicator of ecosystem health, existed both before and after the upgrade at impacted sites. To the best of my knowledge, aquatic N_2O concentrations immediately downstream of the WWTP are the highest known values for a natural system. Concentrations reached as high as 114,000 percent saturation pre-upgrade and 110,000 percent saturation post-upgrade; no significant change was observed pre- vs. post-upgrade across all impacted sites. It was determined that not only did N_2O concentrations from the WWTP effluent span an impact zone of ~5 km in Wascana Creek, but also that the origin of these extremely high concentrations came directly from the effluent. Predictors of both denitrification rates and N_2O concentrations were identified. Nitrate was a predictor of denitrification, while NO_3^- and denitrification rates were significant predictors of N_2O concentrations outside the effluent impact zone. This study showed that enhanced effluent N removal can help mitigate risk of NH_3 toxicity; however, decreases in NH_3 and NH_4^+ concentrations did not significantly impact downstream N_2O emissions or denitrification rates.

FOR SUBMISSION

The following manuscripts prepared in this manuscript-based thesis will be readied for submission:

1. Dylla, N.P., Whitfield, C.J., Schlageter, B., and H.M. Baulch (2018). "The Effect of a Wastewater Treatment Plant Upgrade on In-stream Denitrification" Journal **Vol**(Issue): pg–pg.

   Publisher: TBD

2. Dylla, N.P., Baulch, H.M., and C.J. Whitfield (2018). "The Downstream Effect of a Wastewater Treatment Plant Upgrade on Nitrous Oxide" Journal **Vol**(Issue): pg–pg.

   Publisher: TBD

DEDICATION

This thesis is dedicated to my amazing and supportive family (Maria Dylla[Mom], Daniel P. Dylla[Dad], Daniel J. Dylla[Brother], Allison Dylla[Sister], Daniel Deufel[Brother-in-Law], Lauren Schaafsma[Sister-in-Law], Ryan Dylla[Cousin], and Jacqueline Dylla[Grandma]) who unselfishly encouraged their son, brother, and cousin to leave their home and daily life in order to obtain his degree and accomplish his goals. This is also dedicated to my wonderful partner, Claire Ellen Kohout, who was there for me, stride for stride, while achieving her own degree in the process. Lastly, this is dedicated to my friends from home who kept me motivated throughout this long journey (Evan Gallegos, Christian Fries, E.J. Luna, Tyler Gill, Joseph McGuire, Jorge Castellanos, and Zachary Schneider) as well as the friends I made here in Canada. With all these remarkable people in my life, I can confidently say that I am truly one fortunate man and that I could not have done this without all of their love and support.

ACKNOWLEDGEMENTS

First and foremost, I would like to acknowledge my supervisors, Dr. Helen Baulch and Dr. Colin Whitfield. Their knowledge and experience in this field helped push me through difficult stretches while also creating an environment that stimulated learning. Their "red ink" and criticisms forged better habits and provoked higher-level thinking. I will be forever thankful for their time and effort. I would also like to acknowledge the SaskWatChe group (Emily Cavaliere, Kimberly Gilmour, Katy Nugent, Beauregard Schlageter, Richard Helmle, Carlie Elliott, and Michelle Wauchope-Thompson) for helping with field expeditions, laboratory experiments and analyses, as well as being a great support system. Lastly, I would like to acknowledge my committee members, Dr. Jason Venkiteswaran and Dr. Rich Farrell, for their time, advice, and criticisms throughout this process.

TABLE OF CONTENTS

PERMISSION TO USE STATEMENT i
ABSTRACT ii
FOR SUBMISSION iii
DEDICATION iv
ACKNOWLEDGEMENTS v
TABLE OF CONTENTS vi
LIST OF TABLES ix
LIST OF FIGURES x
LIST OF ABBREVIATIONS xv
Chapter 1: INTRODUCTION 1
1.0 General Introduction 1
1.0.1 Nitrous Oxide Production 1
1.0.2 Microbial Processes of Nitrification and Denitrification 2
1.0.3 Nitrous Oxide from Aquatic Systems 5
1.1 Study Rationale & Background Information 6
1.1.1 Urban Wastewater and other Nutrient and N_2O Sources 6
1.2 Research Objectives 9
1.3 Thesis Structure 11
Chapter 2: THE EFFECT OF A WASTEWATER TREATMENT PLANT UPGRADE ON IN-STREAM DENITRIFICATION 12
2.0 Abstract 12
2.1 Introduction 13
2.2 Materials and Methods 15
2.2.1 Study Area 15
2.2.2 Wastewater Treatment Plant Upgrade Timeline 16
2.2.3 Study Sites 16
2.2.4 Sample Collection 17
2.2.5 Laboratory Analysis 19
2.2.5.1 Water and Sediment Chemistry 19
2.2.6 Denitrification Experiments 20
2.2.7 Statistical Analyses 21
2.2.7.1 Changes in Water Chemistry in Space and Time 21
2.2.7.2 Denitrification Activity 22

2.3 Results....23
2.3.1 Effects of the Wastewater Treatment Plant and Upgrade on Water Chemistry....23
2.3.2 Denitrification Activity—Variation in Space and Time....27
2.3.3 Denitrification Potential and Evidence of Nitrate Saturation....29
2.3.4 Predictors of Denitrification Rates....31
2.4 Discussion....32
2.4.1 Water Quality....32
2.4.2 Temporal and Spatial Changes in Denitrification Rates....34
2.4.2.1 Nitrate Saturation and Kinetics....35
2.4.3 Seasonality....36
2.5 Conclusion....37
2.6 Acknowledgements....37
2.7 Author Contributions....38
Chapter 3: THE DOWNSTREAM EFFECT OF A WASTEWATER TREATMENT PLANT UPGRADE ON NITROUS OXIDE....39
3.0 Preface....39
3.1 Abstract....39
3.2 Introduction....40
3.3 Materials and Methods....42
3.3.1 Study Area....42
3.3.2 Study Sites....44
3.3.3 Water Chemistry....45
3.3.4 Dissolved Gas Collection....46
3.3.5 Dissolved Nitrous Oxide Concentration....46
3.3.6 Gas Transfer Velocity....47
3.3.6.1 BASE model—Dissolved Oxygen for Estimation of Gas Transfer Velocity....47
3.3.6.2 Static Flux Chamber for Estimation of Gas Transfer Velocity....48
3.3.7 Nitrous Oxide Flux....49
3.3.8 Estimating the Downstream Nitrous Oxide Spatial Footprint....50
3.3.9 Diel Sampling....51
3.3.10 Data Analysis....52
3.4 Results....52
3.4.1 Spatial and Temporal Variability of Nitrous Oxide....52
3.4.2 Wastewater Treatment Plant Upgrade's Effect on Nitrous Oxide....55
3.4.2.1 Percent Saturation Pre-upgrade, Post-upgrade, and Comparison....55

3.4.2.2 Spatial Footprint of WWTP-derived Nitrous Oxide 57
3.4.2.3 Nitrous Oxide Flux 58
3.4.3 Diel Variation in Nitrous Oxide and Physico-chemistry 60
3.4.4 Correlations between Nitrous Oxide and Chemical Variables 61
3.5 Discussion 66
3.5.1 Direct Release of Wastewater Treatment Plant N_2O Dominates Emissions 66
3.5.2 Evidence of In-stream Production Downstream of WWTP 68
3.5.3 Controls on In-Stream Production of N_2O 68
3.5.4 WWTP N_2O Emissions 69
3.5.5 Diel Cycles in Nutrient Concentrations and Nitrous Oxide Percent Saturation 70
3.6 Conclusion 72
3.7 Acknowledgements 73
3.8 Author Contributions 73
Chapter 4: GENERAL CONCLUSION 74
4.0 Summary 74
4.1 Limitations and Future Research 77
REFERENCES 79
APPENDIX 103
Supplemental Information Chapter 2: The Effect of a Wastewater Treatment Plant Upgrade on In-Stream Denitrification 103
Supplemental Information Chapter 3: The Downstream Effect of a Wastewater Treatment Plant Upgrade on Nitrous Oxide 112

LIST OF TABLES

Table 2.1 Summary of water chemistry and sediment analyses 19

Table 2.2 Water chemistry and sediment parameters at all sample sites (May 2016–August 2016) prior to the Regina WWTP upgrade. Values shown are averages with standard deviation below in parentheses..... 25

Table 2.3 The difference between mean post-upgrade and pre-upgrade concentrations of NO_3^-, TAN, NH_3, urea, TDN, DOC, and DO (i.e. Post-upgrade–Pre-upgrade). Mean post-upgrade values are in parentheses. A negative value indicates that post-upgrade values were lower than pre-upgrade values. To account for seasonal variability pre-upgrade values were compared to post-upgrade values during the same summer period (i.e. Pre-upgrade: May 2016–August 2016 vs. Post-upgrade: May 2017–August 2017)..... 26

Table 2.4 Multiple correlations between denitrification rates (μg N g^{-1} h^{-1}) and chemical parameters. The numbers represent the Spearman rank correlation coefficient rho (ρ), which signifies the strength of the monotonic correlation..... 32

Table 3.1 Range in observed depth, stream velocity, N_2O concentration, N_2O flux, and sampled atmospheric concentrations of N_2O (N_2O_{atm}) for all study sites through time 53

Table 3.2 Mean excess N_2O–N values transported daily ± standard deviation along and calculated percent loss from downstream of the WWTP. Estimated % loss was estimated using the first-order Eq.(3.9) with the distance from the WWTP (Wascana Creek sites) and the confluence (Qu'Appelle River sites)—negative values mean the site is upstream of the WWTP/ confluence..... 57

Table 3.3 Average observed nitrous oxide percent saturation and flux values found in urban-impacted aquatic riverine systems (ranges are shown in parentheses)..... 67

LIST OF FIGURES

Figure 2.1 Study sites were located near Regina, SK, Canada. Sites were located upstream (triangles) or downstream sites (circles) of the Wastewater Treatment Plant effluent (WWTP: green X) on both Wascana Creek (orange labels) and Qu'Appelle River (blue labels). Wascana Creek flows northwest and Qu'Appelle River flows northeast.....18

Figure 2.2 Mean potential denitrification rates (μg N g^{-1} h^{-1}) for C_2H_2-treated (AT) and C_2H_2-treated and NO_3^--amended (ATNA) samples as well as NO_3^- concentrations (mg NO_3–N L^{-1}) throughout the study (gaps represent the period where sampling did not occur). Panels A and C correspond to both sites on Qu'Appelle River. Panel B and D correspond to the four sites on Wascana Creek. Displayed error bars for panels A and B are the standard error of the triplicate denitrification samples for each experiment (for samples with small standard error, the bars may be covered by the data points). 28

Figure 2.3 Potential denitrification rates (AT; μg N g^{-1} h^{-1}) across six sample sites for the period from May 2016-September 2017. Significant differences in rates are indicated with different letters (those with the same letter are not significantly different from each other; ANOVA $F(5,51) = 25.0$, $p < 0.0001$; TukeyHSD $p < 0.05$). The boxplot and whiskers encompass 95% of the data observed where the outliers are represented as dots, inside the box are the first and third quartiles with the median represented as the center line.....29

Figure 2.4 Denitrification rates (ATNA; μg N g^{-1} h^{-1}) across six sample sites for the period from May 2016-September 2017. Significant differences in rates are indicated with different letters (those with the same letter are not significantly different from each other; ANOVA $F(5,51) = 8.52$, $p < 0.0001$; TukeyHSD $p < 0.05$). The boxplot and whiskers encompass 95% of the data observed where the outliers are represented as dots, inside the box are the first and third quartiles with the median represented as the center line.....30

Figure 2.5 Dose-response curve of (NO_3^--denitrification) from Wascana Creek control site W1 (A) and impacted site W3 (B) showing the change in denitrification rate (μg N g^{-1} h^{-1}) as a function of NO_3^- concentrations (mg NO_3–N L^{-1}). The kinetic parameters V_{max} and K_m are in units of μg N g^{-1} h^{-1} and mg NO_3–N L^{-1}, respectively. 31

Figure 3.1 Left, a riverine network map of the study region with the study sites on Wascana Creek (circles) and Qu'Appelle River (triangles) both upstream (blue) and downstream (red) of the Regina WWTP (purple cross). Right, a land cover map for the surrounding study area. Data was obtained from (Government of Canada and Agriculture and Agri-Food Canada 2018; Government of Canada and Natural Resources Canada 2018).....43

Figure 3.2 Nitrous oxide saturation (%) for all sites throughout the two-year study. Upstream sites are indicated by blue, notched-boxplots while downstream sites are orange, notched-boxplots. The notches show a 95% confidence interval around the median with whiskers encompassing 99% of the data observed where the outliers are represented as dots. Inside the box are the first and third quartiles with the median represented as the center line. Significant differences are indicated with different letters (those with the same letter are not significantly different from each other; ANOVA

F(5,152) = 354, $p < 0.0001$ TukeyHSD $p < 0.05$)..... 54

Figure 3.3 Nitrous oxide % saturation pre-upgrade (Panel A: May–August 2016) and post-upgrade (Panel B: May–August 2017). Significant differences within each period are indicated with different letters for their respective panel. There were no significant differences between the two periods for any given site (e.g. W1 pre-upgrade vs W1 post-upgrade; ANOVA $F(5,93) = 143$, $p < 0.0001$; TukeyHSD $p > 0.05$). Note: the letters only apply within a given panel.....56

Figure 3.4 Nitrous oxide flux rates (μmol N_2O–N m^{-2} d^{-1}) for Qu'Appelle River (Panel A) and Wascana Creek (Panel B). Sites upstream of the WWTP are colored blue while downstream sites are colored orange. Note that the axes are different for each panel.... 59

Figure 3.5 Diel sampling campaign that occurred August 29th–August 31st 2016, for the upstream Wascana Creek site W1 (Top Row, blue points) and the downstream Wascana Creek site W3 (Bottom Row, red points). From left to right, panels consist of nitrous oxide percent saturation, nitrate, total ammonia nitrogen, and total dissolved nitrogen concentrations, dissolved oxygen percent saturation, temperature and pH. Gray bars signify nighttime periods (between sunset at 19:48 and sunrise at 06:10) with white spaces signifying daytime periods. Note that y-axes for each column are on different scales in order to better display the data (except for dissolved oxygen and temperature). The red line for nitrous oxide (% saturation) signifies 100% saturation of nitrous oxide.....62

Figure 3.6 Diel sampling campaign August 29th–August 31st 2016, for the upstream Wascana Creek site W1 (top, blue points) and the downstream Wascana Creek site W3 (bottom, red points). From left to right, panels consist of total dissolved nitrogen, dissolved inorganic nitrogen, dissolved organic nitrogen, and urea. Gray bars signify nighttime periods (between sunset at 19:48 and sunrise at 06:10) with white spaces signifying daytime periods (between sunrise at 06:10 and sunset at 19:48). Note that y-axes for each row are on different scales in order to better display the data although the y-scale within a site is consistent to allow visual assessment of the proportion of TDN pool in each fraction. The urea data for W3 are presented on a finer y-axis in Figure A3.12.... 63

Figure 3.7 Spearman rank correlations for the sites situated in the effluent-N_2O impact zone (W2 and W3), between nitrous oxide (% saturation) and nitrate concentration (mg NO_3–N L^{-1}; Panel A), total ammonia nitrogen concentration (mg TAN L^{-1}; Panel B), and denitrification activity (μg N g^{-1} h^{-1}; Panel C). Note that displayed *p*-values are not Bonferroni corrected ($\alpha_{corrected}$ = 0.0083).....64

Figure 3.8 Spearman rank correlations for the sites not situated in the effluent-N_2O impact zone (W1, W4, QA1, and QA2), between nitrous oxide (% saturation) and nitrate concentration (mg NO_3–N L^{-1}; Panel A), total ammonia nitrogen concentration (mg TAN L^{-1}; Panel B), and denitrification activity (μg N g^{-1} h^{-1}; Panel C). Note that displayed *p*-values are not Bonferroni corrected ($\alpha_{corrected}$ = 0.0083).....65

Appendix Figures

Figure A2.1 Example of the diel cycle of the Wascana Creek flow level during low-flow conditions in 2016. Data obtained from Environment Canada Hydrometric Gauging Station at Wascana Creek (Station ID Number: 05JF005).....103

Figure A2.2 Regina wastewater treatment plant final effluent concentrations of nitrate (green points) and total ammonia nitrogen (purple points). The gray vertical line on May 10th, 2016 signifies when this study began and the black vertical line signifies when the Regina WWTP was substantially upgraded. Data were provided by Kayla Gallant as a personal communication from the Regina WWTP.....104

Figure A2.3 Dissolved oxygen concentration (mg O_2 L^{-1}) during the summer of 2016 at Wascana Creek site W3. Periods of hypoxia (< 4 mg L^{-1}) are observed with a few anoxic occurrences.....104

Figure A2.4 Un-ionized ammonia (NH_3) concentrations (mg NH_3–N L^{-1}) pre-upgrade (panel A) and post-upgrade (panel B). Upstream sites are indicated by blue boxplots while downstream sites are orange boxplots. Significant differences of NH_3 concentrations with-in each site (i.e. W1 pre-upgrade vs W1 post-upgrade) are indicated with an asterisk (*; ANOVA $F(11,33) = 4.43$, $p < 0.001$; TukeyHSD $p < 0.05$). The boxplot and whiskers encompass 95% of the data observed where the outliers are represented as dots, inside the box are the first and third quartiles with the median represented as the center line..... 105

Figure A2.5 Observed pH values at Wascana Creek impact sites (W2 and W3) during pre-upgrade period (solid points) and post-upgrade period (hollow points). 106

Figure A2.6 Denitrification rates (AT; µg N g^{-1} h^{-1}) versus NO_3^- concentrations (NO_3-N mg L^{-1}; Panel A) and temperature (°C; Panel B) at Wascana Creek impact site W3 throughout the study. 107

Figure A2.7 Correlation plot for nitrate concentrations (NO_3-N mg L^{-1}) and denitrification rates (AT; µg N g^{-1} h^{-1}). The reported correlation value and significant level were determined from the Spearman rank correlation test. I acknowledge that although some sites approach saturation points (e.g. W3, W4, and QA2), the overall data maintain a monotnic relationship (i.e. the denitrification rates increase with NO_3^- concentrations even though the relationship begins to slow/plateau under higher NO_3^- concentrations).....108

Figure A2.8 Correlation plot for pH and denitrification rates (AT; µg N g^{-1} h^{-1}). The reported correlation value and significant level were determined from the Spearman rank correlation test. 108

Figure A2.9 Correlation plot for sediment organic carbon (%) and denitrification rates (AT; µg N g^{-1} h^{-1}). The reported correlation value and significant level were determined from the Spearman rank correlation test.....109

Figure A2.10 Correlation plot for lab water temperature (°C) and denitrification rates (AT; μg N g^{-1} h^{-1}). Lab water temperature was kept within ± 2 °C of sampled water temperature. The reported correlation value and significant level were determined from the Spearman rank correlation test 109

Figure A2.11 Correlation plot for dissolved organic carbon (mg L^{-1}) and denitrification rates (AT; μg N g^{-1} h^{-1}). The reported correlation value and significant level were determined from the Spearman rank correlation test. 110

Figure A2.12 Correlation plot for total dissolved nitrogen (mg L^{-1}) and denitrification rates (AT; μg N g^{-1} h^{-1}). The reported correlation value and significant level were determined from the Spearman rank correlation test.....110

Figure A2.13 pH as a function of distance (km) from the wastewater treatment plant for Wascana Creek (Panel A) and Qu'Appelle River (Panel B).....111

Figure A3.1 Date (blue circles) and discharge condition corresponding to dissolved oxygen measurements from HOBO sensors that were used to estimate *k* in Wascana Creek in 2016 (Panel A) and 2017 (Panel B). In total, 133 days were measured for DO across sites W1, W2, and W3.....113

Figure A3.2 Example of BASE model output. The three colors (blue, red, and green) represent each convergence of three-chains used in the model for parameters A, p, R, K, and θ. The x-axis for these variables refers to the number of MCMC iterations used to estimate the aforementioned variables. Dissolved oxygen is shown as the sixth panel with the fitted curve overlaying the data points. Temperature is shown as the seventh panel as well as PAR (smoothed as shown by the red line) as the eighth panel. Dissolved oxygen, temperature, and PAR are shown over the diel period. The x-axis for these parameters refers to the number of time-steps used in the model, since I used 10 min intervals, there were 144 per day (1440 mins d^{-1}).....114

Figure A3.3 Flying flux chamber design as designed from Lorke et al. 2015. Picture A shows the flying flux chamber in the lab after construction and Picture B shows the flying flux chamber in the field. Both pictures describe all parts needed in the construction of flying chamber.....115

Figure A3.4 Static flux chamber *k* values (red point) compared to HOBO dissolved oxygen derived, BASE modeled *k* values (blue point) over time at sites W1 and W3.....115

Figure A3.5 Range of static flux chamber-measured *k* values for each site.....116

Figure A3.6 BASE modeled k values compared to semi-empirical benthic models (h^{-1}, Top Row) and wind models (cm h^{-1}, Bottom Row). Displayed are individual linear regressions with their respective coefficients of determination (R^2) and *p*-value.....117

Figure A3.7 Variability of nitrous oxide percent saturations over time for all sites. Note, a base-10 log scale was used for the y-axis. Upstream sites are distinguished by blue points/lines and

downstream sites are distinguished orange points/lines.....118

Figure A3.8 Directly measured water temperature (˚C) across all study sites for 2016 (Row A) and 2017 (Row B). Upstream sites are distinguished by blue points/lines and downstream sites are distinguished orange points/lines.....119

Figure A3.9 Discharge (m^3 s^{-1}) at Qu'Appelle River gauging site QA1 during 2016 (Panel A) and 2017 (Panel B) as well as discharge at Wascana Creek gauging site W4 during 2016 (Panel C) and 2017 (Panel D). Blue circles denote the dates and flow conditions at which samples were taken.....120

Figure A3.10 Un-ionized ammonia (NH_3) concentrations over the diel sampling campaign that occurred August 29th–August 31st, 2016 at Wascana Creek sites W1 (Top Panel, blue points) and W3 (Bottom Panel, red points). The red horizontal line indicates the freshwater guideline limit of NH_3–N (0.019 mg L^{-1}) in water bodies.....121

Figure A3.11 Wascana flow during 2017 (Panel A) and the diel sampling campaign (August 30th–31st, 2017; Panel B).....122

Figure A3.12 TDN, DIN, DON, and urea concentrations over the diel sampling campaign that occurred August 29th–August 31st, 2016 for the upstream Wascana Creek site W1 (Top Row, blue points) and the downstream Wascana Creek site W3 (Bottom Row, red points). The y-axis range was reduced in order to display the diel cycle of urea at both W1 and W3.....123

Figure A3.13 Seasonal N_2O flux (μmol N_2O–N m^{-2} d^{-1}) across all study sites. Seasons are shown as vertical rectangles as spring (green), summer (yellow), fall (orange), and winter (blue). The y-axes are independent for each site in order to adequately show seasonal variation across sites. Triangles represent sites upstream of the WWTP/ confluence and circles represent sites downstream of the WWTP/ confluence. Black points indicate flux values > 0 μmol N_2O–N m^{-2} d^{-1} (N_2O source) and red points indicate flux values < 0 μmol N_2O–N m^{-2} d^{-1} (N_2O sink). Note that the points are made 65 % transparent to account for visual overlap.....124

LIST OF ABBREVIATIONS

ANOVA	analysis of variance
Ar	argon
AT	acetylene treated
atm	atmosphere, pressure
ATNA	acetylene treated and nitrate amended
BACI	before-after-control-impact
BASE	Bayesian Single-station Estimation, model
BMP	better management practice
BNR	biological nutrient removal
BOD	biochemical oxygen demand
°C	degrees Celsius
C_2H_2	acetylene
CH_4	methane
cm	centimeter
CO_2	carbon dioxide
Cs	concentration of gas dissolved in water when saturated (μmol m^{-3})
Cw	concentration of gas dissolved in water, (μmol m^{-3})
d	day
d^{-1}	per day
DIN	dissolved inorganic nitrogen
DO	dissolved oxygen
DOC	dissolved organic carbon
DON	dissolved organic nitrogen
ECD	electron capturing detector
F	flux/ emission rate of gas (μmol m^{-2} d^{-1})
FTIR	Fourier-transformed infrared spectroscopy
g	gram
GC	gas chromatograph
GHG	greenhouse gas

GLMM	Generalized linear mixed-effects model
GWP_{100}	Global Warming Potential over the next 100 years
h	hour
h^{-1}	per hour
HDPE	high density polyethylene
IPCC	Intergovernmental Panel on Climate Change
k	gas transfer velocity, (m d^{-1})
K	reaeration coefficient, (d^{-1})
k_{600}	standardized gas exchange value for CO_2 at 20°C
kg	kilogram
km	kilometer
Km	substrate concentration when reaction rate is ½ maximal activity
km^2	square kilometer
k_{N2O}	gas transfer velocity for nitrous oxide
KNO_3	potassium nitrate
k_{O2}	gas transfer velocity for oxygen
kPa	kilopascal, pressure
L	liter
L^{-1}	per liter
LMM	linear mixed-effects model
m s^{-1}	meters per second, velocity
m	meter
M	molar
µM	micromolar
m^2	square meter
m^3 s^{-1}	cubic meters per second, discharge
m^3	cubic meter
mg	milligram
min	minute
mL	milliliter
ML	million liters

mm	millimeter
mM	millimolar
mol	mole
N	nitrogen
N_2	dinitrogen gas
N_2O	nitrous oxide
NDIR	non-dispersive infrared detector
ng	nanogram
NH_2OH	hydroxylamine
NH_3	un-ionized ammonia
NH_3-N	ammonia as nitrogen (-N)
NH_4^+	ammonium
NH_4^+-N	ammonium as nitrogen (-N)
NO	nitrogen monoxide
NO_2^-	nitrite
NO_3^-	nitrate
NO_3^--N	nitrate as nitrogen (-N)
N_r	reactive nitrogen
O_2	oxygen
P	phosphorus
PAR	photosynthetically active radiation
ppbv	parts per billion by volume
ppmv	parts per million by volume
ppt	parts per thousand
QA1	Qu'Appelle River site ~5 kilometers upstream of confluence
QA2	Qu'Appelle River site ~12 kilometers downstream of confluence
ρ	rho, Spearman's rank correlation coefficient
rpm	revolutions per minute
S_c	Schmidt number coefficient
SOC	sediment organic carbon
t	water temperature

TDN	total dissolved nitrogen
Tg	teragram
TN	total nitrogen
UV	ultra-violet radiation
Vmax	maximum rate of reaction/ process
W1	Wascana Creek site ~4 kilometers upstream of wastewater treatment plant
W2	Wascana Creek site ~0.2 kilometers downstream of wastewater treatment plant
W3	Wascana Creek site ~3.8 kilometers downstream of wastewater treatment plant
W4	Wascana Creek site ~59.8 kilometers downstream of wastewater treatment plant
WWTP	wastewater treatment plant
yr	year
yr^{-1}	per year
YSI	Yellow Springs Instrument

Chapter 1: INTRODUCTION

1.0 General Introduction

Before the industrial era, reactive nitrogen (N_r) was largely produced directly by lightning or through biological nitrogen (N) fixation i.e. the conversion of unreactive nitrogen (N_2) to a reactive, biologically available form—N_r by microorganisms (Galloway et al. 2003). In modern times, humans have doubled the amount of available N_r through the combustion of fossil fuels, the Haber-Bosch process and biomass burning (Seitzinger and Kroeze 1998; Fowler et al. 2013). This N_r can then be processed further by microorganisms, leading to increased N_2O emissions which is a potent greenhouse gas (GHG) (Knowles 1982; Galloway et al. 1995; Reay et al. 2012; Fowler et al. 2013). Denitrification is a microbially mediated N process that can reduce nitrate (NO_3^-) concentrations, serving as an ecosystem service; however it can produce N_2O in an intermediary step in the pathway (Wrage et al. 2001). With an increasing urban population and as water pollution and water scarcity become more prevalent, water quality and the biological processes that impact it should be assessed (United Nations Environment Program 2010). Eutrophic conditions, or the state of being nutrient rich, can occur in highly impacted aquatic systems that receive nutrient inputs from anthropogenic sources. Eutrophic conditions can be lethal to aquatic life as nutrients such as NO_3^-, total ammonia nitrogen (TAN; $NH_4^+ + NH_3$), urea, and phosphorus (P) can create favorable conditions for the growth of algae, which then ultimately create anoxic waters as seen in the infamous "Dead Zone" in the Gulf of Mexico or in the freshwater Poyang Lake in Eastern China (Rabalais et al. 2002; Liao et al. 2017). Overall, N, in many forms, can significantly impact aquatic ecosystems.

1.0.1 Nitrous Oxide Production

Nitrous oxide is a potent GHG and has a global warming potential (GWP_{100}) ~300 times stronger than that of carbon dioxide (CO_2) which can persist in the atmosphere for more than 100 years (Khalil and Rasmussen 1992; Kanter et al. 2013; IPCC 2014). Since the 19th century, atmospheric N_2O concentrations increased by 20% from 270 ppbv to 330 ppbv (current preliminary data from NOAA and ESRL 2018). During its lifetime, N_2O mixes with the upper layers of the stratosphere, where it can destroy the ozone layer, making it not only a powerful GHG

but also the dominant stratospheric ozone-depleting molecule emitted in the 21st century (Ravishankara et al. 2009).

Nitrous oxide can not only be produced through the aerobic process of nitrification, which oxidizes NH_4^+ to NO_3^-—producing N_2O as a side product, but more importantly through the anaerobic process of denitrification, which reduces NO_3^- to N_2 with N_2O as a regular intermediary step (Wrage et al. 2001; Khalil et al. 2004; Laursen and Seitzinger 2004). Although the greatest anthropogenic N_2O emissions stem from these processes on land (associated with agriculture), both processes can occur in aquatic environments. Rivers, estuaries and coastal zones are estimated to account for ~10% of global N_2O emissions, however these model-derived estimates are highly uncertain (IPCC 2007; Beaulieu et al. 2008; Baulch et al. 2012b).

Microorganisms may produce N_2O via the biological processes of nitrification and denitrification (Knowles 1982; Poth and Focht 1985; Galloway et al. 1995; Fowler et al. 2013). Anthropogenic sources of N_2O stem primarily from stimulation of these microbial processes via N input as agricultural fertilizers with additional emissions from fossil fuel combustion and biomass burning which lead to elevated N deposition (IPCC 2001). However, direct N_2O production by industry (e.g., via nylon manufacturing) is also considered important (Khalil and Rasmussen 1992; Seitzinger 1998). Overall, approximately 40% of total global N_2O emission currently originates from anthropogenic activities (IPCC 2013).

1.0.2 Microbial Processes of Nitrification and Denitrification

Two microbial processes that govern N_2O production—nitrification and denitrification—require quite different environments in order to occur and produce N_2O (Firestone and Davidson 1989). During nitrification, two groups of microorganisms (primary and secondary nitrifiers) oxidize NH_4^+ to NO_3^-:

$$NH_4^+ \rightarrow NH_2OH \rightarrow NO_2^- \rightarrow NO_3^- \quad (1.1)$$

Primary nitrifiers oxidize NH_4^+ to hydroxylamine (NH_2OH) and subsequently nitrite (NO_2^-). Secondary nitrifiers then oxidize NO_2^- to NO_3^- (Wrage et al. 2001). Nitrification can produce N_2O either after NH_4^+ is oxidized to NH_2OH or after producing NO_2^-. The ratio of N_2O to NO_3^-

produced is the N_2O yield for nitrification. During denitrification, a wide range of microbes use nitrogen oxides (chiefly NO_3^-) as an electron acceptor in a sequential reduction pathway:

$$NO_3^- \rightarrow NO_2^- \rightarrow NO \rightarrow N_2O \rightarrow N_2 \quad (1.2)$$

Nitrous oxide is produced in the intermediate steps of denitrification (Wrage et al. 2001). The ratio of N_2O to N_2O+N_2 production is referred to as the N_2O yield for denitrification (Beaulieu et al. 2010). Firestone and Davidson (1989) explained the partitioning of these N gases, such as N_2O, in their "hole-in-the-pipe" model in which a fraction of N_2O is lost from the reaction pathway (e.g. leaking through holes in the pipe). Nitrification and denitrification rates (analogous to the flow of water through a pipe), combined with the "leakiness" of the processes (N_2O yields), controls the amount of N_2O created (Firestone and Davidson 1989).

Nitrogen compounds such as NO_3^- and NH_4^+ are necessary for denitrification and nitrification to occur, respectively, provided there is an ample C source for energy (Wrage et al. 2001; Silvennoinen et al. 2008). Also, O_2 concentration affects the rate at which the processes occur (Rosamond et al. 2012). For nitrification, O_2 facilitates the aerobic oxidation of N substrates by nitrifying bacteria (Wrage et al. 2001; Kemp and Dodds 2002). Nitrification exhibits a strong, positive relationship with NH_4^+ concentration (Seitzinger 1985) under aerobic conditions (Rysgaard et al. 1994; Kemp and Dodds 2002; Strauss et al. 2002). When O_2 concentration is low, however, a negative relationship is observed, most likely due to the lack of O_2 needed to oxidize NH_4^+ in the process; under extremely low O_2 concentrations (i.e. anoxic conditions) the process ceases (Caffrey et al. 1993; Van Luijn et al. 1999; Kemp and Dodds 2002). Notably, with high O_2 and NH_4^+ concentrations, N_2O yields may decline (Goreau et al. 1980; Jørgensen et al. 1984; Anderson and Levine 1986; Jiang and Bakken 1999; Khalil et al. 2004), despite high nitrification rates. Research suggests that when the primary nitrifying bacteria produce NO_2^- under low O_2 conditions, the build-up of NO_2^- becomes detrimental to the cell, causing the production of the nitrite reductase enzyme to reduce the toxic NO_2^- to N_2O. Therefore, when O_2 concentrations are high, N_2O production decreases (Ritchie and Nicholas 1972).

N_2O yields from field studies of nitrification typically range from 0–0.37% (Ji et al. 2015) but values as high as 15% (Santoro et al. 2011) and 25% have been noted (Jørgensen et al. 1984).

Nitrification is favored in a circumneutral to slightly basic environment (Warwick 1986; Antoniou et al. 1990) with highest rates occurring at pH 7.5 (Strauss et al. 2002); however, the highest N_2O yields are observed at pH 6.5 (Stevens et al. 1998). Seasonality of temperature affects nitrification with higher rates occurring in the warmer summer months and lowest rates during the colder winter months (Rudolfs et al. 1986; Antoniou et al. 1990; Starry et al. 2005). Conversely, high temperatures (>10°C) impede N_2O production, with the highest yields occurring between 5°C and 10°C (Maag and Vinther 1996). Along with temperature, dissolved organic carbon (DOC) may indirectly affect nitrification due to the high O_2 demand during heterotrophic bacterial decomposition of the DOC.

While nitrification is strictly an aerobic process, denitrification occurs under anaerobic conditions as O_2 inhibits the enzymatic reduction of NO_3^- by microbes (Knowles 1982; Poth and Focht 1985; Khalil and Rasmussen 1992; Wrage et al. 2001; Harrison et al. 2005; Rosamond et al. 2011, 2012). Nevertheless, in aerobic waters nitrification can produce NO_3^-, which can diffuse into anoxic sediments and enhance the process of denitrification (Rysgaard et al. 1994; Cornwell et al. 1999). Since denitrification and NO_3^- exhibit a strong positive relationship exhibiting Michaelis-Menten kinetics (Oremland et al. 1984; Seitzinger 1988; Kemp and Dodds 2002; Bernot and Dodds 2005; Herrman et al. 2008; Silvennoinen et al. 2008; Garnier et al. 2009), with sufficient time and suitable conditions, denitrifying bacteria can use and fully remove NO_3^-–N from a system (Korom 1992). However, the process of denitrification can become NO_3^--saturated (Herrman et al. 2008). Once denitrifying bacteria have become NO_3^--saturated, the maximal rate of denitrification shifts from NO_3^- concentrations to the other main rate-limiting substrate—C (Knowles 1982; Kim 2014). Since denitrifying bacteria are generally heterotrophic (some species are chemoheterotrophic) they need a C source for survival as C provides the electron necessary for heterotrophic metabolism to occur. Moreover, Garcia-Ruiz et al., 1998 found that not only did denitrification rates follow Michaelis-Menten kinetics but also denitrification rates were likely NO_3^--saturated in a eutrophic river, meaning that the NO_3^- concentration at half-maximal activity (K_m, mg NO_3–N L^{-1}) was lower than the available NO_3^- concentration in the water column. In addition to determining K_m for assessing possible NO_3^- saturation, V_{max}, or the maximal denitrification rate (μg N_2O-N g^{-1} dried sediment h^{-1}), can be useful for estimating how much NO_3^- can be denitrified in a system. Several studies found NO_3^- saturation thresholds to be between 0.68

mg NO_3^-–N L^{-1} (Gooding and Baulch 2017) and 2.0 mg NO_3^-–N L^{-1} (Herrman et al. 2008), however kinetic studies on denitrification in freshwater riverine sediments is sparse (Kaspar 1982; Oremland et al. 1984). Therefore, assessing the kinetic parameters (K_m and V_{max}) on denitrification rates becomes important when characterizing an ecosystem with regards to N removal.

Denitrifying bacteria prefer an alkaline environment (Seitzinger 1988; Rysgaard et al. 1994; Maag and Vinther 1996; Herrman et al. 2008), i.e. they have respiration rates that reach a maximum at pH between 7.0 and 8.5 (Van Cleemput and Patrick 1974; Davies and Pretorius 1975; Müller et al. 1980). At the same time the N_2O yield increases at lower pH (Martikainen 1985; Cavigelli and Robertson 2000) because reduction of N_2O to N_2 is inhibited in acidic conditions (Willer and Delwiche 1954). Temperature is often positively related to denitrification rates (Davies and Pretorius 1975; Cavari and Phelps 1977; Martin et al. 2001; Veraart et al. 2011). Overall, N_2O yields from denitrification are found to be ≤ 5% of N_2 produced (Seitzinger 1988; Silvennoinen et al. 2008; Chen et al. 2015) but yields as high as 80% have been reported from nutrient rich, eutrophic rivers (Garcia-Ruiz et al. 1998).

Nitrogen cycling can undergo diel changes (Rosamond et al. 2011; Baulch et al. 2012a). During the daytime, when primary production is high, dissolved oxygen (DO) concentrations tend to be high as well. Moreover, since temperature rises and photosynthesis removes CO_2 from aquatic bodies during the day, increasing pH, nitrification activity may follow a diel cycle (Warwick 1986). These high O_2 daytime conditions inhibit denitrifying bacteria and can limit their N_2O production. However, during the night, respiration dominates the system causing a decrease in DO which may increase the microbial consumption of NO_3^- as an electron acceptor (Venkiteswaran et al. 2014).

1.0.3 Nitrous Oxide from Aquatic Systems

The amount of total N_2O emitted from riverine systems globally has been estimated at ~1.26 Tg N yr^{-1} (Kroeze et al. 2010). The 4th Intergovernmental Panel on Climate Change (IPCC) Assessment report estimates that these emissions are ~30% of the total global anthropogenic N_2O budget (IPCC 2007); however, rates of emission are highly variable. For example, in a study on streams in a small urban-agricultural area of Canada, flux rates ranged from –3.2 μmol N_2O m^{-2} d^{-1} (net sinks) to 776 μmol N_2O m^{-2} d^{-1} (net sources) across multiple systems in the small region

(Baulch et al. 2011). In sewage affected systems, N_2O concentrations at sites downstream/near treated sewage outflows were ten times that of concentrations at upstream sites (Toyoda et al. 2009). Moreover, downstream sites often had the highest reported values of N_2O concentrations/ emissions (McElroy et al. 1978; Hemond and Duran 1989; Harrison and Matson 2003; Toyoda et al. 2009; Beaulieu et al. 2010; Rosamond et al. 2012; Yu et al. 2013). The IPCC estimates that up to 25% of this wastewater N can be directly converted into N_2O (IPCC 2006). The addition of nutrients from a wastewater treatment plant's (WWTP) effluent provide N compounds such as NO_3^- and NH_4^+ that undergo nitrification and denitrification, producing N_2O in the processes. Therefore, treated wastewater can cause dramatic increases in the amount of N_2O produced and emitted from riverine systems. Despite this evidence of elevated emissions from N-enriched rivers, global estimates of N_2O emissions from rivers contain high levels of uncertainty due to a poorly constrained understanding of variability in the N_2O yield as well as variability in N loads and cycling in riverine systems.

1.1 Study Rationale & Background Information

1.1.1 Urban Wastewater and other Nutrient and N_2O Sources

Although urban inputs have increased due to the growth of urban populations (Vitousek et al. 1997; United Nations Environment Program 2010), direct agricultural emissions account for a majority of current anthropogenic global N_2O emissions (IPCC 2014). Conversion of N_2 to N_r for agriculture and industrial feedstock accounts for nearly 60% of anthropogenic produced N_r (Fowler et al. 2013; IPCC 2013). In addition to the production of N_r for crop fertilizer and cattle feed, P is also commonly used for both fertilizer and dietary supplement to cattle (Sharpley et al. 2000). The agriculture sector (e.g. crops and animal production) accounts for 38% of P loads to freshwater while also producing ~6.1 Tg N_2O-N yr^{-1} (Mosier et al. 1998; Mekonnen and Hoekstra 2018). While agriculture and animal production substantially impact the environment, the domestic sector accounts for 54% of P loads to freshwater with the production of ~0.2 Tg N_2O-N yr^{-1} from WWTPs. However, the amount of N or P that WWTPs release largely depends on the level of treatment. For example, in a city in Japan, where 67% of the population sent their waste to WWTPs with only 10% P removal, the city produced 0.26 kg of P per capita as compared to a city in Germany where 100% of the population treated their sewage with 86% P removal,

ultimately resulting in the production of only 0.07 kg of P per capita (Mekonnen and Hoekstra 2018).

Wastewater treatment plants operate at differing levels of treatment from preliminary to tertiary (advanced treatment). Preliminary treatment removes larger debris such as sticks and rags, while primary treatment aims to separate and remove suspended materials. Secondary treatment is often the biological removal of dissolved organic matter and some nutrients through the use of aerobic bacteria (Sonune and Ghate 2004). The effluent from secondary treatment can still contain high levels of nutrients such as N and P which can enter and impact receiving water bodies (McMahon and Dennehy 1999; Mulholland et al. 2008). This inflow of nutrients can drive in-stream N_2O production as wastewater effluent can dominate biogeochemical processes such as nitrification and denitrification in receiving aquatic systems (Carey and Migliaccio 2009). Tertiary/ advanced wastewater treatment can further reduce not only inputs of N and P, but quite possibly subsequent downstream production of N_2O (IPCC 2006).

While many cities, regions, or nations impose strict regulations to control nutrient levels and monitor effects of wastewater treated effluent on chemistry and biota, there is limited information on the downstream impacts on N_2O production. The few studies that have observed the effect of treated effluent from WWTPs on riverine systems showed an increase in N_2O emissions from rivers and streams (McElroy et al. 1978; Hemond and Duran 1989; Harrison and Matson 2003; Toyoda et al. 2009; Beaulieu et al. 2010; Rosamond et al. 2012; Yu et al. 2013). These studies universally show the effects of enriched waters from WWTPs on aquatic N_2O concentrations and that the sites nearest to the effluent formed hotspots of N_2O emissions. It should be noted that N_2O production can occur during the wastewater treatment process; data suggest that the contribution of N_2O produced during WWTP process ranges from negligible (primary treatment) to substantial (advanced treatment), largely depending on the specific treatment processes and stages (Czepiel et al. 1995; Schulthess and Gujer 1996; Kimochi et al. 1998; Kampschreue et al. 2009; Law et al. 2012). For studies that focused on N_2O emissions from WWTPs, the amount of influent N converted to N_2O (N_2O yield) ranged between 0–5% (Gejlsbjerg et al. 1998; Park et al. 2000; Foley et al. 2009), although biological nutrient removal (BNR) chains (as implemented in the Regina WWTP) have been estimated to convert 0.003–25% of inflowing N into N_2O (Law et al. 2012).

Urban aquatic systems, especially downstream of WWTPs, often contain hypoxic waters due to high biochemical oxygen demand (BOD) (Fair 1939; Arbabi et al. 1974; Munodawafa and Chitata 2012) and increased nutrient load of treated effluent (Yang et al. 2011; Rosamond et al. 2012; Venkiteswaran et al. 2015; Wang et al. 2015). The release of BOD laden effluent creates an "oxygen sag" where DO levels decrease significantly at the source of the organic matter (Arbabi et al. 1974; Ramalho 1977). In these extremely low DO environments, denitrification activity is promoted because NO_3^- is favored as the terminal electron acceptor for denitrifying bacteria (Seitzinger 1988) thereby forming hotspots of N_2O production (Smith et al. 1998; Canfield et al. 2010). Even though downstream DO concentrations will eventually return to upstream conditions, due to dilution of anaerobic bacteria, growth of algae, and reaeration of O_2, DO concentrations would vary greatly following a diel cycle because of the high BOD (Bartsch 1948; O'Connor 1967; Chambers et al. 1997).

Along with denitrification, nitrification can contribute to N_2O hotspots downstream of a WWTP where NH_4^+ is an important component of N loading. Additionally, coupled nitrification to denitrification or the single-organism (*Nitrosomonas europaea*) process of nitrifier denitrification can further produce N_2O in the aerobic, nutrient-rich waters downstream (Wrage et al. 2001). Moreover, the process of anaerobic NH_4^+ oxidation (anammox) can combine NO_2^- with NH_4^+ to produce N_2 (Kartal et al. 2011), which provides another path to aid in permanently removing NO_3^- from the system (Burgin and Hamilton 2007). Even though there have been few studies on anammox and the process is not directly linked to N_2O production (Jetten et al. 1999; Dalsgaard et al. 2005), studies have begun to focus on this process in freshwater as it can be an important N sink (Schubert et al. 2006; Hamersley et al. 2009; Moore et al. 2011; Hu et al. 2012). Lastly, the process of complete NH_4^+ oxidation (comammox) allows for the full conversion of NH_4^+ to NO_3^- in a single organism (versus two organisms necessary for nitrification to occur). Not only have species capable of performing comammox (*Nitrospira*) recently been discovered, but those microorganisms were found in more-extreme conditions inside of biofilms (Daims et al. 2015; Kessel et al. 2016). Because these findings are recent, research on N_2O production is sparse; however Sabba et al., 2018 investigated biofilms as a source of N_2O in wastewater treatment processes and found that electron donor limitation for denitrification and low DO concentrations in biofilms promote N_2O production.

1.2 Research Objectives

In Regina, Saskatchewan the Regina WWTP underwent an upgrade to reduce nutrient concentrations in its effluent, including N compounds such as NH_4^+, un-ionized ammonia (NH_3) referred to herein as TAN, total dissolved N (TDN), and P. The purpose of this research was to determine the effect of this WWTP upgrade on downstream water chemistry of Wascana Creek and Qu'Appelle River, denitrification rates and N_2O concentrations and emissions. More specifically, for Chapter 2 I aimed to answer the following questions:

Q1. Did the Regina WWTP upgrade significantly reduce concentrations of nutrients, specifically NO_3^-, TAN, NH_3, TDN, urea, and/or DOC?

Q2. Does wastewater effluent increase denitrification rates when compared to un-impacted sites?

H_0: Wastewater effluent does not increase denitrification rates when compared to un-impacted sites.

H_a: Wastewater effluent increases denitrification rates when compared to un-impacted sites.

Q3. Does the WWTP upgrade affect denitrification rates?

H_0: The WWTP upgrade will not affect denitrification rates.

H_a: The WWTP upgrade will affect denitrification rates.

Q4. Are denitrification rates NO_3^--saturated in effluent-impacted reaches?

H_0: Nitrate saturation will not be observed at high nitrate concentrations downstream of the WWTP.

H_a: Nitrate saturation will be observed at high NO_3^- concentrations downstream of the WWTP.

Q5. Does wastewater effluent impact denitrification kinetics?

H_0: Denitrification kinetics at non-effluent impacted sites will not be different from downstream sites.

H_a: Denitrification kinetics at non-effluent impacted sites will be different from downstream sites.

Q6. Is there a correlation between physicochemical factors (NO_3^-, pH, sediment organic carbon; SOC) and denitrification rates?

H_0: There will be no significant correlation between [individual] physicochemical factors and denitrification rates.

H_a: There will be a significant correlation between [individual] physicochemical factors and denitrification rates.

While for Chapter 3, I aimed to answer these following questions:

Q1. Does the WWTP cause an increase in downstream N_2O concentrations/emissions?

H_0: The WWTP does not cause an increase in N_2O concentrations/emissions downstream.

H_a: The WWTP causes an increase in N_2O concentrations/emissions downstream.

Q2. Does the WWTP upgrade cause a significant reduction in N_2O concentrations and emissions downstream?

H_0: The WWTP upgrade will not cause a reduction in N_2O concentrations and emissions downstream.

H_a: The WWTP upgrade will cause a reduction in N_2O concentrations and emissions downstream.

Q3. Is there a significant correlation between chemical factors (NO_3^-, TAN) or denitrification rates and N_2O concentrations?

H_0: There will be no significant correlation between (individual) chemical factors or denitrification rates and N_2O concentrations.

H_a: There will be a significant correlation between (individual) chemical factors or denitrification rates and N_2O concentrations.

Q4. Do physicochemical factors (urea, NO_3^-, TAN, TDN, DO, pH, and temperature) and N_2O follow a diel pattern?

H_0: N_2O and/or (individual) physicochemical factors will not follow a diel pattern.

H_a: N_2O and/or (individual) physicochemical factors will follow a diel pattern.

1.3 Thesis Structure

This introduction is followed by two draft manuscripts where each manuscript addresses a set of research questions as outline above as individual, yet complementary chapters. Chapter 3 (second manuscript) is followed by conclusions, then followed by a list of references, and lastly followed by appendices.

Chapter 2: THE EFFECT OF A WASTEWATER TREATMENT PLANT UPGRADE ON IN-STREAM DENITRIFICATION

Citation: Dylla, N.P., Whitfield, C.J., Schlageter, B., and H.M. Baulch (2019). "The Effect of a Wastewater Treatment Plant Upgrade on In-stream Denitrification" Journal Vol(Issue): pg–pg.

Status: Prepared for Publication

2.0 Abstract

Nutrient-rich effluent from wastewater treatment plants (WWTPs) can drive biological processes in rivers and create major impacts on ecosystem health. Improving effluent quality can help minimize these effects. Here I capitalize on a novel opportunity to understand the impacts of WWTP upgrade on in-stream water quality and denitrification rates, using a before-after-control-impact (BACI) design in both an effluent-dominated river where effluent can constitute more than 90% of the discharge, and in a larger river in the stream network. It was demonstrated that a WWTP upgrade led to major and immediate changes in in-stream concentrations of total ammonia nitrogen (TAN; NH_4^+ + NH_3). Total ammonia nitrogen declined by up to 35-fold, mitigating potential toxicity. Large spatial differences were observed in denitrification rates, with high denitrification rates commonly observed downstream of the WWTP. Sites downstream of the effluent had >1200-fold higher denitrification rates when compared to upstream sites in the effluent dominated stream and were commonly nitrate (NO_3^-)-saturated. A more muted, but still substantive 20-fold increase in denitrification rates was observed downstream of the confluence with a larger river. Results suggest that NO_3^- concentrations are dynamic both in space and in time. Denitrification rates remained NO_3^--saturated in areas of the river following the upgrade. Nitrate saturation continued in part because NO_3^- concentrations at our downstream sites did not show major changes post-upgrade. Instead, this work demonstrates that enhanced N removal in the effluent has helped mitigate potential NH_3 toxicity, while high in-stream denitrification rates continue. Ultimately, particularly within effluent dominated ecosystems, engineering design should consider not only in-stream sensitivity to the effluent, but also in-stream capacity to mitigate nutrient pollution, for example, by helping to maximize N removal capacity via denitrification.

2.1 Introduction

Agriculture and urbanization have increased the amount of nutrients entering bodies of water (Vitousek et al. 1997; Galloway et al. 2003; Leavitt et al. 2006; IPCC 2013). Nutrient-enriched waters provide the conditions necessary for primary producing organisms to flourish, then die, ultimately forming zones of hypoxic or anoxic conditions in the rivers, lakes, or oceans (Smith et al. 1998). With respect to urban point sources, significant efforts have been made to decrease wastewater loads through technological upgrades, and to decrease agricultural nutrient loads through implementation of beneficial management practices (BMPs) (Cherry et al. 2008). Upgrades to wastewater treatment plants (WWTPs) can show immediate benefits to downstream ecosystems (Sosiak 2002; Zhou and Smith 2002; Holeton et al. 2011); however, these upgrades are often expensive. Agricultural BMPs may be less expensive, but can be slow to show benefits, in part due to long nutrient legacies and high uncertainty in terms of their efficacy (Meals et al. 2010; Sharpley et al. 2013). This leaves difficult decisions in balancing cost, uncertainty and timescale in efforts to improve water quality in systems influenced by both urban and agricultural environments.

Wastewater treatment plants can affect the receiving ecosystem in many ways. Effluent concentrations typically and vastly exceed those in receiving water bodies (Carey and Migliaccio 2009); this can alter downstream biogeochemical processes (Dodds and Welch 2000; Rabalais et al. 2002). For example, WWTP effluent containing high concentrations of nutrients and organic matter regularly causes in-stream biochemical oxygen demand (BOD) to rapidly increase, which can lead to hypoxia in enriched, eutrophic waters (Fair 1939; Mulholland et al. 2008; Venkiteswaran et al. 2015). In turn, this may potentially inhibit processes such as nitrification, or stimulate phosphorus (P) release from sediments (Mortimer 1941; Schindler 1974; Orihel et al. 2017). Increased primary productivity resulting from elevated nutrient loads may also contribute to hypoxia due to associated carbon (C) inputs, and nighttime respiration (Correll 1998; Rabalais et al. 2002; Camargo and Alonso 2006). Wastewater treatment plants can also affect pH, conductivity and temperature of receiving aquatic systems (Andersen et al. 2004; Hershey et al. 2004; Ekka et al. 2006).

While ecosystems can be influenced by influxes of nutrients from WWTPs, in-stream microbial processes can help abate these high nutrient loads. One process—denitrification—can

permanently remove nitrogen (N) from the water by sequentially reducing nitrate (NO_3^-) to dinitrogen gas (N_2) (Firestone and Davidson 1989). Since N_2 is biologically unavailable to most organisms and returns to the atmosphere, denitrification is considered an ecosystem service (Inwood et al. 2005; Burgin and Hamilton 2007; Mulholland et al. 2009). Denitrification is a ubiquitous process in soils and in both fresh and salt water (Knowles 1982). This process is assumed to be a substantial sink of NO_3^- (Seitzinger and Kroeze 1998; IPCC 2013); however, the rate of denitrification can be affected by a multitude of parameters (Galloway et al. 2004; Canfield et al. 2010). Nitrate is often the limiting factor, although dissolved oxygen (DO), pH, temperature, sediment organic carbon (SOC), and dissolved organic carbon (DOC) can also play a role (Davies and Pretorius 1975; Oren and Blackburn 1979; Caffrey et al. 1993). When NO_3^- concentrations are high, C may control rates (Arango and Tank 2008), although this is not always the case (Cooke and White 1987; Martin et al. 2001).

Since denitrification rates exhibit Michaelis-Menten kinetics when assessing NO_3^- concentrations, kinetic parameters such as K_m (the NO_3^- concentration at half-maximal activity) and V_{max} (the maximum denitrification rate) can be determined. These parameters help determine possible NO_3^- saturation as well as how active rates of denitrification are in particular sediments. If K_m values are below in-stream NO_3^- concentrations, then denitrification may be NO_3^--saturated. Where NO_3^- concentrations do not limit rates, the process may instead be limited by other factors (C, temperature, pH, and DO) (Garcia-Ruiz et al. 1998). Comparing V_{max} values across sediments or study sites is also important as it helps characterize the denitrification potential across sites. Although kinetic experiments are limited, several studies found NO_3^- saturation to occur between 0.68 mg NO_3^-–N L^{-1} (Gooding and Baulch 2017) and 2.0 mg NO_3^-–N L^{-1} (Herrman et al. 2008), however research in freshwater sediments is sparse (Kaspar 1982; Oremland et al. 1984). Because many nutrients first enter freshwater bodies from leaching and run-off, characterizing the kinetic parameters of denitrification in freshwater systems is vital to further understanding the process of denitrification. Nitrification, a process which can lead to the in-stream production of NO_3^- from ammonium (NH_4^+), can be important to oxygen demand (O'Connor 1967; Khalil et al. 2004), and in some ecosystems coupled nitrification-denitrification is the major pathway stimulating removal of reactive nitrogen (N_r).

By creating low-oxygen, nutrient and C-rich conditions, often with high NO_3^- concentrations, wastewater effluents can create hotspots of N removal via denitrification (Garcia-

Ruiz et al. 1998; Lofton et al. 2007). These hotspots mitigate transport of N_r to downstream ecosystems. While studies focused on wastewater impacts on denitrification are relatively sparse (Bradley et al. 1995; Lofton et al. 2007; David et al. 2011; Ribot et al. 2017), there are important questions about how effluents influence nutrient removal in receiving waters and how improved WWTP effluent quality may alter these processes.

Therefore, in this study, I assessed how denitrification rates vary spatially in a creek dominated by treated effluent and a downstream river where the WWTP inputs play a lesser role in the nutrient budget. I assessed whether the upgrade of a WWTP, and resultant changes to the receiving waters, including a decreasing N load, led to lower denitrification rates (pre-upgrade to post-upgrade) using a before-after-control-impact (BACI) design. Specifically, this study aimed to answer the following questions: 1) Did the Regina WWTP upgrade significantly reduce in-stream nutrients? 2) Does wastewater effluent increase denitrification rates when compared to un-impacted sites? 3) Does the WWTP upgrade affect denitrification rates? 4) Are denitrification rates NO_3^--saturated in effluent-impacted reaches? 5) Does wastewater effluent impact denitrification kinetics? 6) Is there a correlation between physicochemical factors (NO_3^-, SOC, and pH) and denitrification rates?

2.2 Materials and Methods

2.2.1 Study Area

The two studied riverine systems—Wascana Creek and the Qu'Appelle River—are situated northwest of Regina, Saskatchewan, Canada (Figure 2.1) and experience a cold semi-arid continental climate (Köppen climate class BSk/Dfb) (Köppen and Geiger 1936; Lohmann et al. 1993). Wascana Creek slowly flows northwest for ~60 km where it is a tributary to the Qu'Appelle River, flowing east. Wascana Creek and Qu'Appelle River upstream of the study location have effective drainage areas of 1740 km^2 and 6950 km^2, respectively (Environment Canada 2017a; b). The dominant land use in the region is agriculture (Allan and Roy 1980), though the Wascana Creek watershed also features a large urban area. Annual flow in Wascana Creek and the Qu'Appelle River averages 2.4 $m^3\ s^{-1}$ and 6.3 $m^3\ s^{-1}$ at W4 and QA2, respectively. However, flow rates are seasonal peaking after the spring snow-melt while rates are lowest (with transient peaks from precipitation events) during the warm/dry months from May-September. The creek and river

become ice-covered in ~November. Air temperature varies greatly through the year with an average temperature for July and January of 19.1ºC and –16.5ºC, respectively (Environment Canada 2018). In winter, during ice-covered conditions, treated effluent can provide up to 100% of the flow of Wascana Creek (Waiser et al. 2011b).

2.2.2 Wastewater Treatment Plant Upgrade Timeline

The Regina WWTP, servicing a population of approximately 215,000, is located ~15 km northwest of Regina, Saskatchewan and discharges directly into Wascana Creek. During low-flow, discharge from the WWTP results in diel water level fluctuations as far as 60 km downstream (Figure A2.1). Prior to the recent upgrade, wastewater was treated through the following sequence: primary treatment, followed by transit through a five-cell lagoon system, treatment with alum to facilitate P removal, followed by ultraviolet disinfection (Waiser et al. 2011a; b). Although the WWTP employed tertiary treatment, there was concern regarding both NH_4^+ and un-ionized ammonia (referred to herein as NH_3) and nutrient loading to Wascana Creek (Waiser et al. 2011a; b). Upgrade construction started in June 2014 to implement a biological nutrient removal (BNR) process in order to meet enhanced regulations for effluent quality and increase capacity to support a population of 258,000. The WWTP upgrade retrofitted both the primary filtration (separating liquids from solids) as well as the biosolids management systems (solids digesters). The WWTP upgrade was designed to enhance water quality by reducing N loading in its effluent as total nitrogen (TN) and total ammonia nitrogen (TAN; $NH_4^+ + NH_3$). The upgrade featured secondary clarifiers (further separation of solids and liquids) as well as a new UV disinfection system, and three advanced bio-reactors to enhance BNR (N and P). Enhanced nutrient removal was online August 11th, 2016 as determined by the reduction of TAN at our first downstream site as well as in effluent concentrations (Kayla Gallant, personal communication, November 20, 2018; Figure A2.2).

2.2.3 Study Sites

Four sites situated on Wascana Creek (W1–4) and two on the Qu'Appelle River (QA1–2) were sampled. Sites were selected based on a before-after-control-impact (BACI) design and site access, incorporating upstream (control) and downstream (impact) sites of the Regina WWTP for both Qu'Appelle River and Wascana Creek. The Wascana Creek sites were: W1 (control: ~4 km

upstream of the WWTP), W2 (impact: ~0.2 km downstream of the WWTP), W3 (impact: ~3.8 km downstream), and W4 (impact: ~59.8 km downstream). The Qu'Appelle River sites were: QA1 (control: ~5 km upstream of the Wascana Creek confluence) and QA2 (impact: ~12 km downstream of the confluence) (Figure 2.1). I note that the control sites are not true controls, and instead should be considered reference sites unaffected by the WWTP upgrade; however, I use the term 'control' for simplicity based on the BACI design.

2.2.4 Sample Collection

Water sampling was performed twice monthly while sampling sediment for denitrification experiments occurred monthly during the open-water seasons from May–November in 2016 and April–September in 2017. Water quality parameters (DO, pH, specific conductance, and temperature) were measured with a YSI (Yellow Springs Instrument) Multi-Probe System 556 (YSI Environmental, Yellow Springs, Ohio) by wading into the middle of the creek/ river and placing the probe at half-depth. Bulk water samples were collected via grab sampling and kept cool, processed, preserved, and analyzed according to standard methods (Table 2.1) for NO_3^-, TAN, urea, SOC, DOC, and total dissolved nitrogen (TDN).

An open-ended coring tube (4.5 cm diameter) was used (Schaller et al. 2004; Inwood et al. 2005) to collect the upper 5 cm of sediment for denitrification rate measurements. Sediment cores were taken across the width of the stream and composited to obtain a sample representative of sediment characteristics within the stream bed. Sediment cores were placed into 1 L HDPE (high density polyethylene) bottles and homogenized. One liter of raw water was also taken from each site (HDPE bottle) for denitrification assays. Both sediment and site water were stored on-ice or refrigerated prior to initiating experiments the next day.

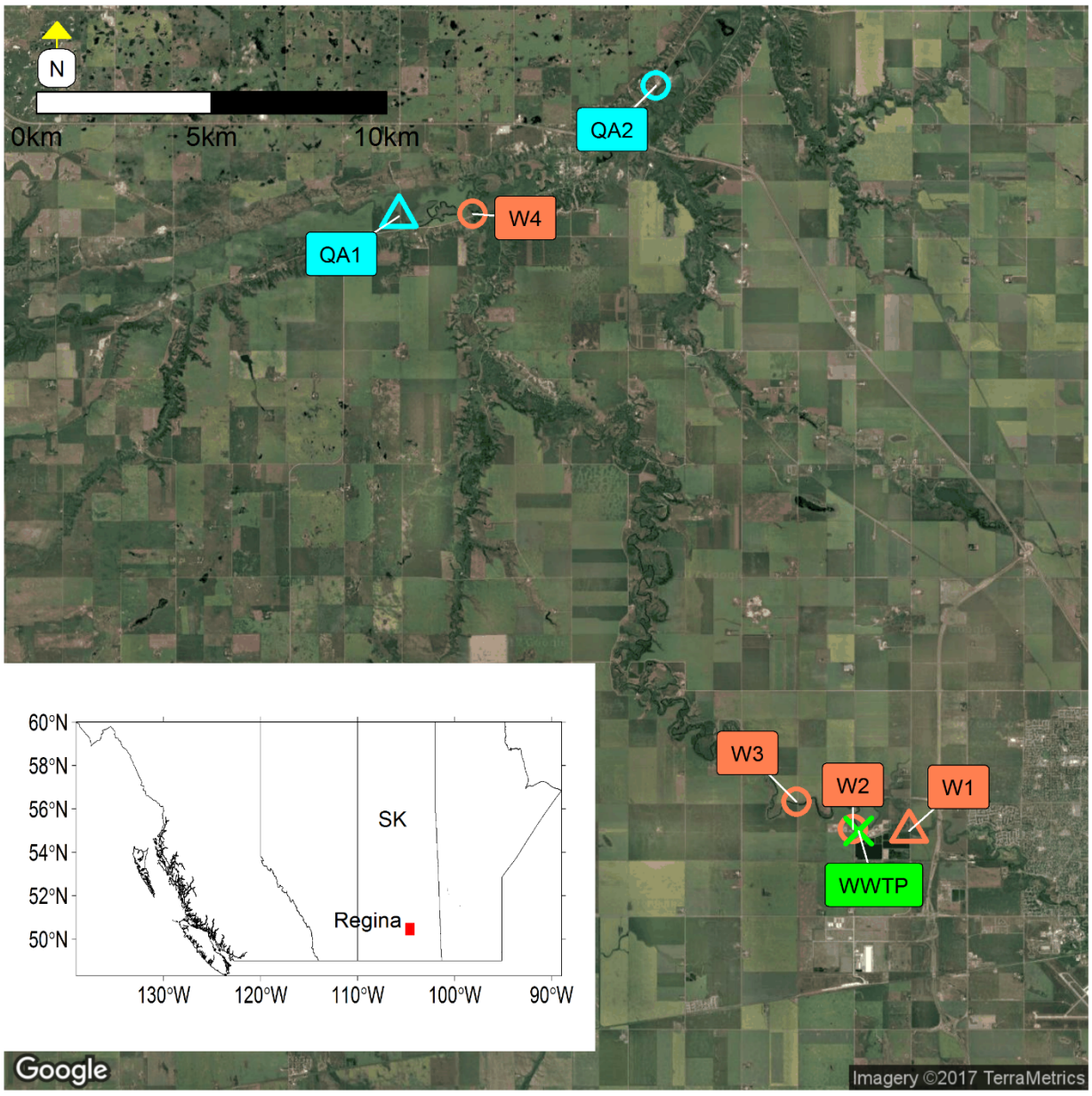

Figure 2.1 Study sites were located near Regina, SK, Canada. Sites were located upstream (triangles) or downstream sites (circles) of the Wastewater Treatment Plant effluent (WWTP: green X) on both Wascana Creek (orange labels) and Qu'Appelle River (blue labels). Wascana Creek flows northwest and Qu'Appelle River flows northeast.

Table 2.1 Summary of water chemistry and sediment analyses.

Analyte	Method	Sample Treatment	Storage
NO_3^-	Open tubular copperized cadmium reduction (OTCR) followed by diazotization with sulfanilamide[1]	Filtered (0.45 µm cellulose acetate filters with a GFF)	Frozen (–40°C)
TAN[†]	Indophenol blue method with a borate buffer[2]	Filtered (0.45 µm cellulose acetate filters with a GFF) and acidified with 10% H_2SO_4	Frozen (–40°C)
Urea	Phenol yellow method[3]	Filtered (0.45 µm cellulose acetate filters with a GFF)	Frozen (–40°C)
SOC	Loss on ignition method[4]	Dried, combusted (360°C)	Refrigerated (4°C)
DOC	Catalytic combustion to CO_2 and IR detection[5]	Filtered (0.45 µm cellulose acetate filters with a GFF)	Refrigerated (4°C)
TDN	Combustion and conversion of N species to NO_2[6]	Filtered (0.45 µm cellulose acetate filters with a GFF) and acidified with 10% H_2SO_4	Refrigerated (4°C)

[1](Wetzel and Likens 1991); [2](Ministry of the Environment 2001); [3](Emmet 1969); [4](Schumacher 2002); [5](ASTM International 2018); [6](ASTM International 2016); [†]TAN is dominated by NH_4^+ in our systems but the analysis also includes NH_3

2.2.5 Laboratory Analysis

2.2.5.1 Water and Sediment Chemistry

Nitrate was measured in duplicate and analyzed using a colorimetric technique on a SmartChem 170 (WestCo Scientific Instruments, Inc.) auto-analyzer. This method includes the small amount of NO_2^- in the analysis for NO_3^-; therefore, NO_3^- reported here is NO_2^- + NO_3^- (Johnston et al. 1990; Avanzino and Kennedy 1993; Baulch 2009). Ammonia (NH_3) and ammonium (NH_4^+) concentrations are referred to in aggregate as total ammonia nitrogen (TAN). Un-ionized ammonia (NH_3) was estimated from TAN concentrations based on measured stream temperature and pH (Emerson et al. 1975; Canadian Council of Ministers of the Environment 2010; Waiser et al. 2011b). Urea and TAN were also measured in duplicate on SmartChem 170 according to the indophenol blue and phenol yellow methods, respectively (Emmet 1969; Ministry

of the Environment 2001). Dissolved organic carbon was analyzed in duplicate on a Shimadzu TOC-L analyzer where samples were combusted (> 680˚C) and converted to CO_2 and analyzed using non-dispersive infrared (NDIR) detectors (ASTM International 2018).

Sediment organic carbon (SOC) samples were stored at 4ºC and dried at room temperature. Once dry, sediment was passed through a 2 mm sieve and analyzed for organic matter according to the loss-on-ignition method (Schumacher 2002). Total dissolved nitrogen was analyzed in duplicate on a Shimadzu TOC-L analyzer with TN module where samples were combusted (720˚C) to nitrogen monoxide (NO), cooled by passing through a thermoelectric cooler, and analyzed via a chemiluminescence analyzer (ASTM International 2016).

2.2.6 Denitrification Experiments

Potential denitrification rates were quantified using a chloramphenicol-amended acetylene (C_2H_2)-block method (Smith and Tiedje 1979; Arango and Tank 2008). Although, the chloramphenicol-amended C_2H_2-block allows for high-throughput experimentation at relatively low-costs, this method can underestimate rates of denitrification, due to the inhibition of nitrification (which produces NO_3^-) especially in low or dynamic NO_3^- environments (Groffman et al. 2006). Likewise, acetylene has been shown to be degraded by bacteria, which could also underestimate rates of denitrification, since the build-up of gases would not stop at N_2O (Flather and Beauchamp 1992). Notwithstanding these limitations, because the experimental procedure stops the denitrification process at N_2O, the rates generated with this method may be viewed as potential rather than true rates. However, for processing a large number of samples this method is most viable (Groffman et al. 1999).

For each site, 25 mL aliquots of homogenized sediment were added to eight glass media bottles (140 mL) equipped with lids containing a rubber septum. Then, 50 mL of site water + chloramphenicol was added to create a slurry (75 mL total sediment + site water). Chloramphenicol was added to all bottles to reach a final concentration of 6.0 mM to inhibit the production of new enzymes (Knowles and Yoshinari 1976; Schaller et al. 2004; Inwood et al. 2005). The sample bottles were then purged with N_2 for 5 mins. The eight samples were comprised of two controls (no C_2H_2), three C_2H_2-treated replicates (AT), and three C_2H_2-treated replicates with NO_3^--amendments (ATNA). Potassium nitrate (KNO_3) was added to ATNA samples to ensure 100 mg NO_3–N kg sediment^{-1} (~700 mg NO_3–N L^{-1}) as the NO_3^- amendment and used to

determine if ambient samples were NO_3^--saturated. All bottles were dark-incubated at stream temperature (± 2°C) and shaken at 165 rpm for 170 mins. Gaseous headspace samples were taken at 20, 70, 120, and 170 min. Nitrous oxide (N_2O) concentrations were analyzed using a Scion 456 Gas Chromatograph (Bruker; Electron Capture Detector; injector and column temperature 60°C, detector temperature 350°C, and Ar carrier gas). Rates of denitrification (μg N g^{-1} h^{-1}) were calculated from the increase in N_2O (μg N) over time, divided by the dry weight of sediments.

A kinetics experiment was also carried out for one upstream site (W1) and one downstream site (W3) to find the maximum rate of denitrification (V_{max}) as well as the concentration at half-maximal activity (K_m). The same C_2H_2-block method as used for the ATNA samples was also applied for this experiment, with the exception that a range of concentrations 0.20 mg NO_3^- L^{-1} (ambient in-stream concentration), 0.30 mg NO_3^- L^{-1}, 0.50 mg NO_3^- L^{-1}, 1.00 mg NO_3^- L^{-1}, 1.20 mg L^{-1}, 3.20 mg NO_3^- L^{-1}, and 5.20 mg NO_3^- L^{-1} were chosen to provide a range of NO_3^- concentrations. Also, instead of using respective site water for each site, water from W1 was used for both W1 and W3 sediments to limit NO_3^- concentrations below those measured at W3, while maintaining an otherwise similar water matrix.

2.2.7 Statistical Analyses

A BACI design was employed which allowed for multiple impact sites to be compared to an upstream control site, before and after an event (Eberhardt 1976; Bernstein and Zalinski 1983; Stewart-Oaten et al. 1986). Several statistical analyses were employed to assess: a) whether the WWTP upgrade affected nutrient concentrations and denitrification rates, b) spatial variation in rates and potential factors driving variation in denitrification rates, and c) whether denitrification is NO_3^--limited. All data analyses were performed using R: A Language and Environment for Statistical Computing, 2018 (R Core Team 2018; version 1.1383) where $\alpha = 0.05$ was considered statistically significant. Where I assessed the effects of the WWTP upgrade on chemistry, or denitrification rates, I restricted comparisons to the summer months, where I have both pre-upgrade data and post-upgrade data (i.e., pre: May–August 2016; post: May–August 2017).

2.2.7.1 Changes in Water Chemistry in Space and Time

To find possible differences amongst sites and through time, a linear mixed-effects model (LMM) was used (package: ‘lmerTest’; function: (lmer)) with parameter inferences (*F*-statistic

and *p*-value) obtained using an analysis of variance (ANOVA; package: 'lmerTest; function: (anova)) (Kuznetsova et al. 2017). This LMM analysis was employed as it handles unbalanced designs (i.e. missing data), confounding variables, inconsistent sampling dates and treats time as a continuous variable (Lindstrom and Bates 1990; Cnaan et al. 1997; Nakagawa and Schielzeth 2010). To further investigate significant differences between sites, a TukeyHSD test was run using a general linear hypothesis with multiple comparisons (package: 'multcomp'; function: (glht)) (Hothorn et al. 2008). A TukeyHSD test was chosen as the post-hoc test because it allows for comparison of multiple means. After producing the LMM the residuals were checked for normality and were found to be non-normal, therefore they were transformed using the Box-Cox log-transformation method ($\lambda = 0.101$; package: 'MASS'; function: (boxcox)) and the model re-run with transformed data (Box and Cox 1964; Venables and Ripley 2002). The transformation also helped with achieving equality of variance (homoscedasticity) which was confirmed using the Levene's Test (package: 'car'; function: (leveneTest) (Fox and Weisberg 2011). Chemical parameters (NO_3^-, NH_4^+, urea, TDN, DO, pH, and SOC) were individually assessed for normality through visual inspection of a quantile-quantile plot (package: 'stats' ; function: (qqnorm)) and using the Shapiro-Wilk test (package: 'stats'; function: (shapiro.test)) (R Core Team 2018); where data were considered parametric having a *p*-value > 0.05. After individually checking for normality for correlation analysis, NO_3^- ($W = 0.73$, $p = 1.3 \times 10^{-10}$), NH_4^+ ($W = 0.49$, $p = 7.9 \times 10^{-15}$), TDN ($W = 0.77$, $p = 3.6 \times 10^{-13}$), urea ($W = 0.87$, $p = 1.0 \times 10^{-6}$), and SOC (W=0.92, $p = 0.01$) data were non-parametric while DO ($W = 0.96$, $p = 0.09$) and pH ($W = 0.98$, $p = 0.36$) data were parametric. In order to reduce the chance of a type I error, all *p*-values were Bonferroni corrected, providing each analysis with a 95% confidence interval.

2.2.7.2 Denitrification Activity

Potential denitrification rates (μg N g^{-1} h^{-1}) were calculated as the accumulation of N_2O over time, indicating active denitrification (Groffman et al. 2006). Replicates were only included for further analysis if they showed statistically significant linear relationships ($p < 0.05$). Non-linearity may occur due to experimental error or potentially through chloramphenicol interfering with denitrifying enzymes (Wu and Knowles 1995). Non-linearity was rare (1.2% of cases), and non-linear replicates were removed from analysis. However, a second analysis to test for potential bias of removing these samples, by setting their rates to zero, found no significant effect. The

residuals from the LMM analysis for denitrification rates were tested for normality (were non-normal) and normalized following the Box-Cox log-transformation ($\lambda = 0.101$). The LMM was used to determine if denitrification activity differed within sites before and/or after the upgrade and if impacted sites differed from control sites (Smith 2002). Nitrate saturation was identified as occurring for samples where denitrification rates did not increase when NO_3^- was added. A paired t-test (package: 'stats' ; function: [t.test]) (R Core Team 2018) was used to test for NO_3^- saturation by comparing the denitrification activity of AT and ATNA samples for each site. Samples were considered saturated when there was no difference between rates (Bonferroni corrected $p > 0.05$). To solve for the variables from the denitrification kinetics experiment—V_{max} (maximal rates at saturating NO_3^- concentrations) and K_m (substrate concentration at ½ V_{max})—a general dose-response model was employed (package: 'drc'; function: [drm]) (Ritz et al. 2015) for sites W1 and W3.

To identify physicochemical predictors (NO_3^-, SOC, and pH) of denitrification activity (AT samples), individual correlation analyses (package: 'stats'; function: [cor.test]) (R Core Team 2018) were used. Non-parametric analysis (Spearman's rank) was used for the combination of both parametric (pH) and non-parametric data (NO_3^- and SOC). Bonferroni correction was used to maintain a 95% confidence interval for each test.

2.3 Results

2.3.1 Effects of the Wastewater Treatment Plant and Upgrade on Water Chemistry

The most chemically impacted sites were situated on the smaller Wascana Creek (W2, W3, and W4). Pre-upgrade TAN concentrations for the site upstream of the WWTP on Wascana Creek (site W1) averaged 0.05 mg TAN L^{-1}. Concentrations increased more than 100-fold to 8.18 mg TAN L^{-1} at W2 then slightly decreased downstream to an average of 6.29 mg TAN L^{-1} at W3, and 1.42 mg TAN L^{-1} at W4 (Table 2.2). The Qu'Appelle River sites averaged 0.01 mg TAN L^{-1} at QA1 (upstream of the Wascana Creek confluence) and 0.34 mg TAN L^{-1} at QA2 (downstream of the Wascana Creek confluence) and were not significantly different (ANOVA $F(5,30) = 19.9$, $p < 0.0001$; TukeyHSD $p > 0.1$). Pre-upgrade NH_3 concentrations were significantly higher at W2 and W3, compared to W1 (ANOVA $F(5,30) = 19.9$, $p < 0.0001$; TukeyHSD $p < 0.0001$) (Table 2.2). Prior to the upgrade, NO_3^- concentrations were significantly greater at all downstream sites,

respective to their system (ANOVA $F(5,30) = 13.5$, $p < 0.0001$; TukeyHSD $p < 0.001$). Nitrate concentrations were over 100 times greater downstream of W1 (0.02 mg NO_3–N L^{-1}) on Wascana Creek (W2: 3.31 mg NO_3–N L^{-1}; W3: 2.81 mg NO_3–N L^{-1}; W4: 4.69 mg NO_3–N L^{-1}) and over 10 times greater downstream of QA1 (0.17 mg NO_3–N L^{-1}) on the Qu'Appelle River (QA2: 2.09 mg NO_3–N L^{-1}; Table 2.2). Urea was significantly higher only at the downstream site W2 relative to control (W1) with an average concentration of 0.10 mg urea–N L^{-1} (ANOVA $F(5,30) = 11.54$, $p < 0.0001$; TukeyHSD $p < 0.0001$). The highest urea concentrations were observed for both Qu'Appelle River sites with QA1 having an average concentration of 0.17 mg urea–N L^{-1} and QA2 of 0.12 mg urea–N L^{-1}. Pre-upgrade TDN concentrations exhibited high temporal variability across the impact sites downstream of the WWTP on Wascana Creek and at W2 were TDN concentrations significantly greater than at W1 (ANOVA $F(5,41) = 3.72$, $p < 0.01$; TukeyHSD $p < 0.01$) (Table 2.2). Within site pre-upgrade DOC concentrations were also highly variable, and there were no significant differences between control and impact sites. Overall, the control sites (W1 and QA1) observed the lowest concentrations of nutrients and conductivity. They were slightly basic, and well-oxygenated (daytime data; Table 2.2). In contrast, the downstream site—W3 experienced multiple periods of hypoxia, sometimes even in the daytime (Figure A2.3). Pre-upgrade, SOC was significantly greater at the downstream Wascana Creek sites (W2 and W4) when compared to W1 (ANOVA $F(5,14) = 35.0$, $p < 0.0001$; TukeyHSD $p < 0.0001$). Pre-upgrade DO was significantly greater at W4 than W1 (ANOVA $F(5,15) = 14.1$, $p < 0.0001$; TukeyHSD $p < 0.0001$), while pH was significantly lower (closer to neutral) at W2 and W3 than at W1 (ANOVA $F(5,20) = 60.9$, $p < 0.0001$; TukeyHSD $p < 0.0001$). Pre-upgrade, conductivity was significantly greater at W2, W3, and W4 when compared to W1 (ANOVA $F(5,20) = 4.80$, $p < 0.01$; TukeyHSD $p < 0.05$).

Table 2.2 Water chemistry and sediment parameters at all sample sites (May 2016–August 2016) prior to the Regina WWTP upgrade. Values shown are averages with standard deviation below in parentheses.

Site	TAN[§] (mg L^{-1})	NH_3–N (mg L^{-1})	NO_3–N (mg L^{-1})	Urea–N (mg L^{-1})	TDN (mg L^{-1})	DOC (mg L^{-1})	DO (%)	pH	Conductivity (µS cm^{-1})	SOC (%)
W1	0.05 (0.06)	0.002 (0.002)	0.02 (0.04)	0.02 (0.01)	1.02 (0.30)	12.07 (2.99)	90.23 (10.2)	8.03 (0.24)	1219 (421.3)	3.08 (0.23)
W2	**8.18**[†] (5.41)	**0.079**[†] (0.054)	**3.31**[†] (4.6)	**0.10**[†] (0.05)	**10.11**[†] **(8.38)**	9.00 (4.73)	108.03 (13.3)	**7.22**[†] (0.14)	**1899**[†] (545.8)	**5.07**[†] (0.22)
W3	**6.29**[†] (3.98)	**0.073**[†] (0.049)	**2.81**[†] (3.81)	0.06 (0.04)	5.80 (4.25)	9.38 (4.72)	81.63 (26.9)	**7.29**[†] (0.21)	**1786**[†] (763.7)	2.46 (1.28)
W4	1.42 (3.10)	0.127 (0.242)	**4.69**[†] (2.73)	0.05 (0.03)	5.82 (5.58)	9.52 (4.84)	**125.73**[†] (14.4)	8.14 (0.13)	**1662**[†] (396.3)	**0.42**[†] (0.24)
QA1	0.01 (0.01)	0.001 (0.001)	0.17 (0.41)	0.17 (0.08)	0.95 (0.19)	11.65 (3.24)	128.70 (27.8)	8.36 (0.09)	1529 (135.8)	2.26 (0.19)
QA2	0.34 (0.68)	0.028 (0.047)	**2.09**[‡] (2.70)	0.12 (0.06)	3.32 (3.31)	9.98 (5.22)	113.00 (20.2)	8.11 (0.08)	1646 (161.0)	1.74 (0.14)

[†]Denotes significant differences between Wascana Creek site W1 and downstream sites W2, W3, and W4 pre-upgrade. [‡]Denotes significant differences between Qu'Appelle River site QA1 and downstream site QA2 pre-upgrade. Statistical test performed (ANOVA, Tukey post hoc $p < 0.05$ [Bonferroni corrected]). [§]TAN consists of both NH_4^+ and NH_3

Comparing post-upgrade to pre-upgrade conditions, TAN concentrations were dramatically reduced from 8.18 to 0.23 mg TAN L^{-1} at W2 (ANOVA $F(11,56) = 15.0$, $p < 0.0001$; TukeyHSD $p < 0.001$) and at W3 from 6.26 to 0.51 mg TAN L^{-1} (ANOVA $F(11,56) = 15.0$, $p < 0.0001$; TukeyHSD $p < 0.05$) (Table 2.3). Post-upgrade NH_3 concentrations were significantly reduced from 0.079 to 0.003 mg NH_3–N L^{-1} at W2 (ANOVA $F(11,33) = 4.43$, $p < 0.0001$; TukeyHSD $p < 0.05$) and from 0.073 to 0.006 mg NH_3–N L^{-1} at W3 (ANOVA $F(11,33) = 4.43$, $p < 0.0001$; TukeyHSD $p < 0.05$; Table 2.3, Figure A2.4). While NH_3 concentrations decreased at W2 and W3, time series plots do not suggest pH caused those reduced values as pH values did not significantly change (ANOVA $F(11,47) = 12.7$, $p > 0.05$; Figure A2.5). Nitrate, TDN, DOC, and DO concentrations did not significantly change following the upgrade across all sites ([NO_3^-: ANOVA $F(11,56) = 19.7$, $p < 0.0001$; TukeyHSD $p > 0.05$)], [TDN: ANOVA $F(11,63) = 0.31$, $p > 0.5$], [DOC: ANOVA $F(11,35) = 2.18$, $p < 0.05$; TukeyHSD $p > 0.05$], [DO: ANOVA $F(11,63) = 0.011$, $p > 0.5$]; Table 2.3). Urea was only significantly lower at QA1 (ANOVA $F(11,56) = 6.02$, $p < 0.0001$; TukeyHSD $p < 0.001$).

Table 2.3 The difference between mean post-upgrade and pre-upgrade concentrations of NO_3^-, TAN, NH_3, urea, TDN, DOC, and DO (i.e. Post-upgrade–Pre-upgrade). Mean post-upgrade values are in parentheses. A negative value indicates that post-upgrade values were lower than pre-upgrade values. To account for seasonal variability pre-upgrade values were compared to post-upgrade values during the same summer period (i.e. Pre-upgrade: May 2016–August 2016 vs. Post-upgrade: May 2017–August 2017).

Site	NO_3–N (mg L^{-1})	TAN (mg L^{-1})	NH_3–N (mg L^{-1})	Urea–N (mg L^{-1})	TDN (mg L^{-1})	DOC (mg L^{-1})	DO (%)
W1	0.016 (0.04)	–0.02 (0.03)	0.001 (0.003)	0.04 (0.06)	1.03 (2.05)	–1.03 (11.04)	13.75 (103.98)
W2	1.33 (4.64)	**–7.95*** (0.23)**	**–0.08* (0.003)**	0.1 (0.20)	–5.79 (4.32)	–3.49 (5.52)	12.82 (120.85)
W3	0.73 (3.54)	**–5.78* (0.51)**	**–0.07* (0.006)**	0.14 (0.20)	–0.38 (5.41)	–0.77 (8.61)	49.00 (113.60)
W4	–3.24 (1.45)	–1.29 (0.13)	–0.12 (0.006)	0.05 (0.10)	–3.03 (2.79)	–0.23 (9.29)	–2.76 (122.97)
QA1	–0.13 (0.04)	0.008 (0.02)	0.0001 (0.001)	**–0.15*** (0.02)**	–0.36 (0.59)	–5.19 (6.46)	–20.90 (107.78)
QA2	–1.55 (0.54)	–0.26 (0.08)	–0.02 (0.007)	–0.07 (0.05)	–1.99 (1.33)	–3.24 (6.74)	–10.42 (102.58)

*Denotes Bonferroni corrected $p \leq 0.05$
***Denotes Bonferroni corrected $p \leq 0.001$

2.3.2 Denitrification Activity—Variation in Space and Time

Denitrification rates at the impacted sites were significantly higher than at the control sites (ANOVA $F(5,51) = 25.0$, $p < 0.0001$; TukeyHSD $p < 0.005$). The most immediate downstream site, W2, showed the highest average denitrification rates of 5.9 x 10^{-1} μg N g^{-1} h^{-1}—rates over 1000-fold higher than the upstream control site, but the denitrification rates decreased with distance from the effluent (W2 > W3 > W4; Figure 2.3). Rates at QA2 exhibited high variability and were not significantly different from Wascana Creek impact sites W3 and W4 (ANOVA $F(5,51) = 25.0$, $p < 0.0001$; TukeyHSD $p > 0.1$). Denitrification rates did not significantly change between the between the pre and post upgrade periods (May–August 2016 vs. May–August 2017; ANOVA $F(11, 51) = 0.904$, $p > 0.5$, TukeyHSD $p > 0.5$; Figure 2.2). Both control sites (W1 and QA1) had the lowest mean denitrification rates throughout the study 5.0 x 10^{-4} μg N g^{-1} h^{-1} and 1.0 x 10^{-2} μg N g^{-1} h^{-1}, respectively, and were not statistically significant from each other (ANOVA $F(5,51) = 25.0$, $p < 0.0001$; TukeyHSD $p > 0.1$; Figure 2.3).

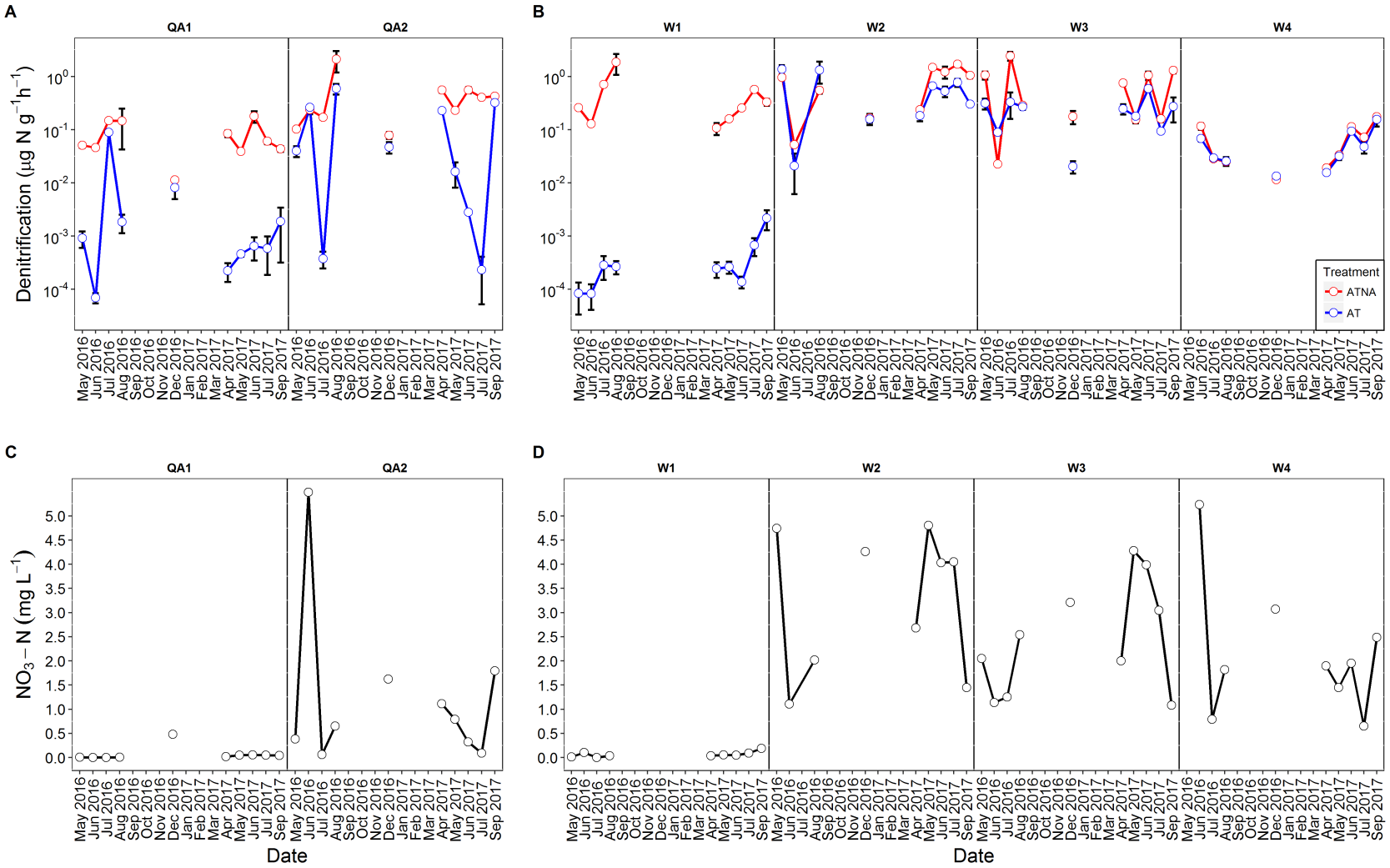

Figure 2.2 Mean potential denitrification rates (μg N g^{-1} h^{-1}) for C_2H_2-treated (AT) and C_2H_2-treated and NO_3^--amended (ATNA) samples as well as NO_3^- concentrations (mg NO_3–N L^{-1}) throughout the study (gaps represent the period where sampling did not occur). Panels A and C correspond to both sites on Qu'Appelle River. Panel B and D correspond to the four sites on Wascana Creek. Displayed error bars for panels A and B are the standard error of the triplicate denitrification samples for each experiment (for samples with small standard error, the bars may be covered by the data points); y-axis is a base-10 log scale.

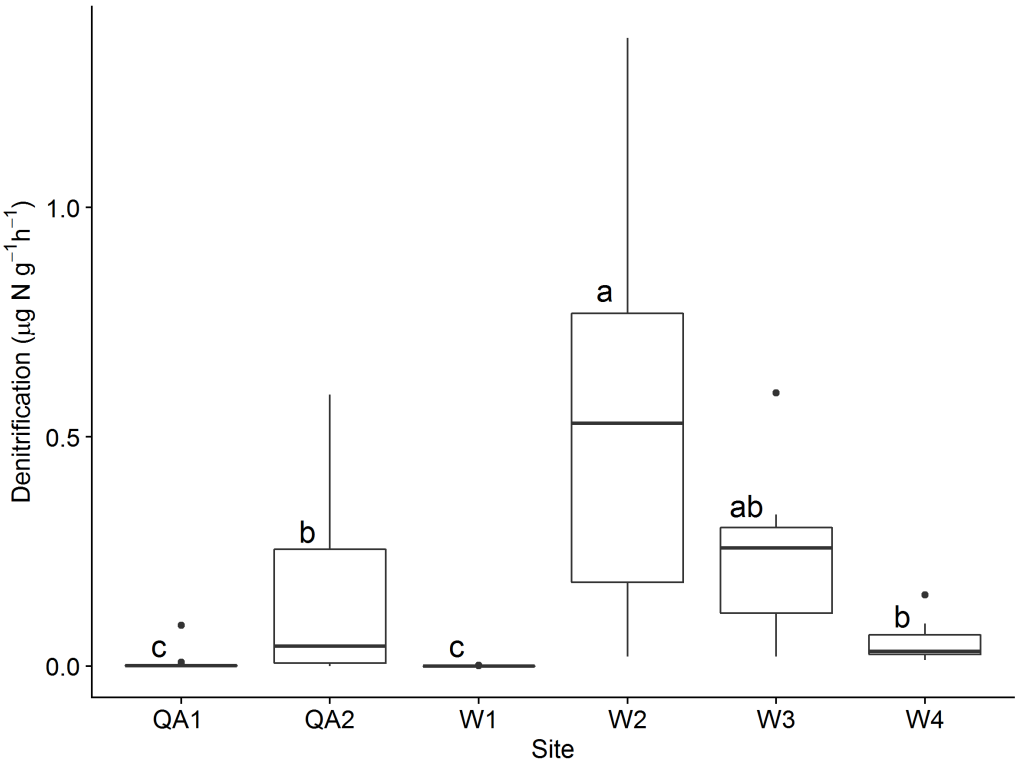

Figure 2.3 Potential denitrification rates (AT; µg N g^{-1} h^{-1}) across six sample sites for the period from May 2016-September 2017. Significant differences in rates are indicated with different letters (those with the same letter are not significantly different from each other; ANOVA F(5,51) = 25.0, p < 0.0001; TukeyHSD p < 0.05). The boxplot and whiskers encompass 95% of the data observed where the outliers are represented as dots, inside the box are the first and third quartiles with the median represented as the center line.

2.3.3 Denitrification Potential and Evidence of Nitrate Saturation

Impacted sites on Wascana Creek (W2 and W4) exhibited NO_3^- saturation (W2: *t*-test(8) = 1.67, $p > 0.1$; W4: *t*-test(8) = 2.04, $p > 0.1$). There was no significant difference between the ATNA and AT treatments, thus denitrification was NO_3^--saturated under ambient conditions. Although W3 and QA2 did not statistically demonstrate NO_3^- saturation throughout the study (W3: *t*-test(9) = 2.49, $p < 0.05$; QA2: *t*-test(9) = 3.22, $p < 0.01$ there were several periods that showed evidence of NO_3^- saturation (Figure 2.2; Figure A2.6). Neither control site showed evidence of NO_3^- saturation (W1: *t*-test(8) = 16.0, $p < 0.0001$; QA1: *t*-test(9) = 6.23, $p < 0.001$) at any point in the study. The potential denitrification rate (ATNA samples) appears to vary spatially, with W1 and W4 exhibiting significantly lower median potential denitrification rates (Figure 2.4) than W2 and W3. QA2 also showed a higher median potential denitrification rate than the upstream QA1 site (Figure 2.4).

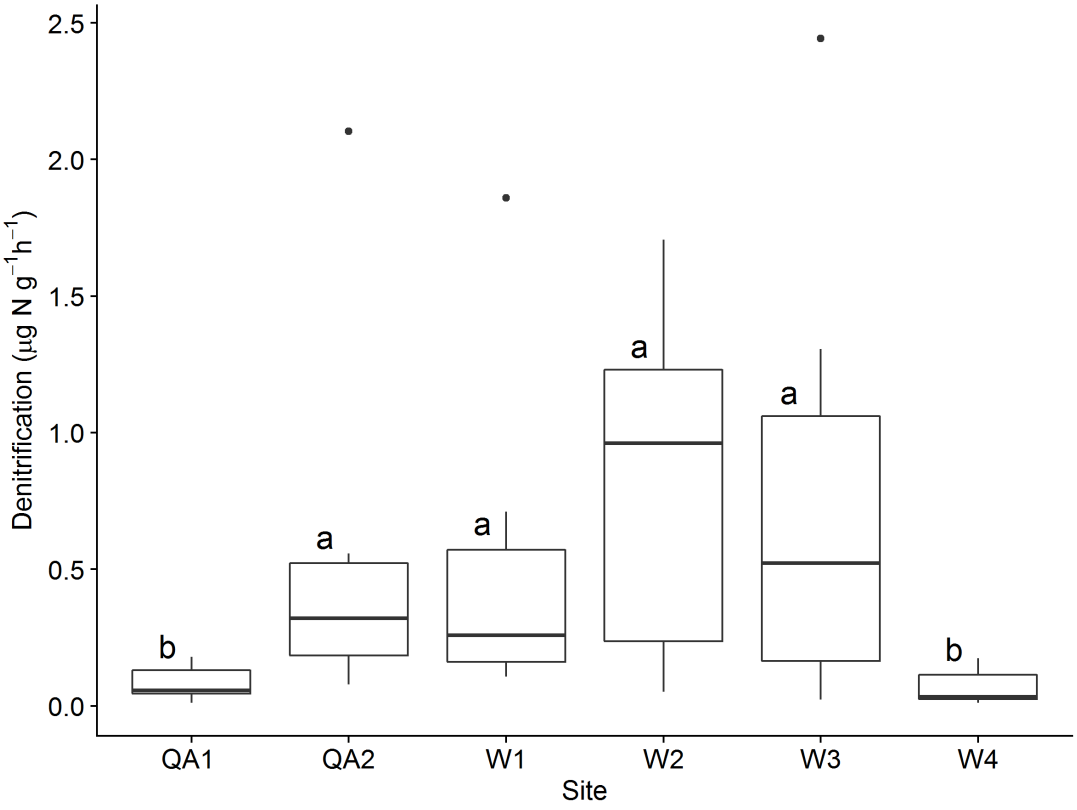

Figure 2.4 Potential denitrification rates (ATNA; µg N g^{-1} h^{-1}) across six sample sites for the period from May 2016-September 2017. Significant differences in rates are indicated with different letters (those with the same letter are not significantly different from each other; ANOVA $F(5,51) = 8.52$, $p < 0.0001$; TukeyHSD $p < 0.05$). The boxplot and whiskers encompass 95% of the data observed where the outliers are represented as dots, inside the box are the first and third quartiles with the median represented as the center line.

The kinetics of denitrification rates (AT) were assessed at two contrasting sites on Wascana Creek—W1 (control: upstream of effluent) and W3 (impact: second site downstream of the effluent)—to assess differences in their responses to enhanced substrate availability at finer intervals than tested using a potential denitrification assay. A Michaelis-Menten type curve was observed for W1 sediment with observed V_{max} and K_m values of 7.0 x 10^{-5} µg N g^{-1} h^{-1} and 1.47 mg NO_3–N L^{-1}, respectively (Figure 2.5). W3 did not reach a point of saturation (under the same range of NO_3^- concentrations), with a linear relationship observed across the range of NO_3^- concentrations.

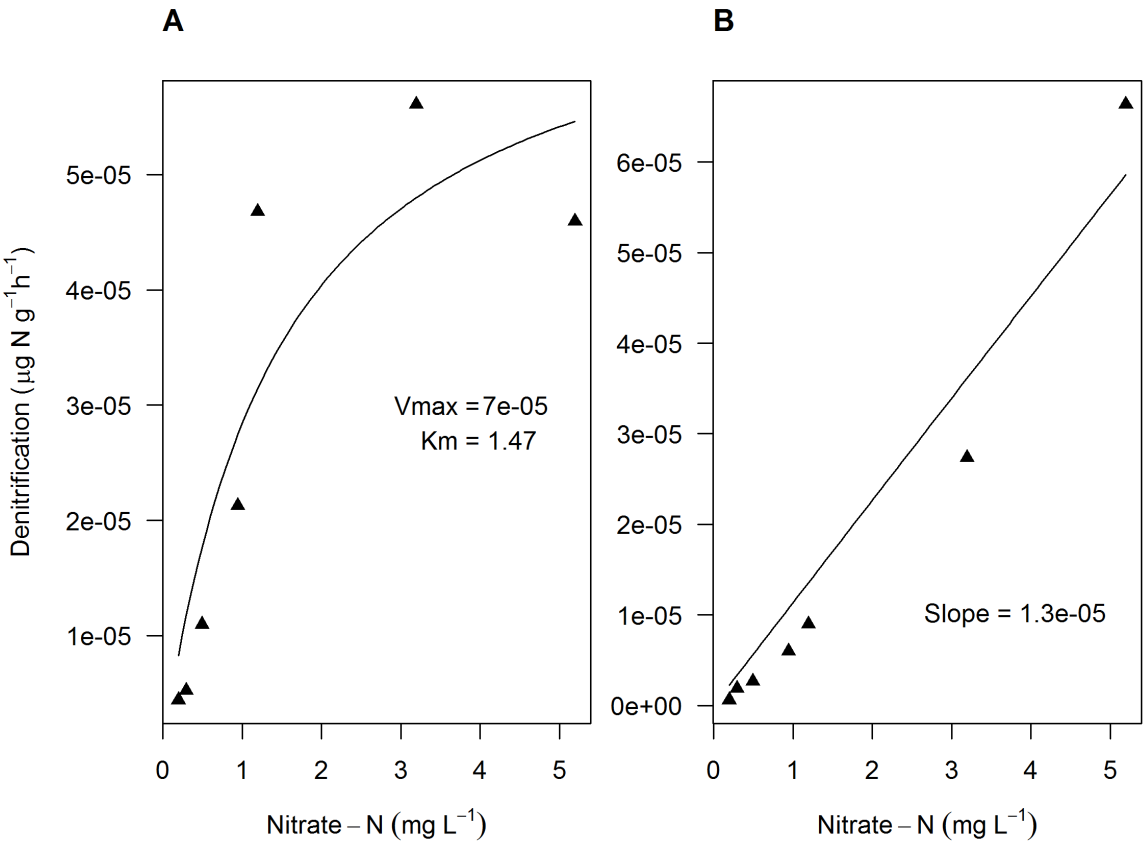

Figure 2.5 Dose-response curve of (NO_3^--denitrification) from Wascana Creek control site W1 (A) and impacted site W3 (B) displaying the change in denitrification rate (µg N g^{-1} h^{-1}) as a function of NO_3^- concentrations (mg NO_3–N L^{-1}). The kinetic parameters V_{max} and K_m are in units of µg N g^{-1} h^{-1} and mg NO_3–N L^{-1}, respectively.

2.3.4 Predictors of Denitrification Rates

Denitrification rates were significantly related to some chemistry parameters (Table 2.4, Figures A2.7–12). Strength of correlations are defined as weakly ($\rho \geq 0.30$), moderately ($\rho \geq 0.50$), and highly ($\rho \geq 0.70$) correlated. Denitrification rates were highly, positively correlated with NO_3^- concentrations (Spearman rank correlation, $\rho = 0.77$, $p < 0.001$, while moderately, negatively correlated with pH ($\rho = -0.60$, $p < 0.001$ (as conditions became more basic, denitrification activity decreased). There was no significant correlation between denitrification rates and SOC ($\rho = 0.036$, $p = 0.79$) or DOC ($\rho = -0.083$, $p = 0.51$).

Table 2.4 Multiple correlations between denitrification rates (μg N g^{-1} h^{-1}) and chemical parameters. The numbers represent the Spearman rank correlation coefficient rho (ρ), which signifies the strength of the monotonic correlation.

NO_3^- (mg L^{-1})	SOC (%)	pH
0.77***	0.04	–0.60***

***Denotes Bonferroni corrected $p \leq 0.001$

2.4 Discussion

In this study, I capitalized on a novel opportunity to assess how a WWTP upgrade impacted water quality and in-stream denitrification rates in two rivers. In the fifteen months following the upgrade, marked improvements in water quality were seen. Specifically, concentrations of NH_4^+ and NH_3 decreased by over an order of magnitude at the impact site closest to the WWTP effluent, W2. While this study was motivated by questions about how changing N loads might affect in-stream N attenuation via denitrification, I observed no effect of the upgrade, or changing river conditions, on denitrification rates, likely due to the lack of impact of the upgrade on NO_3^- concentrations. Instead, the effluent continued to stimulate elevated denitrification rates, with N removal via this process by up to 1200 times higher than control sites.

2.4.1 Water Quality

The Regina WWTP effluent strongly impacted water quality in the effluent dominated Wascana Creek both before and after the upgrade, while the effects at the larger Qu'Appelle River were more subtle. Nutrient concentrations (NO_3^-, TAN, and TDN) were highest at the downstream Wascana Creek sites (W2, W3, and W4); however, concentrations were often much lower in Qu'Appelle River. Because of these high nutrient loadings in the Wascana Creek, hypoxic/anoxic zones formed at Wascana Creek site W3. In one effluent-impacted system, it took O_2 concentrations > 160 km to recover back to O_2 values observed upstream of the outflow (Ramalho 1977).

Nitrate, TAN, and TDN concentrations were significantly elevated downstream of the WWTP which is consistent with many studied effluent-impacted systems (Andersen et al. 2004;

Ekka et al. 2006; Popova et al. 2006; Migliaccio et al. 2007; Toyoda et al. 2009). However, in Wascana Creek, TAN concentrations incrementally decreased downstream of the WWTP (W2 > W3 > W4) during the pre-upgrade period, likely reflective of biological assimilation of NH_4^+ into algal, plant, and bacterial biomass (Wester et al. 2003, Gammons et al. 2011). No significant change in NO_3^- concentrations were seen, despite evidence of increased NO_3^- concentrations in effluent (Kayla Gallant, personal communication, November 20, 2018; Figure A2.2). Although a realized goal of the WWTP upgrade was the reduction of NH_3 released in its effluent, the lack of change for in-stream NO_3^- concentrations is interesting and may reflect a variety of factors altering nitrification rates, denitrification rates, other NO_3^- sinks such as algal uptake, along with changes in effluent NO_3^- loads. While nitrification rates could decrease due to lower NH_4^+ concentrations, it appears this was not sufficient to impact in-stream NO_3^- concentrations. This raises important questions about whether nitrification rates are substrate limited or whether other NO_3^- sinks dominate in-stream processing.

An important topic when discussing TAN concentrations is the equilibrium of NH_4^+ and NH_3. The proportion of NH_3:NH_4^+ that comprises TAN depends on both pH and temperature (Jofre and Karasov 1999; Environmental Protection Agency 2013); increasing temperature by 5°C can cause a 40–50% increase while increasing pH (more alkaline) by one unit leads to an order of magnitude increase from pH 6.0–9.0 (Environment Canada 1999; Canadian Council of Ministers of the Environment 2010). Since the pKa of NH_3 is ~9.5 at 15°C, an increase in pH from 8.5 to 9.5 results in an increase from 7.97% NH_3:NH_4^+ to 46.4% NH_3:NH_4^+, while an increase in temperature (at constant pH 8.5) from 15°C to 25°C results in an increase from 7.97% NH_3:NH_4^+ to 15.3% NH_3:NH_4^+ (Emerson et al. 1975; Perrin 1982). The freshwater quality guideline for NH_3 in Canada is set at 0.019 mg L^{-1} but ranges up to 0.063 mg L^{-1} depending on the organism, with larger organisms, such as fish, being more susceptible to toxicity (Canadian Council of Ministers of the Environment 2010). The calculated pre-upgrade average for the Qu'Appelle River impact site surpassed the lower limit (QA2: 0.028 mg NH_3–L^{-1}) and all Wascana Creek impact sites surpassed the upper limit (averages of W2: 0.079, W3: 0.073, and W4: 0.127 mg NH_3–L^{-1}). At these high concentrations, NH_3 has been shown to become toxic to both vertebrates and invertebrates (Environment Canada 1999). Fortunately, the WWTP upgrade successfully reduced NH_3 concentrations below these possibly lethal values, causing average post-upgrade NH_3

concentrations to decrease significantly below the lower suggested limit of 0.019 mg L^{-1} across all impacted sites (W2: 0.003, W3: 0.006, W4: 0.006, and QA2: 0.007 mg NH_3–L^{-1}). The large decline in effluent TAN drove the decline in NH_3. The pH—a major control on the proportion of NH_3 in the TAN pool—did not change (ANOVA $F(11,47) = 12.7$, $p > 0.05$; Figure A2.5).

2.4.2 Temporal and Spatial Changes in Denitrification Rates

Denitrification rates were relatively stable throughout the upgrade process—unaffected by the reduced N loads, likely because NO_3^- concentrations were unaffected, and other environmental variables such as DO did not appear to change. It should be noted that the sampling campaigns occurred during the day, which is important when discussing the timescale of DO as concentrations vary greatly over 24h periods (lowest overnight) while nutrient concentrations remain relatively constant. While denitrification rates did not change through time, they did vary across sites. The highest rates were observed downstream of the WWTP on Wascana Creek. Denitrification rates at the downstream sites were nearly 1200 times higher on Wascana Creek (W2 vs W1) and nearly 20 times on Qu'Appelle River (QA2 vs QA1). Clearly the discharged effluent created conditions to strongly stimulate NO_3^- removal. Although in-stream NO_3^- concentrations did not change significantly post-upgrade at our downstream sites, directly sampled effluent appeared to have increased post-upgrade (Kayla Gallant, personal communication, November 20, 2018; Figure A2.2). Since there was no observed change of in-stream NO_3^- concentrations or denitrification rates there could be substantial assimilation of NO_3^- into biomass downstream between the effluent outfall and W2 (~200 m); however, future studies may look to assess assimilation of NO_3^- into biomass. Although agricultural inputs may contribute NO_3^- concentrations in both riverine systems, surface inflows are generally minimal across sites.

Denitrification activity exhibited a strong positive correlation with NO_3^- concentrations consistent with past work in other nutrient rich systems (Bradley et al. 1995; Herrman et al. 2008; Thuan et al. 2017). I acknowledge that the in-stream NO_3^- concentrations were sampled from the water column and were not porewater samples. Because denitrifying bacteria most likely utilize porewater NO_3^-, future studies may look to obtain porewater nutrient chemistry to build the denitrification/ nutrient relationship. However, it is likely that overlying NO_3^- concentrations are rapidly transported into the sediment, but future studies may aim to sample both the water column

and porewater (Van Kessel 1978; Garcia-Ruiz et al. 1998). Denitrification rates were also correlated with pH, an effect that appears to be related to spatial changes in pH associated with the effluent (Figure A2.13). Denitrification rates were highest at the two downstream sites closest to the effluent (W2, W3), where pH was depressed (closer to a neutral pH of 7). However, denitrification rates were lowest where pH was higher (W1, W4, and at the Qu'Appelle River sites). Ultimately, the impact of spatial changes in NO_3^- concentrations was likely more important than the potential role of pH change in influencing denitrification rates, particularly within the observed pH range, which is near the optimal range of 7 to 8.5 (Van Cleemput and Patrick 1974; Davies and Pretorius 1975; Müller et al. 1980). Although denitrification rates were not correlated with SOC, future studies may look to compare porewater DOC concentrations to rates of denitrification as denitrifying bacteria most likely utilize porewater DOC for their C source (Martin et al. 2001).

2.4.2.1 Nitrate Saturation and Kinetics

While NO_3^- saturation has been reported across a wide range of sewage and agriculturally impacted systems, few studies have described Michaelis-Menten kinetics of denitrification in lotic systems (Garcia-Ruiz et al. 1998; Figueroa-Nieves et al. 2016). Interestingly, these studies exhibited extremely high variation, with K_m values as low 1.0 mg NO_3–N L^{-1} in an agricultural, headwater stream (Herrman et al. 2008) to as high as 9.0 mg NO_3–N L^{-1} in an urban, sewage-effluent system (Garcia-Ruiz et al. 1998). In this study, K_m for the upstream, Wascana Creek control site (W1) was 1.47 mg NO_3–N L^{-1} (105 µM) based on Michaelis-Menten experiments. This is considerably higher than the threshold for NO_3^- saturation reported for prairie agricultural streams (0.68 mg NO_3–N L^{-1}), although similar values were reported for small agriculturally influenced reservoirs (1.38 mg NO_3–N L^{-1}; Gooding and Baulch 2017). While K_m was not determined at W3 with NO_3^- concentrations as high as 5.20 mg L^{-1}, saturation events occurred under lower in-stream concentrations. Importantly, the threshold for these NO_3^--saturation events appear to vary through time. For example, at one point in time W3 exhibited saturation at NO_3^- concentrations as low as 1.14 mg L^{-1} but at another point in time W3 did not exhibit NO_3^- saturation with in-stream concentrations as high as 4.28 mg NO_3–N L^{-1} (Figure 2.2). Effluent dominated rivers are known to be highly dynamic in terms of NO_3^- availability, O_2, and C

concentrations (Bradley et al. 1995), thus it should not be surprising that the kinetics of denitrification could vary markedly through time. However, this is clearly an area where more work is required to understand dynamics of change and support modelling of this key, but highly dynamic NO_3^- removal process.

Nitrate saturation—where NO_3^- concentrations were not limiting denitrification rates—may be considered an indicator of poor ecological status (Gooding and Baulch 2017). Continued NO_3^- saturation occurred following the upgrade (e.g., W2 and W4). Nonetheless, there are some indications that recovery may be underway. At site W2, denitrification rates for AT samples appear to incrementally decrease relative to ATNA samples after December 2016, and the site did not experience NO_3^- saturation again for the remainder of the study. Given the lack of change in NO_3^- concentrations in the system following the upgrade, more work is required to understand whether a change is occurring, and the potential drivers of that change. Interestingly, the risk of NO_3^- saturation was highest at the furthest downstream site on Wascana Creek, W4, which was consistently NO_3^--saturated. This appears to be due to the low SOC in the sandy sediments of this site, as this is known to limit potential denitrification rates (Evrard et al. 2013). In the downstream Qu'Appelle River, NO_3^- saturation at QA2 seemed to co-occur with periods of elevated NO_3^- concentrations. However, more work to fully understand the process under changing hydrological conditions is warranted.

2.4.3 Seasonality

Although denitrification is optimal at temperatures ranging from 18–35°C (Brin et al. 2017), with temperatures below 10°C shown to reduce denitrification rates (Davies and Pretorius 1975; Martin et al. 2001), the studied sites did not exhibit this seasonality. Denitrification rates varied markedly over time, but the coldest sampling date in December was often associated with intermediate rates (e.g. W2, QA1, and QA2). Interestingly, recent work in prairie lakes under ice suggests that denitrification rates remain relatively constant through winter and summer, associated with hierarchical control of denitrification rates—controlled first by NO_3^- concentrations, then by temperature (Cavaliere and Baulch 2018), suggesting that in this NO_3^--rich environment, denitrification remains an important N sink year-round. Questions of seasonality of denitrification rates remain important, as variable seasonal patterns appear widespread

(Christensen and Serrensen 1988; Holmes et al. 1996; Arango and Tank 2008; Grantz et al. 2012), but the importance of NO_3^- removal via denitrification in many ecosystems will be closely tied to hydrology and seasonal changes in flow and concentrations.

2.5 Conclusion

This work illustrates the very large impact that WWTP effluent can have on in-stream denitrification rates in a wastewater dominated stream. This includes increases in denitrification rates at impacted sites of up to 1200-fold as compared to upstream sites along with large differences in the potential denitrification rates under NO_3^--amended conditions between downstream and upstream sites. Given that effluent quality affects the ecosystem service of in-stream NO_3^- removal, this raises interesting questions about whether engineering design should consider ways to maximize in-stream nutrient removal in effluent-dominated ecosystems, for example, considering factors such as managing benthic substrates, O_2, or the C and N stoichiometry of the effluent to help maximize in-stream denitrification rates.

Within effluent dominated streams, even upgrades using advanced technology do not mitigate all impacts. Herein I observed significant and immediate improvements in water quality with the decrease in concentrations of TAN and NH_3—a major design goal of the upgrade. However, in-stream NO_3^- concentrations did not change substantively following the plant upgrade despite large decreases in NH_3 and TAN concentrations and an apparent increase in NO_3^- in the effluent in the study season (Kayla Gallant, personal communication, November 20, 2018; Figure A2.2). The lack of change in NO_3^- concentrations likely explains the absence of change in denitrification rates following the upgrade. Denitrification rates were very strongly stimulated downstream of the effluent (e.g., 1200 fold increase from W1 to W2).

2.6 Acknowledgements

I would like to acknowledge the SaskWatChe (Saskatchewan Water Chemistry) lab group, specifically Kimberly Gilmour and Katy Nugent for their support with field expeditions, laboratory analyses, and experiments. I would like to acknowledge the National Sciences and Engineering Research Council (NSERC) of Canada's Collaborative Research and Training Experience Program for scholarship. Also, I want to acknowledge the NSERC Discovery Grant to HMB for funding, support of the Global Institute for Water Security, and the Centennial Enhancement Chair

Program, and start-up funding awarded to CJW at the U of S. Lastly, I would like to thank Dr. Vijay Tumber for assistance with experimental design though his past experience with the study area.

2.7 Author Contributions

NPD and BS performed the denitrification experiments and field work. NPD conducted the laboratory and statistical analyses. NPD was lead author on manuscript, with editing and commenting of thesis chapters provided by CJW and HMB. CJW and HMB also obtained funding for the research as well as provided knowledge for project design.

Chapter 3: THE DOWNSTREAM EFFECT OF A WASTEWATER TREATMENT PLANT UPGRADE ON NITROUS OXIDE

Dylla, N.P., Baulch, H.M., and C.J. Whitfield (2019). "The Downstream Effect of a Wastewater Treatment Plant Upgrade on Nitrous Oxide" Journal **Vol**(Issue): pg–pg.
Status: Prepared for Publication

3.0 Preface

Chapter 2 not only provided an in-depth view on the microbial process of denitrification and how the Regina WWTP effluent affected denitrification rates within Wascana Creek and Qu'Appelle River, but also demonstrated that denitrification rates were unaffected by the upgrade. Chapter 2 also identified possible controls on denitrification rates and showed that few parameters were affected by the upgrade process, although concentrations of TAN and NH_3 declined. Chapter 3 further investigates a greenhouse gas byproduct of nitrogen cycling—nitrous oxide (N_2O)—by measuring N_2O concentrations and estimating N_2O emissions associated with the Regina WWTP before and after its upgrade.

3.1 Abstract

Nitrous oxide (N_2O) is a powerful stratospheric ozone depleting chemical and potent greenhouse gas (GHG) emitted chiefly as a consequence of nitrification and denitrification. Because point-sources, such as wastewater treatment plants (WWTPs), can have significant impacts on downstream nutrient chemistry and biogeochemical cycling, I aimed to see how a WWTP upgrade, designed to improve effluent water quality and decrease un-ionized ammonia (NH_3) concentrations, impacted riverine N_2O emissions. In-stream N_2O concentrations were unaffected by the WWTP upgrade and were the highest values ever published for an aquatic system (up to 1.39×10^5 percent saturation), and extremely high areal emissions resulted downstream of the effluent outfall (up to 7.28×10^4 μmol N_2O–N m^{-2} d^{-1}). The N_2O impact zone, or the stream length over which 95% of N_2O originating in the WWTP effluent dissipated, spanned ~5 km of Wascana Creek. Because in-stream processes were consistently masked by supersaturated effluent at sites

within ~5 km of the WWTP, I did not observe correlations between N_2O concentrations and concentrations of dissolved oxygen (DO) or with rates of denitrification. Downstream of the WWTP, but outside of the N_2O impact zone, N_2O concentrations were correlated with nitrate (NO_3^-), total ammonia nitrogen (TAN), and denitrification rates. However, I found no significant changes in N_2O concentrations or emissions when comparing the pre-upgrade period to the post-upgrade period at both the impacted and non-impacted sites.

3.2 Introduction

Nitrous oxide (N_2O) is a potent greenhouse gas (GHG) ~300 times stronger than carbon dioxide (CO_2; GWP_{100}) that can persist in the atmosphere for more than 100 years (Khalil and Rasmussen 1992; Kanter et al. 2013; IPCC 2014). Over the last two centuries, N_2O concentrations increased by over 20% to a global atmospheric concentration of 330 ppbv (current preliminary data from NOAA and ESRL 2018). Nitrous oxide is produced through the aerobic process of nitrification, by which ammonium (NH_4^+) is oxidized to nitrate (NO_3^-)—producing N_2O as a side product, but also through the anaerobic process of denitrification, which reduces NO_3^- to inert, dinitrogen gas (N_2) with N_2O formed as an intermediate step (Wrage et al. 2001; Khalil et al. 2004; Laursen and Seitzinger 2004). Although the greatest anthropogenic N_2O emissions stem from these processes on land (associated with agriculture), both processes also occur in aquatic environments.

Even though treatment systems can vary greatly across nations, most developed countries employ closed, underground sewers that discharge into centralized wastewater treatment plants (WWTPs) (IPCC 2006). These treatment plants process incoming sewage with differing levels of treatment (primary, secondary, and tertiary/advanced) through the use of screens, chemical treatments and bacterial processors in order to create an effluent that can enter a receiving water body with minimal impact (Carey and Migliaccio 2009). However, even treated effluent often contains high concentrations of N compounds and high biochemical oxygen demand (BOD), which often cause receiving water bodies to experience stretches of anoxic zones (Fair 1939; Rosamond et al. 2012; Venkiteswaran et al. 2015). Before the stream is depleted of oxygen (O_2), nitrifying bacteria can consume O_2 and process the effluent NH_4^+ by oxidizing it to NO_3^-. During this aerobic conversion, N_2O can be produced as a byproduct. The rate of nitrification can be increased by higher NH_4^+ concentrations, pH, and temperature, but inhibited by lower O_2

concentrations (Antoniou et al. 1990; Kemp and Dodds 2002; Strauss et al. 2002; Starry et al. 2005). The nitrification N_2O yield, or N_2O:NO_3^-, can also be impacted by the aforementioned factors, with yields decreasing with increased temperature, NH_4^+ concentrations, pH, and O_2 (Goreau et al. 1980; Maag and Vinther 1996; Jiang and Bakken 1999; Khalil et al. 2004). Nitrification N_2O yields have generally been found to range from 0–0.37% (Eastern South Tropical South Pacific Oxygen Minimum Zone; Ji et al. 2015) but yields upwards of 15% (Marine sediment; Santoro et al. 2011) and 25% have been noted (Marine sediment; Jørgensen et al. 1984).

Denitrification is the anaerobic process that reduces NO_3^- to N_2 while producing N_2O in an intermediate step. Rates of denitrification can increase with increasing NO_3^- concentration, temperature, pH, and with decreasing O_2 concentrations (Martin et al. 2001; Herrman et al. 2008; Teixeira et al. 2010; Veraart et al. 2011). The denitrification yield, N_2O:N_2O+N_2, is known to increase with higher NO_3^- concentrations and to decrease with higher pH values (>7) (Cavigelli and Robertson 2000; Silvennoinen et al. 2008). Downstream of wastewater effluents, high rates of denitrification associated with anoxic conditions can lead to the formation of hotspots or hot moments of N_2O production in rivers; however, inflowing effluent can also contain high concentrations of N_2O (Smith et al. 1998; Canfield et al. 2010). Fortunately, WWTPs can be modified or upgraded to reduce the amount of nutrients they release into the receiving streams, rivers, lakes or oceans (IPCC 2006; Holeton et al. 2011), and these modifications may alter in-stream GHG production and emissions.

Typically, WWTPs deposit their treated waste into large water bodies, thereby allowing receiving systems to dilute, assimilate, and process the influx of nutrients. However, in the semi-arid Canadian prairies, freshwater is limited, hence smaller water bodies are sometimes used as receiving ecosystems even for large amounts of wastewater. Wascana Creek is a small, effluent-dominated system which receives the wastewater from the City of Regina, Canada. Flow can be up to ~100% treatment plant effluent (Waiser et al. 2011b), and high NH_3 concentrations have been a particular cause of concern, due to toxicological impacts (Environment Canada 1999; Jofre and Karasov 1999; Environmental Protection Agency 2013). Herein I investigate the impact of an upgrade to the Regina WWTP on N_2O concentrations and emissions from Wascana Creek and the downstream Qu'Appelle River using a before-after-control-impact (BACI) design. This design not only compares upstream "control" sites to impact sites, but it also allows for them to be assessed

through time, before and after the upgrade. Therefore, this study addressed the following questions: 1) Does the WWTP cause an increase in downstream N_2O concentrations and emissions? 2) Does the WWTP upgrade cause a significant reduction in N_2O concentrations and emissions downstream 3) Is there a significant correlation between chemical factors (NO_3^-, TAN) or denitrification rates and N_2O concentrations? 4) Do physicochemical factors (urea, NO_3^-, TAN, total dissolved nitrogen [TDN], DO, pH, and temperature) and N_2O follow a diel pattern?

3.3 Materials and Methods

3.3.1 Study Area

Wascana Creek begins southeast of Regina, Saskatchewan, Canada where it flows northwest and eventually enters the Qu'Appelle River near Lumsden, Saskatchewan (Figure 3.1). These riverine systems drain from their own respective watersheds into the larger Assiniboine watershed. Wascana Creek is a smaller riverine system as compared to the larger, wider, and deeper Qu'Appelle River. Wascana Creek has an effective drainage area of 1740 km^2, while the Qu'Appelle River effective drainage area upstream of the study sites is 6950 km^2 (Environment Canada 2017). Flow on Wascana Creek is naturally low which, combined with meandering through low creek walls, allows the build-up of ~6 mm of sediment per year (Waiser et al. 2011b). Annual flow in Qu'Appelle River is much greater with an average rate of 6.3 $m^3 s^{-1}$ as compared to 2.4 $m^3 s^{-1}$ for Wascana Creek (Environment Canada 2017b; a). Both systems are surrounded by agricultural fields featuring wheat, barley, and oat crops with cattle grazing the low-land pastures. Wascana Creek flows through the City of Regina (pop. 215,000; Statistics Canada 2016) and receives effluent from the Regina WWTP.

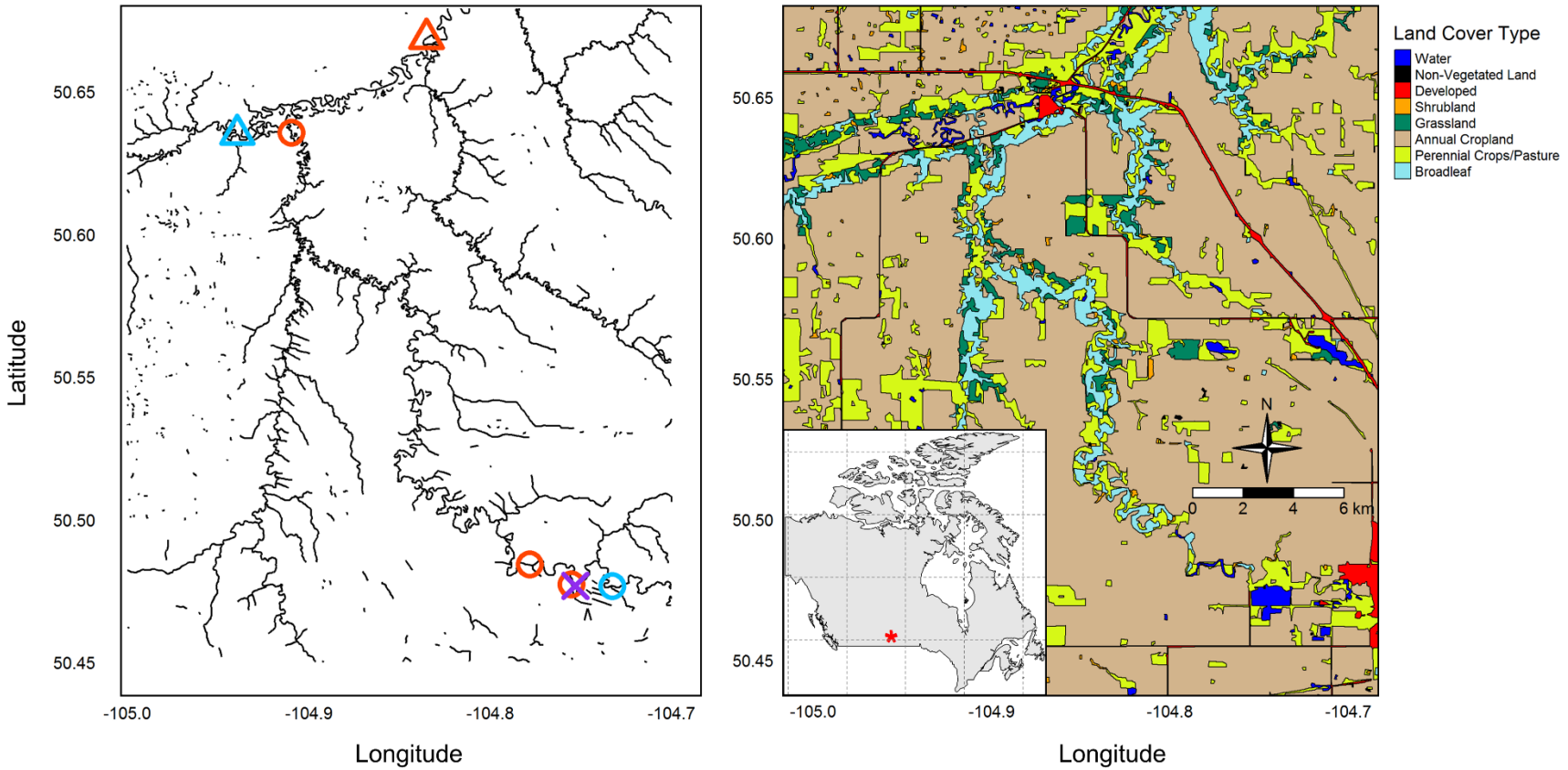

Figure 3.1 Left, a riverine network map of the study region with the study sites on Wascana Creek (circles) and Qu'Appelle River (triangles) both upstream (blue) and downstream (red) of the Regina WWTP (purple cross). Right, a land cover map for the surrounding study area. Data was obtained from (Government of Canada and Agriculture and Agri-Food Canada 2018; Government of Canada and Natural Resources Canada 2018).

The semi-arid climate in southern Saskatchewan exhibits strong seasonality, with relatively long, cold winters and warmer summers with shorter shoulder seasons. The region has a Köppen climate classification of BSk/Dfb (Köppen and Geiger 1936). Monthly average air temperature varies from highs in the month of July (19.1°C) to lows in January (–16.5°C). The Qu'Appelle River and Wascana Creek generally freeze in November, with ice cover thawing in March/April, shortly before maximum stream discharge. A short reach downstream of the WWTP remains open through the winter months due to the warmer temperature of the effluent. Due to the seasonally semi-arid and cold climate, riverine systems in Saskatchewan can experience seasonal periods of low flow. Summer flows are low with transient peaks driven by large precipitation events. Average annual precipitation in Regina is 390 mm and potential evapotranspiration is greater than precipitation. Approximately 20% of precipitation falls as snow, while the majority of rain falls between April and August (Hammer 1971; Government of Canada 2017); however snowmelt is a disproportionately important contributor to runoff generation in the region. Wind velocities average 20.9 km h^{-1} with southeastern prevailing winds (Hammer 1971).

3.3.2 Study Sites

This study includes six regularly sampled sites on two riverine systems. Sites were chosen based on locations of previous water quality studies and include upstream (reference or 'control') and downstream (impact) sites for the BACI (before-after-control-impact) design. There are four sites situated on Wascana Creek: W1 (control: ~4 km upstream of the WWTP), W2 (impact: ~0.2 km downstream), W3 (impact: ~3.8 km downstream), and W4 (impact: ~60 km downstream). There are no significant inflows between W1 and W2 besides the WWTP effluent outflow (with an average pre-upgrade inflow of 71 ML d^{-1}). The Qu'Appelle River features two additional sites, QA1 (control: ~5 km upstream of the Wascana Creek confluence) and QA2 (impact: ~12 km downstream of the Wascana Creek confluence) (Figure 3.1). As part of the WWTP upgrade, N removal processes were operational in mid-August 2016 (the plant was substantially complete on December 19, 2016). As such, dates prior to August 11th, 2016 were considered part of the pre-upgrade period while dates after were considered post-upgrade due to the focus on N chemistry and N_2O emissions.

3.3.3 Water Chemistry

All six study sites were sampled twice monthly from thaw (March/April) to freeze-up (November/December) for water chemistry and dissolved gases. All sites were sampled on the same day between sunrise and sunset, although on rare occasions individual sites were not sampled because road closures prevented site access. A YSI Multi-Probe System 556 (YSI Environmental, Yellow Springs, Ohio) was used to measure dissolved oxygen (DO), pH, specific conductance, and temperature by wading into the middle of the creek/ river and placing the probe at mid-depth. Urea, NO_3^-, TAN, TDN, and dissolved organic carbon (DOC) were collected by grab sampling water at mid-depth from the middle of the creek/ river. Urea and NO_3^- were filtered and placed in 100 mL HDPE (high density polyethylene) bottles and frozen at –40°C, while TAN was filtered and acidified with 10% H_2SO_4 and then frozen at –40°C. Total dissolved N and DOC were filtered then refrigerated at 4°C. Urea, NO_3^-, and TAN were analyzed on a colorimetric auto-analyzer SmartChem 170 (WestCo Scientific Instruments, Inc.). Urea was measured in duplicate and analyzed with the phenol yellow method (Emmet 1969). Nitrate was measured in duplicate and analyzed following the copperized cadmium reduction followed by diazotization with sulfanilamide (Wetzel and Likens 1991; Unity Scientific SmartChem 2011a). This method includes the small amount NO_2^- in the analysis for NO_3^-; therefore, NO_3^- reported here is NO_2^- + NO_3^- (Johnston et al. 1990; Avanzino and Kennedy 1993; Baulch 2009). Total ammonia N (NH_4^+ + NH_3, but herein referred to as TAN) was measured in duplicate and analyzed using the indophenol blue method (Ministry of the Environment 2001; Unity Scientific SmartChem 2011b). Un-ionized ammonia (NH_3) was estimated from TAN concentrations and was dependent on in-stream temperature and pH (Emerson et al. 1975; Canadian Council of Ministers of the Environment 2010; Waiser et al. 2011b). Dissolved organic carbon was analyzed in duplicate on a Shimadzu TOC-L analyzer where samples were combusted (>680°C) and converted to CO_2 and analyzed using non-dispersive infrared (NDIR) detectors (ASTM International 2018). Total dissolved N was analyzed in duplicate on a Shimadzu TOC-L analyzer with TN module where samples were combusted (720°C) to nitrogen monoxide (NO), cooled by passing through a thermoelectric cooler, and analyzed via a chemiluminescence analyzer (ASTM International 2016). Total dissolved N consists of both dissolved organic nitrogen (DON; urea, proteins, amino

acids, etc.) as well as dissolved inorganic nitrogen (DIN; NO_3^-/NO_2^- and TAN). Since I measured both TDN and DIN species, DON was estimated as the difference between TDN and DIN.

3.3.4 Dissolved Gas Collection

Dissolved N_2O concentrations were sampled biweekly at all sites while direct, in-stream effluent was collected at the outflow of the WWTP (~10 m downstream) twice during this study; both campaigns utilized the headspace equilibration technique to extract N_2O from solution (Kampbell et al. 1989). Water for dissolved N_2O analysis was collected by wading upstream with an open ~1.1 L thick-walled glass bottle. The bottle was inverted (mouth facing the sediment), placed at half stream depth, and inverted again (mouth facing towards the surface) to fill. Once full, a rubber stopper, affixed with two tubes (air line and water line), was depressed into the bottle while ejecting the water it had displaced. Sixty mL of ambient air was then collected in a syringe and injected into the bottle to create a headspace; the displaced 60 mL water was simultaneously captured in a second syringe. The bottle was immediately shaken in the shade for two minutes to equilibrate dissolved gases with the headspace. Once equilibrated, duplicate 20 mL headspace samples were removed and stored in evacuated 5.9 mL double-wadded (chlorobutyl septum + PTFE/Silicon) gas Exetainers® (Labco Ltd, Lampeter, UK). Nitrous oxide concentrations were analyzed using a Scion 456 Gas Chromatograph (Bruker; Electron Capture Detector; injector and column temperature 60°C, detector temperature 350°C, and Ar carrier gas). Stream temperature was measured at time of sample collection (above). Ambient, local atmospheric N_2O concentrations were collected using a 20 mL syringe ~2 m above water level and stored in a 5.9 mL exetainer. Wind velocity (m s^{-1}) and barometric pressure (atm) were measured 2 m above water level using a handheld anemometer (Kestrel 5500).

3.3.5 Dissolved Nitrous Oxide Concentration

Percent (%) saturation was calculated using the concentration of N_2O in the stream (C_w) and the concentration of N_2O at equilibrium with local atmospheric pressure (C_s) as follows:

$$\%\ N_2O\ Saturation = [(C_w\ /\ C_s)] \times 100\% \quad (3.1)$$

where C_w (μmol m^{-3}) is the in-stream concentration of N_2O and C_s (μmol m^{-3}) is the concentration of N_2O when the stream is in equilibrium with the local atmosphere as determined by duplicate ambient air samples collected at each site through time (Table 3.1). C_s is dependent on stream temperature which was used to calculate the solubility of N_2O as follows (Liu et al. 2011; Audet et al. 2017).

$$C_s = H \times C_A \tag{3.2}$$

where C_A is the partial pressure (atm) of N_2O in the atmosphere calculated from the local, ambient atmospheric N_2O concentrations and barometric pressures (atm) for each site. The equilibrium constant, H (mol L^{-1} atm^{-1}), in moist air, was calculated from Henry's Law as follows (Weiss and Price 1980):

$$lnH = -165.8806 + 222.8743\left(\frac{100}{T}\right) + 92.0792\ln\left(\frac{T}{100}\right) - 1.48425\left(\frac{T}{100}\right)^2 \tag{3.3}$$

where T is the temperature (Kelvin) of the stream when the gas sample was collected.

3.3.6 Gas Transfer Velocity

The gas transfer velocity (k) is a physical component of an aquatic system that determines the rate of gas emitted from a system. Two approaches were used to quantify k. First, k_{N2O} was calculated from k_{O2} values (as described in 3.3.7) which were determined using the BASE model (Grace et al. 2015; Giling et al. 2018) as described in 3.3.6.1. Second, k_{N2O} was determined based on linear flux chamber measurements (Lambert and Fréchette 2005); see section 3.3.6.2.

3.3.6.1 BASE model—Dissolved Oxygen for Estimation of Gas Transfer Velocity

Diel variation in oxygen can be used for estimating the gas transfer velocity (Chapra and Di Toro 1991; McBride and Chapra 2005). Here, the reaeration coefficient (K; d^{-1}) and ultimately the gas transfer velocity (k; m d^{-1}) were estimated based on measured DO (mg O_2 L^{-1}) and temperature (°C) via HOBO sensors (Hoskin Scientific; U26-001 Data Logger) deployed at

Wascana Creek sites W1 and W3 periodically (~every 3 weeks) throughout the two-year study (Figure A3.1).

The R package "BASEmetab" and function "bayesmetab" (Grace et al. 2015) were used to analyze the DO curves for each day. This semi-automated method uses HOBO sensor-derived DO concentrations and temperature, photosynthetically active radiation (PAR), atmospheric pressure (atm) and salinity as the main input parameters into the BASE model in order to compute *K* for each daily DO observation. In this model, *K* is estimated through the use of Markov Chain Monte Carlo iterations (three-chains with 1000 iterations each) that fit the modeled DO series with the measured DO data. This model simultaneously estimates photosynthesis based on PAR data as well as *K* and ecosystem respiration which are both temperature dependent. PAR data (~1 m above surface; LI-COR LI-190), and average daily barometric pressure (~2 m above surface; Vaisala WXT520) were obtained from a station on a nearby reservoir (Buffalo Pound Lake). After visual inspection of each model run, the individual models were then assessed for goodness-of-fit through several recommended output checks (Figure A3.2; Giling et al. 2018).

3.3.6.2 Static Flux Chamber for Estimation of Gas Transfer Velocity

Static flux chambers have been used to establish a linear relationship between the build-up of gases and time in order to estimate *k* (Duchemin et al. 1998; Kremer et al. 2003; Lorke et al. 2015). Although chambers may overestimate the flux of gases into the chamber due to the artificial turbulence created by placing the chamber in flowing water, chambers employed for this study were designed to limit turbulence following the "flying chamber" design (Lorke et al. 2015; Figure A3.3). Herein, I deployed static flux chambers across a range of flow conditions and across all sites throughout the open-water season in 2017 (May–November). Chamber derived *k* values were calculated as described in Lambert and Fréchette (2005), where linear relationships of gas concentrations were built over the course of 45 mins. Criteria were established (linear relationship and $R^2 > 0.90$ and percent saturation > 200%) in order to filter out inaccurate or unreliable chamber measurements.

When comparing both the BASE modeled *k* values and chamber measured *k* values at sites W1 and W3 (where both HOBO sensors and chambers were deployed), broadly similar *k* values were observed during those periods (Figure A3.4). Although rarely was there direct overlap in

available measurements, BASE modeled *k* appeared higher than the results obtained from flux chamber measurements. Also, chamber measured *k* values were relatively similar across sites (Figure A3.5).

3.3.7 Nitrous Oxide Flux

Although *k* was modeled using diel DO curves over multiple periods, continuous measurements of DO throughout the duration of the study were not made. I assessed the potential to use semi-empirical models to scale *k* estimates in time by testing semi-empirical wind-driven models (Wanninkhof 1992; Cole and Caraco 1998; Raymond and Cole 2001; Laursen and Seitzinger 2005) and benthic turbulence driven models (O'Connor and Dobbins 1958; Churchill et al. 1962; Owens et al. 1964). Since depth measurements were not continuously recorded at these sites, the downstream Environment Canada gauging stations at W4 and QA2 were used to estimate changes in stream velocity (m s^{-1}) and stream depth (m). For sites without gauges (W1, W2, W3, and QA1) I built a linear curve based on depth measurements made at those sites, relative to depths recorded at the gauging stations. After several depth measurements were obtained at the un-gauged sites, depth curves were built for each un-gauged site based on the depths recorded at their relative downstream gauging site. Based upon several model validation metrics and individual visual inspection, none of the semi-empirical models tested performed adequately for this study system (Figure A3.6). Therefore, instead of relying on models, I opted to bound estimates based on the observed variation in *k*. Although in-stream DO concentrations were not continuously measured, they covered a wide range of flow conditions (Figure A3.1), hence are assumed to represent the range in *k* values within the ecosystem.

In brief, to estimate N_2O flux over time, I used the average BASE model *K* (d^{-1}) values (from sites W1 and W3), multiplied by stream depth (m), and applied these *k* values (m d^{-1}) across sites. The standard deviation (± 1 STD) of BASE model *k* values was used to help constrain variability across the range of conditions over the course of two years.

The depth dependent, DO modeled k_{O2} (m d^{-1}) was converted to the gas transfer velocity for N_2O (k_{N2O}) as follows (Wanninkhof 1992):

$$k_{N2O} = k_{O2} \times \left(\frac{SN2O}{SO2}\right)^{-n} \quad (3.4)$$

where k_{N2O} is units of (m d^{-1}), n is the unitless Schmidt number coefficient based upon the roughness of surface water—here I used 0.5 as it best describes a wave-covered surface caused by the flowing water in these riverine systems (Jähne et al. 1987; Jähne and Haußecker 1998). S_{N2O} and S_{O2} are the temperature dependent unitless Schmidt numbers for N_2O and O_2, respectively, and are calculated as follows (Wanninkhof 1992):

$$S_{N2O} = 2055.6 - 137.11t + 4.3173t^2 - 0.054350t^3 \quad (3.5)$$

$$S_{O2} = 1800.6 - 120.10t + 3.7818t^2 - 0.047608t^3 \quad (3.6)$$

where t is stream temperature (°C).

Nitrous oxide flux, or the emission rate of N_2O, was quantified following the thin-boundary layer diffusion model (Broecker and Peng 1974). Using C_w, C_s, and k_{N2O}, flux was calculated as follows (Liss and Slater 1974):

$$F = k_{N2O}(C_w - C_s) \quad (3.7)$$

where flux, F, is the emission rate of N_2O from the river in units of (μmol N_2O–N m^{-2} d^{-1}).

3.3.8 Estimating the Downstream Nitrous Oxide Spatial Footprint

BASE modeled K values were used to determine the extent of the WWTP's effect on dissolved N_2O concentrations at downstream sites through the use of a first-order loss, exponential equation (Chapra and Di Toro 1991; Demars et al. 2015):

$$L = \frac{-ln(C) \times v}{K} \quad (3.8)$$

where L is the distance (m) from W2 to downstream sites, C is the fraction of N_2O that remained in the system, v is stream velocity (m s^{-1}), and K is the reaeration coefficient (converted units from d^{-1} to s^{-1}). It should be noted that it is assumed that there is insignificant production of N_2O between W2 and W3, but if there was significant in-stream production between those sites, % loss

values would be underestimated. Through the rearrangement and exponential transformation of Eq.(3.8), values of excess N_2O that remained in solution, based on distances from W2 (L), were calculated/ estimated by the following equation (Demars et al. 2015):

$$C = C_0 \times e^{\left(\frac{-K \times L}{v}\right)} \quad (3.9)$$

where C_0 was the relative concentration of N_2O at W2 (i.e. sites downstream of W2 have C values < 1). These estimated C values (% loss) were compared with directly measured % loss of excess N_2O transported from W2 using the following equation:

$$E_{N_2O} = Q \times d_{N_2O} \times MW \quad (3.10)$$

where E_{N2O} was the excess dissolved N_2O (kg d^{-1}; i.e. the daily mass of N_2O discharged in excess of atmospheric saturation), Q was stream discharge (m^3 s^{-1} converted to m^3 d^{-1}), d_{N2O} was the measured concentration of N_2O–N (mol L^{-1} converted to mol m^{-3}) in the stream above atmospheric saturation, and MW is the molecular weight for N_2O-N (kg mol^{-1}). Percent loss was calculated based on relative E_{N2O} values from W2 to downstream sites. Estimated % loss from Eq.(3.9) was then directly compared to calculated % loss from Eq.(3.10). It should be noted that Eq.(3.9) is an estimation based on modeled K values using a first-order loss equation, while Eq.(3.10) values were empirically derived values based on measured dissolved N_2O concentrations. Where the results were broadly similar, I conclude that degassing of the effluent is the dominant driver of change.

3.3.9 Diel Sampling

Diel sampling at W1 and W3, spanning 36 hours, was carried out once during the study to identify possible variations in in-stream physicochemical conditions. Water was sampled every 2.5 h for the following: a) dissolved N_2O, NO_3^-, TAN, urea, TDN, DOC, and DO concentrations, b) pH, and c) water temperature (at both W1 and W3) in order to characterize system variability across diel conditions.

3.3.10 Data Analysis

All statistical analyses were performed using R: A Language and Environment for Statistical Computing, 2018 (R Core Team 2018; version 1.1383) where $\alpha = 0.05$ was considered statistically significant (95% confidence level). A generalized linear mixed-effects model (GLMM) (package: 'lmerTest'; function: [glmer]) was employed to test for significant differences in N_2O % saturation and flux across sites and through time (Kuznetsova et al. 2017). Therefore, the GLMM aimed to discover general differences across sites (e.g. W2 vs QA2) as well as through time at individual sites (e.g. W2 pre-upgrade vs W2 post-upgrade). To obtain GLMM model parameter values (*p*-values and *F*-statistics) an analysis of variance (ANOVA) was used (package: 'car; function: [Anova]) (Kuznetsova et al. 2017); residuals were confirmed to be normal through visual inspection. Homoscedasticity was confirmed for the ANOVA analysis using the Levene's Test (package: 'car'; function: [leveneTest]) (Fox and Weisberg 2011). To further investigate specific significant differences across sites and between time periods while accounting for seasonal variability (e.g. N_2O % saturation during May–August 2016 vs. May–August 2017), Tukey's Honest Significant Difference (HSD) test (package: 'multcomp'; function: [glht]) was carried out (Hothorn et al. 2008). Spearman rank correlation tests were employed to explore the relationship between denitrification rates (N. Dylla: Chapter 2) and N_2O % saturation and between chemical parameters (NO_3^- and TAN) and N_2O % saturation (package: 'ggpubr'; function: [ggscatter]) (Kassambara 2018). To investigate general differences in water temperature across both periods (pre- vs post-upgrade) for each site, a one-way ANOVA (package: 'stats'; function: [aov]) was used with a Tukey's HSD test (package: 'stats'; function: [TukeyHSD]) to infer differences between sites (R Core Team 2018). A student's t-test was used to compare flow rates when samples were taken both pre- and post-upgrade (package: 'stats'; function: [t.test]). All statistical tests were Bonferroni corrected, providing each individual test with a 95% confidence interval.

3.4 Results

3.4.1 Spatial and Temporal Variability of Nitrous Oxide

Nitrous oxide concentrations varied more than 300-fold across sites and dates. The upstream sites on Wascana Creek (W1) and Qu'Appelle River (QA1) had the lowest mean N_2O % saturation with values of 120 and 134% saturation, respectively. The sites most impacted by N_2O

from the WWTP effluent (W2 and W3) were extremely supersaturated, averaging 4.51 x 10^4 and 2.54 x 10^4% saturation, respectively. By W4, the extent of the supersaturation had dropped markedly to 310% saturation. The downstream site on the Qu'Appelle River (QA2)—with an average of 345% saturation—exhibited significantly greater concentrations of N_2O as compared to QA1 (ANOVA $F(5,152) = 354$, $p < 0.0001$; TukeyHSD $p < 0.05$; Figure 3.2). All downstream sites on Wascana Creek observed significantly higher N_2O % saturation than W1 (ANOVA $F(5,152) = 354$, $p < 0.0001$; TukeyHSD $p < 0.005$; Figure 3.2 and Table 3.1). Moreover, two separate, in-stream point measurements immediately downstream of effluent outflow indicated N_2O % saturation values of 5.30 x 10^4 (September 2016) and 1.01 x 10^5 (August 2017), as compared to N_2O % saturation values at W2 of 4.85 x 10^4 (September 2016) and 1.12 x 10^5 (August 2017). In-stream N_2O concentrations were highly variable in time, with the lowest concentrations occurring in May, associated with snowmelt driven dilution associated with higher discharge (Figure A3.7).

Table 3.1 Range in observed depth, stream velocity, N_2O concentration, N_2O flux, and sampled atmospheric concentrations of N_2O (N_2O_{atm}) for all study sites through time.

Site	Depth (m)	Velocity (m s^{-1})	N_2O Saturation (%)	N_2O Flux (µmol N_2O–N m^{-2} d^{-1})	N_2O_{atm} (ppmv)
W1	1.83–4.12	0.003–0.236	64.9–398	–32.5 to 109	0.242–0.843
W2	2.37–5.34	0.003–0.322	617–139000	227 to 72800	0.241–0.459
W3	1.56–3.51	0.001–0.138	1040–92000	398 to 40800	0.253–0.823
W4	1.59–3.59	0.006–0.236	125–2370	9.78 to 788	0.151–0.486
QA1	5.22–5.26	0.009–0.714	107–257	3.03 to 69.1	0.241–0.371
QA2	4.91–4.95	0.004–0.325	111–2970	4.17 to 907	0.239–0.256

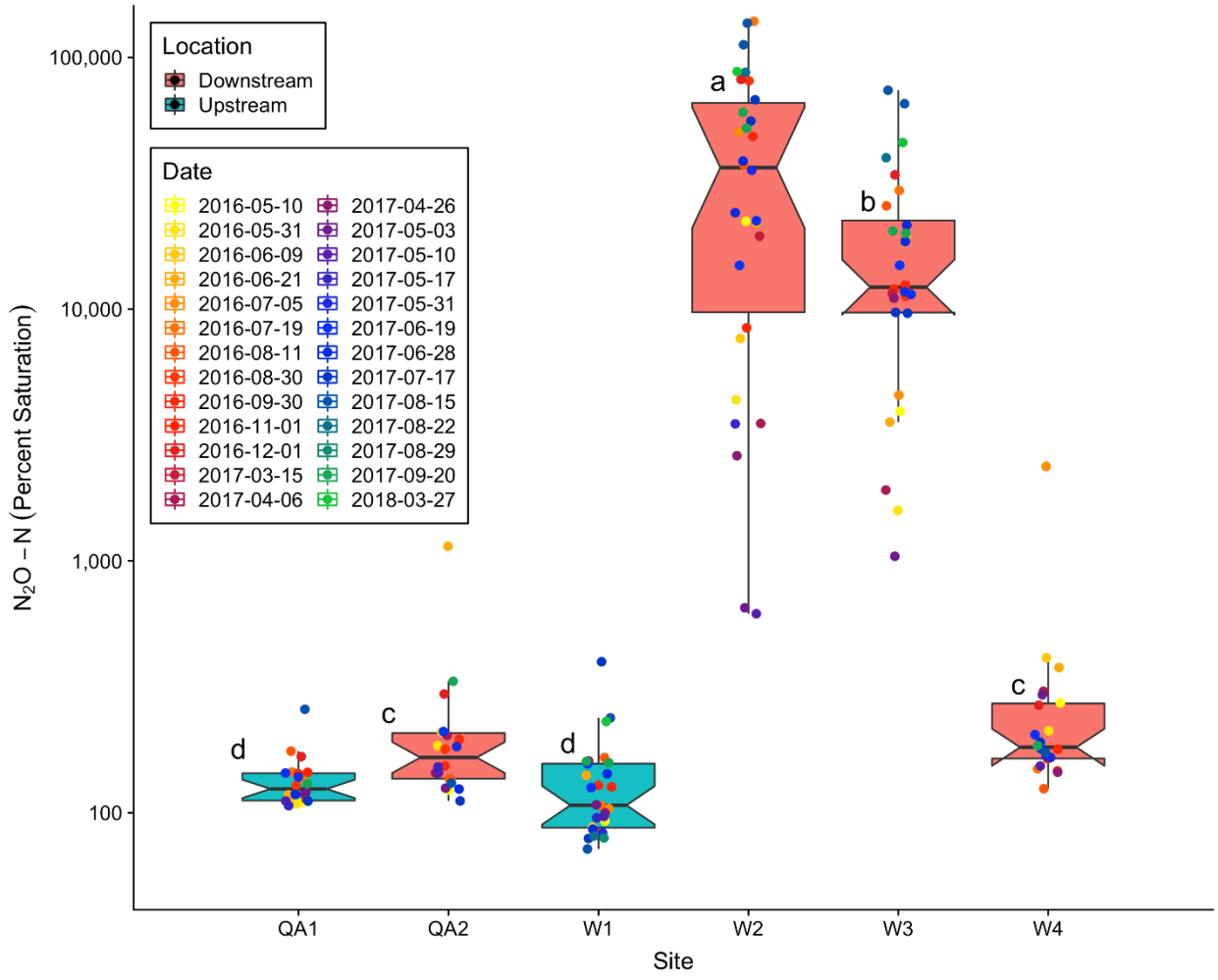

Figure 3.2 Nitrous oxide saturation (%) for all sites throughout the two-year study. Upstream sites are indicated by blue, notched-boxplots while downstream sites are orange, notched-boxplots. The notches show a 95% confidence interval around the median with whiskers encompassing 99% of the data observed where the outliers are represented as dots. Inside the box are the first and third quartiles with the median represented as the center line. Significant differences are indicated with different letters (those with the same letter are not significantly different from each other; ANOVA $F(5,152) = 354$, $p < 0.0001$ TukeyHSD $p < 0.05$).

3.4.2 Wastewater Treatment Plant Upgrade's Effect on Nitrous Oxide

3.4.2.1 Percent Saturation Pre-upgrade, Post-upgrade, and Comparison

In order to compare pre-upgrade conditions to post-upgrade conditions, N_2O concentrations and emissions were assessed after physical conditions such as water temperature and flow rates were confirmed to be similar. Results showed that the physical conditions were comparable between the two periods (pre-upgrade vs. post-upgrade). Water temperature, for the dates that were sampled, was not significantly different for all sites (ANOVA $F(11,123) = 0.405$, $p > 0.5$; TukeyHSD $p = 1$; Figure A3.8). Flow rates for the sampling dates, were not significantly different when comparing pre-upgrade vs. post-upgrade conditions at each gauging station (Qu'Appelle River: t-test$(24) = –0.171$ $p = 0.866$) and (Wascana Creek: t-test$(19) = –0.327$, $p = 0.747$; Figure A3.9).

Pre-upgrade, N_2O concentrations were greatest at the Wascana Creek impacted sites W2 and W3. Percent saturation values for these sites, during the pre-upgrade period, were as high as 1.39×10^5 for W2 and 2.96×10^4 for W3. All downstream Wascana Creek sites (W2–4) were significantly greater than the upstream site W1 (ANOVA $F(5,41) = 51.5$, $p < 0.0001$; TukeyHSD $p < 0.005$). The upstream control sites demonstrated the lowest concentrations pre-upgrade with no significant difference between the furthest downstream Wascana Creek site (W4) and downstream Qu'Appelle River site (QA2) (ANOVA $F(5,41) = 51.5$, $p < 0.0001$; TukeyHSD $p = 1$; Figure 3.3).

No evidence was found of significant change in % saturation associated with the upgrade using data for the period May 2016–August 2016 vs May 2017–August 2017 to directly assess upgrade impacts, (ANOVA $F(11,93) = 143$, $p < 0.0001$; TukeyHSD $p = 1$; Figure 3.3). However, a high degree of spatial variation in % saturation was also exhibited, similar to what was observed for the full time series of data. Post-upgrade, N_2O concentrations remained highest at the most immediately impacted Wascana Creek sites W2 and W3. Percent saturation values reached maxima at 1.37×10^5 for W2 and 7.40×10^4 for W3. Percent saturation values were significantly greater than all the other sites at Wascana Creek sites W2 and W3 but were not significantly different from each other (ANOVA $F(5,52) = 145$, $p < 0.0001$; TukeyHSD $p = 0.175$).

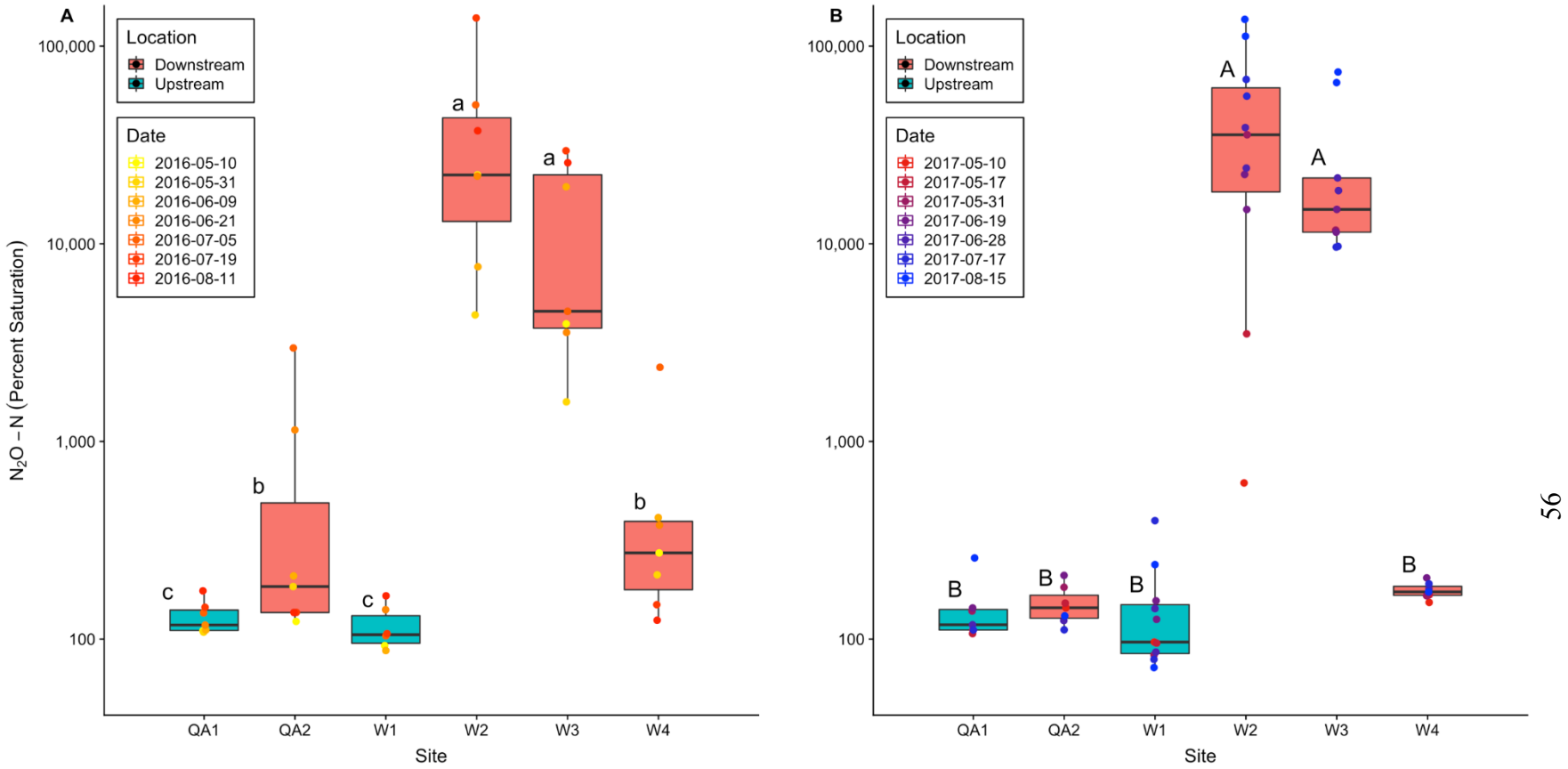

Figure 3.3 Nitrous oxide % saturation pre-upgrade (Panel A: May–August 2016) and post-upgrade (Panel B: May–August 2017). Significant differences within each period are indicated with different letters for their respective panel. There were no significant differences between the two periods for any given site (e.g. W1 pre-upgrade vs W1 post-upgrade; ANOVA $F(5,93) = 143$, $p < 0.0001$; TukeyHSD $p > 0.05$). Note: the letters only apply within a given panel.

3.4.2.2 Spatial Footprint of WWTP-derived Nitrous Oxide

Through the use of Eq.(3.8), the distance at which 95% of N_2O was lost from the system ($L_{5\%}$) was determined to be ~5 km. Site W3 was ~3.8 km downstream of the WWTP and therefore was determined to be inside the impact zone; no other sites were impacted by WWTP effluent originating N_2O (Table 3.2). Using Eq.(3.9), the estimated amount of N_2O that remained in the system by W3 was 22%. Therefore, on average, 78% of N_2O was estimated to be lost from W2 to W3 (Table 3.2). Using Eq.(3.10) and directly measured concentrations of N_2O at W2 and W3, I found that, on average, there was a 62% loss from W2 to W3 (Table 3.2). Therefore, on average, there was a 16% difference between the estimated off-gassing and measured N_2O concentration at the only site in the impact zone, site W3. The highest average excess N_2O–N (N_2O in excess of saturation concentrations) transported downstream was observed at W2, with an average value of 18.0 kg d^{-1} followed by W3 with 6.77 kg d^{-1}. The upstream sites had similar excess N_2O-N values of 0.021 kg d^{-1} at W1 and 0.029 kg d^{-1} at QA1. The furthest downstream Wascana Creek site, W4, observed an excess N_2O-N value of 0.114 kg d^{-1}, similar to QA2 with 0.196 kg d^{-1}.

Table 3.2 Mean excess N_2O–N values transported daily ± standard deviation along and calculated percent loss from downstream of the WWTP. Estimated % loss was estimated using the first-order Eq.(3.9) with the distance from the WWTP (Wascana Creek sites) and the confluence (Qu'Appelle River sites)—negative values mean the site is upstream of the WWTP/ confluence.

Site	Distance from WWTP/ Confluence (m)	Estimated Percent Loss (%)	Excess N_2O–N (kg transported d^{-1})	Calculated Percent Loss (%)
W1	–4000	—	0.021 ± 0.064	—
W2	200	0	18.0 ± 14.5	0
W3	3800	78	6.77 ± 4.73	62
W4	60000	100	0.114 ± 0.235	99
QA1	–5000	—	0.029 ± 0.043	—
QA2	12000	—	0.196 ± 0.418	—

3.4.2.3 Nitrous Oxide Flux

Flux was determined through Eq.(3.7) using measured, dissolved N_2O concentrations and *k*. Note that the *k* values were estimated from DO sensors at the upstream site (W1) and downstream site (W3). The averaged standardized k_{600} (20°C, CO_2; Wanninkhof 1992) value was 18.2 ± 16.4 cm h^{-1}.

The highest N_2O flux rates were observed at the Wascana Creek site immediately downstream of the WWTP, W2, with a maximum observed flux rate of 7.28 x 10^4 µmol N_2O–N m^{-2} d^{-1} (Figure 3.4). The average rate of emission at W2 was 2.02 x 10^4 ± 1.83 x 10^4 µmol N_2O–N m^{-2} d^{-1}, which was the highest flux rates for any site. Further downstream on Wascana Creek, site W3 observed the second highest average flux rates with a value of 1.32 x 10^4 ± 1.20 x 10^4 µmol N_2O–N m^{-2} d^{-1}. The upstream sites, W1 and QA1, as well as the downstream Qu'Appelle River site, QA2, were often sinks of (atmospheric) N_2O, although on average represented minor sources, with respective average emissions of 8.31 ± 7.53 µmol N_2O–N m^{-2} d^{-1}, 16.1 ± 14.6 µmol N_2O–N m^{-2} d^{-1}, and 88.2 ± 79.9 µmol N_2O–N m^{-2} d^{-1} (Figure 3.4). While QA2 showed periods of net uptake, there were many occurrences of emission, with the greatest event in June 2016 (907 µmol N_2O–N m^{-2} d^{-1} ± 822 µmol N_2O–N m^{-2} d^{-1}; Figure 3.4). It should be noted that assuming the major source of error is the estimation of *k*, the error bounds of these flux estimates are constrained by standard deviation calculated from each BASE model run. Moreover, BASE modeled *k* values fell within the reported range of values for lotic systems (Raymond and Cole 2001; Lorke et al. 2015).

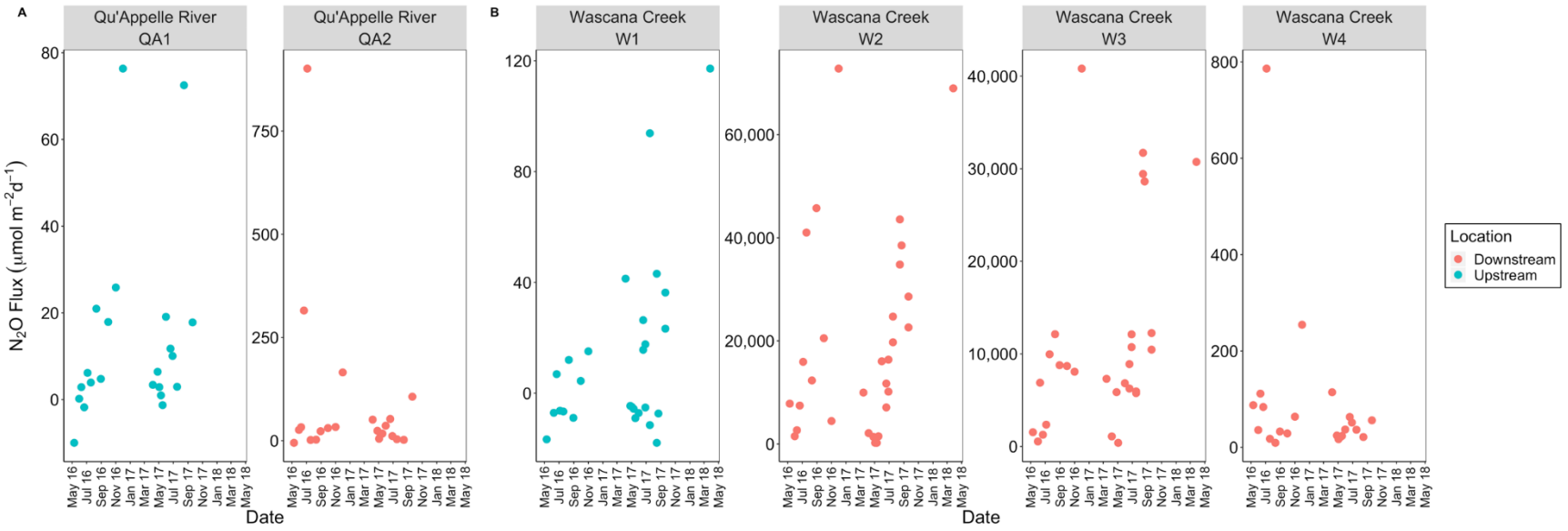

Figure 3.4 Nitrous oxide flux rates (μmol N_2O–N m^{-2} d^{-1}) for Qu'Appelle River (Panel A) and Wascana Creek (Panel B). Sites upstream of the WWTP are colored blue while downstream sites are colored orange. Note that the axes are different for each panel.

3.4.3 Diel Variation in Nitrous Oxide and Physico-chemistry

Over the course of diel sampling period (~36 h), N_2O and TAN did not show a consistent diel pattern at Wascana Creek W1, although N_2O concentrations at W3 show possible diel variation (Figure 3.5). Nitrate concentrations showed some evidence of diel change at W3 with maximal values occurring during the day, ranging from 2.74–4.30 mg L^{-1} over the course of a diel cycle with peak concentrations occurring ~3 h before sunset (16:48). The magnitude of change in N_2O % saturation during the diel cycles ranged from 64–190% at W1 and 1.35 x 10^4–9.20 x 10^4 % at W3 (Figure 3.5), suggesting 3.0–6.8-fold variation over a 36-hour period in summertime. Nitrous oxide % saturation at W1 varied between below 100 % saturation and supersaturation with the highest value occurring during the night. Nitrous oxide concentrations at W3 exhibited an overall decreasing trend through the 36 h sampling period, although this was not a monotonic decline as small N_2O concentrations increases were observed during the day (Figure 3.5). Total dissolved N appeared to increase during the day (W1 range = 0.77–0.96 mg L^{-1}; W3 range = 3.84–5.25 mg L^{-1}) while declining overnight (Figure 3.5) for both sites, but the trend was more apparent at W3. Since TDN is comprised of both DIN (analyzed in this study as NO_2^-/NO_3^- and TAN) and DON, I further examined the composition of TDN with regards to urea and DON. At the upstream site, W1, TDN mainly consisted of DON species which was comprised of only a small fraction of urea (Figure 3.6). Conversely, at the downstream site W3, TDN mainly consisted of DIN species, which also experienced a diel cycle (Figure 3.6), mostly driven by changes in NO_3^- concentrations (Figure 3.5). At W3, DON remained relatively constant throughout the diel campaign, while DON at W1 experienced a slight diel trend (similar to TDN) with higher concentrations occurring in the daytime. Interestingly, urea concentrations exhibited a diel cycle at both sites, with maximum concentrations occurring during the day (W1 range = 0.07–0.61 mg L^{-1}; W3 range = 0.21–0.41 mg L^{-1}) and decreased concentrations during the night (Figure 3.6). At W1, urea abruptly increased throughout the day before decreasing to minimal concentrations overnight.

Dissolved oxygen (% saturation), temperature, and pH followed a strong diel pattern across both sites, with values decreasing overnight and increasing during the day (Figure 3.5). pH values were closer to neutral at W3 and ranged from 7.12–7.92, while the pH at W1 was more basic and ranged from 8.38–8.83 (Figure 3.5). Un-ionized ammonia (NH_3), directly related and estimated from TAN concentrations, pH, and temperature did not surpass the freshwater guideline of 0.019

mg L^{-1} even when pH and temperature increased during the day (Figure A3.10). Flow during the diel sampling remained stable as no precipitation events occurred (Figure A3.11).

3.4.4 Correlations between Nitrous Oxide and Chemical Variables

To assess correlations between N_2O and chemical variables, data were grouped by sites situated inside the effluent-N_2O impact zone (< 5 km downstream of the WWTP; W2 and W3) and outside the effluent-N_2O impact zone (Upstream of the WWTP/Confluence; W1/QA1 or > ~5 km downstream of the WWTP/Confluence; W4/ QA2). Nitrate concentrations and denitrification rates were significant predictors of N_2O % saturation at only the non-impacted sites. No significant correlations between N_2O % saturation and denitrification rates were observed at W2 and W3; (Figure 3.7). It should be noted that if there were any correlations observed at the effluent-N_2O impacted sites (W2 and W3) the relationships would be further scrutinized due to the possible artefact of the WWTP process and its impact on nutrients and dissolved gases in its effluent. Nitrate was highly correlated with N_2O % saturation with a Spearman coefficient and *p*-value of ($\rho = 0.72$, $p < 0.0001$; Figure 3.8A). Denitrification rates were also highly correlated with N_2O % saturation ($\rho = 0.72$, $p < 0.0001$; Figure 3.8C)

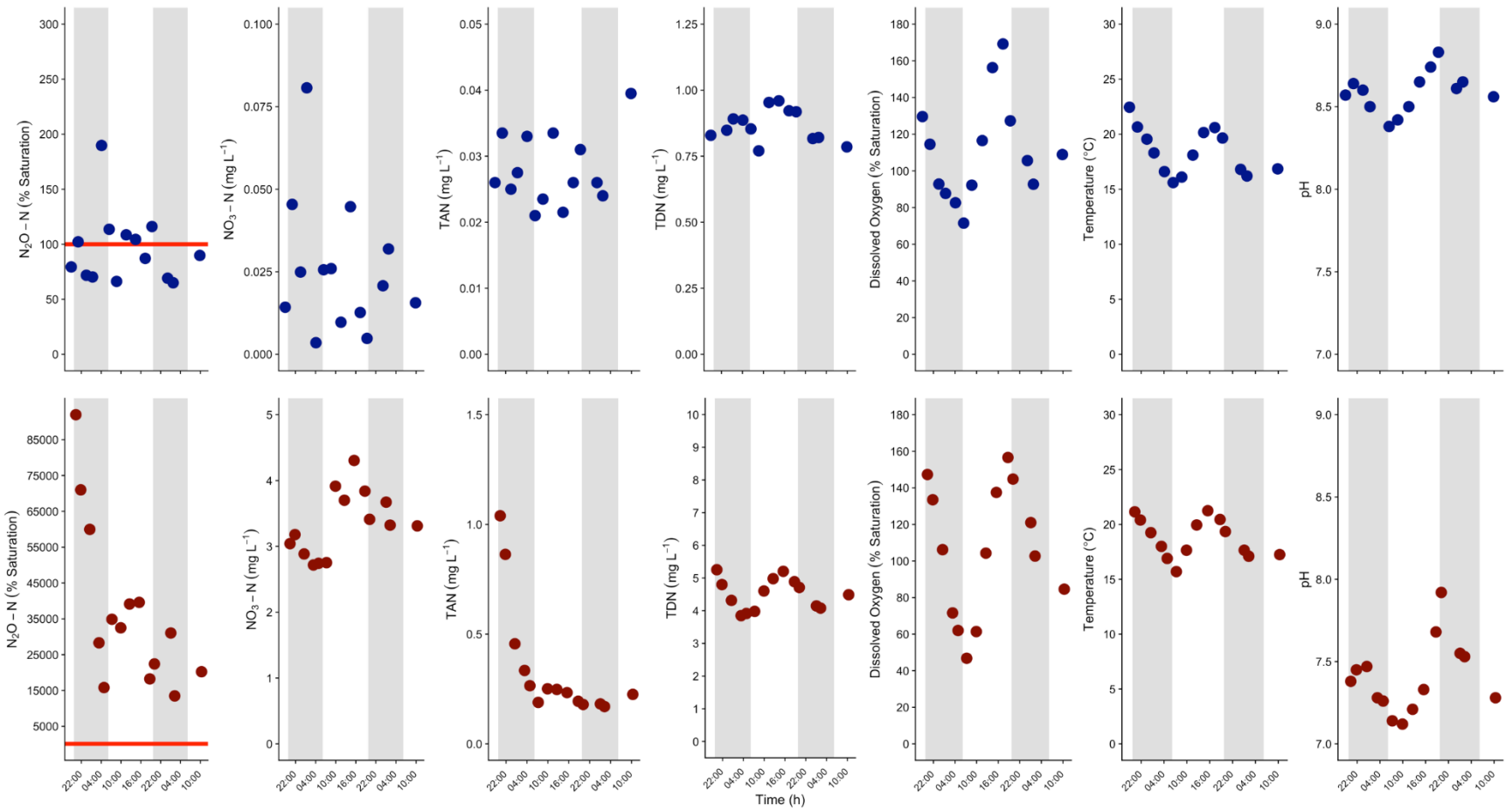

Figure 3.5 Diel sampling campaign that occurred August 29th–August 31st 2016, for the upstream Wascana Creek site W1 (Top Row, blue points) and the downstream Wascana Creek site W3 (Bottom Row, red points). From left to right, panels consist of nitrous oxide percent saturation, nitrate, total ammonia nitrogen, and total dissolved nitrogen concentrations, dissolved oxygen percent saturation, temperature and pH. Gray bars signify nighttime periods (between sunset at 19:48 and sunrise at 06:10) with white spaces signifying daytime periods. Note that y-axes for each column are on different scales in order to better display the data (except for dissolved oxygen and temperature). The red line for nitrous oxide (% saturation) signifies 100% saturation of nitrous oxide.

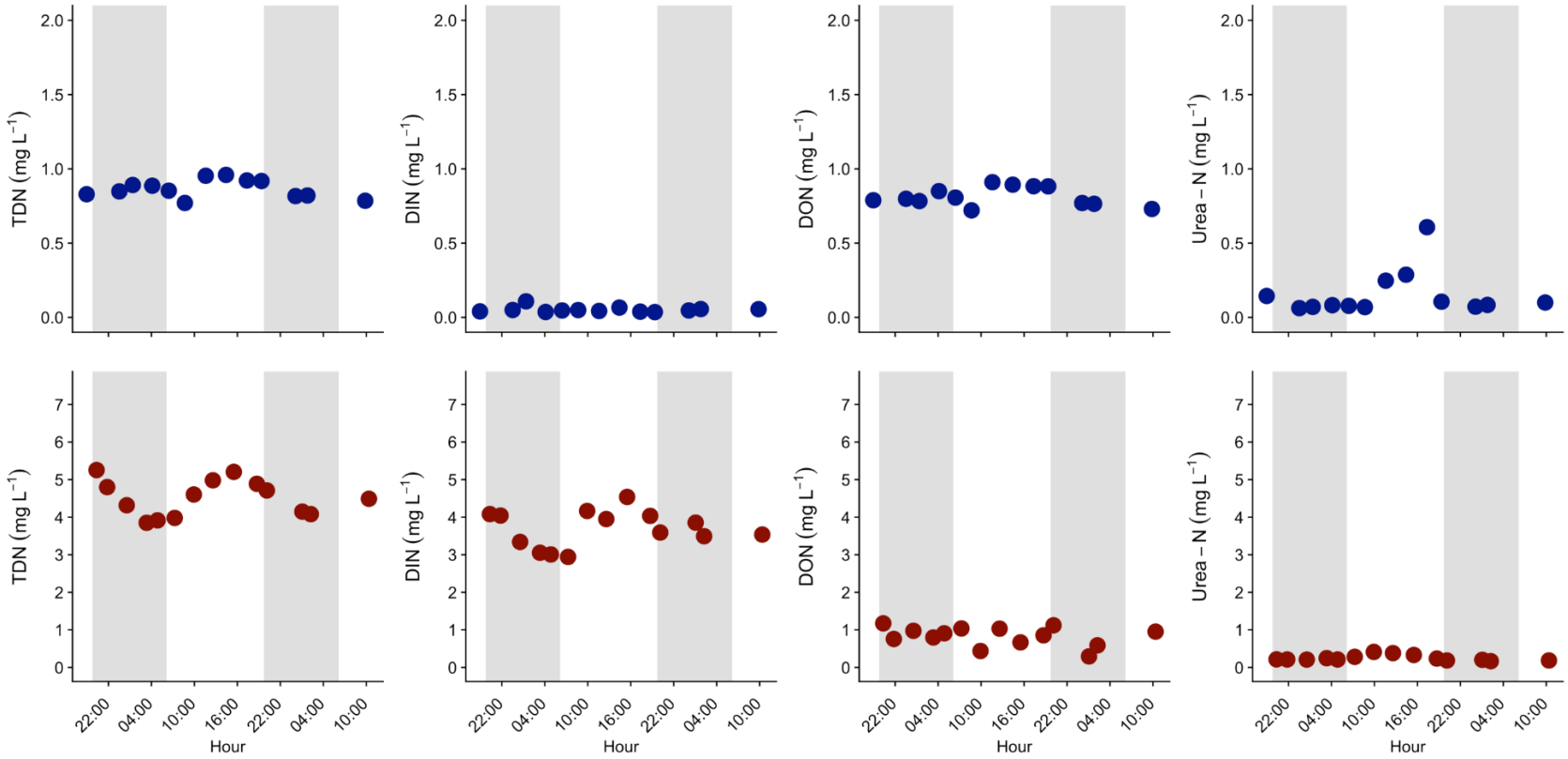

Figure 3.6 Diel sampling campaign August 29th–August 31st 2016, for the upstream Wascana Creek site W1 (top, blue points) and the downstream Wascana Creek site W3 (bottom, red points). From left to right, panels consist of total dissolved nitrogen, dissolved inorganic nitrogen, dissolved organic nitrogen, and urea. Gray bars signify nighttime periods (between sunset at 19:48 and sunrise at 06:10) with white spaces signifying daytime periods (between sunrise at 06:10 and sunset at 19:48). Note that y-axes for each row are on different scales in order to better display the data although the y-scale within a site is consistent to allow visual assessment of the proportion of TDN pool in each fraction. The urea data for W3 are presented on a finer y-axis in Figure A3.12.

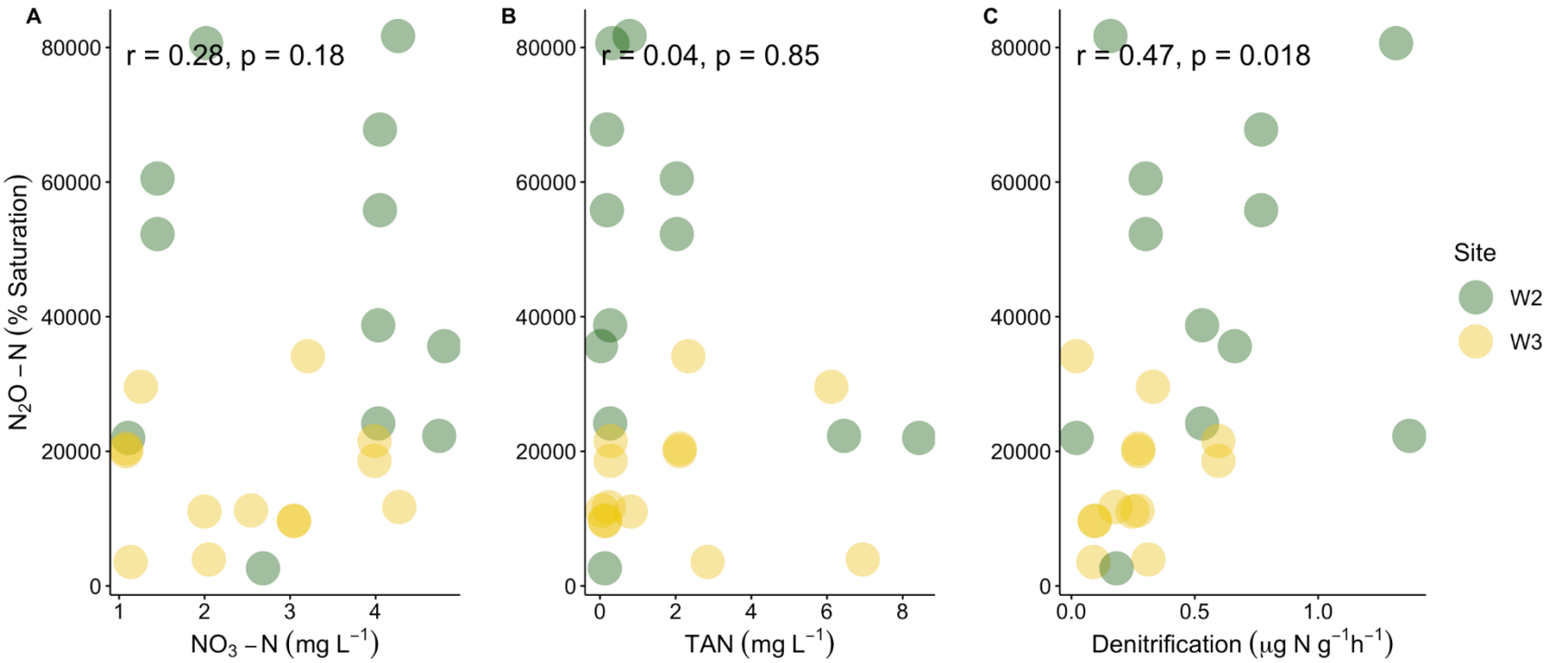

Figure 3.7 Spearman rank correlations for the sites situated in the effluent-N_2O impact zone (W2 and W3), between nitrous oxide (% saturation) and nitrate concentration (mg NO_3–N L^{-1}; Panel A), total ammonia nitrogen concentration (mg TAN L^{-1}; Panel B), and denitrification activity (μg N g^{-1} h^{-1}; Panel C). Note that displayed *p*-values are not Bonferroni corrected ($\alpha_{corrected} = 0.0083$).

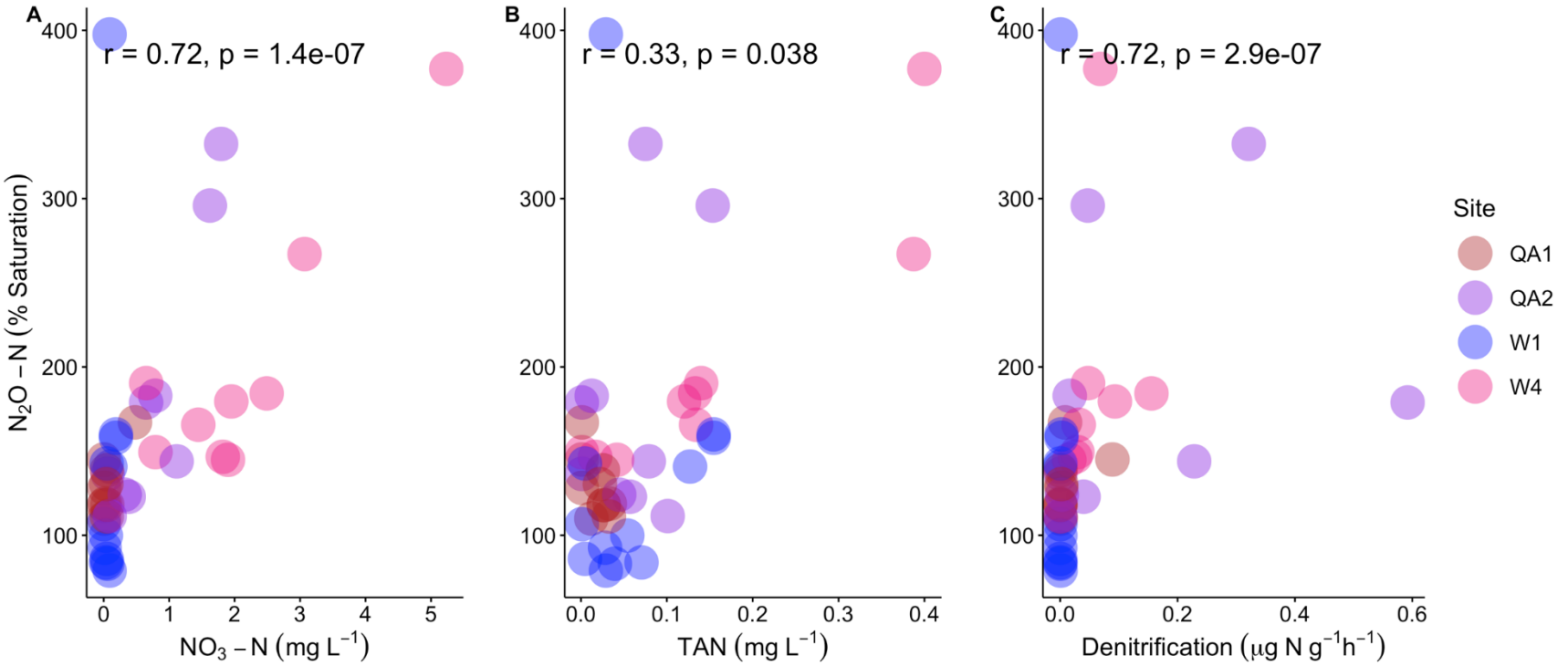

Figure 3.8 Spearman rank correlations for the sites not situated in the effluent-N_2O impact zone (W1, W4, QA1, and QA2), between nitrous oxide (% saturation) and nitrate concentration (mg NO_3–N L^{-1}; Panel A), total ammonia nitrogen concentration (mg TAN L^{-1}; Panel B), and denitrification activity (µg N g^{-1} h^{-1}; Panel C). Note that displayed *p*-values are not Bonferroni corrected ($\alpha_{corrected} = 0.0083$).

3.5 Discussion

3.5.1 Direct Release of Wastewater Treatment Plant N_2O Dominates Emissions

Nitrous oxide released from the Regina WWTP effluent markedly impacted downstream N_2O concentrations and emissions along an ~5 km reach of Wascana Creek. As this system can be up to 100% effluent during winter and 90% during summer, it is considered an effluent dominated system, which means the flow and biogeochemical processes are driven by the effluent from the Regina WWTP (Waiser et al. 2011b). The data also suggest that emissions of the potent GHG, N_2O, at W2 and W3 are driven directly by the effluent. Further downstream, emissions are impacted by the elevated N loads of the effluent, although emissions decrease dramatically once the effluent-derived N_2O is degassed. Measured effluent concentrations were extremely high, in excess of measurements at W2. This finding of effluent-derived N_2O impacting emissions is not novel. The larger Grand River in Ontario (Rosamond et al. 2012) as well as the Potomac River near Washington D.C. (McElroy et al. 1978) both experienced supersaturation of N_2O downstream of a WWTP, while it was not clear if the N_2O was directly from the effluent or indirectly produced via in-stream N cycling. However, areal N_2O emissions in Wascana Creek were significantly higher, to the best of my knowledge, than published values from any urban impacted aquatic ecosystem (Table 3.3). Immense production of N_2O by denitrification and nitrification during the BNR process created the supersaturated concentrations of N_2O (> 100,000 %) in Wascana Creek. The effluent, as confirmed by two point-measurements, entered Wascana Creek supersaturated and largely dissipated (95 %) within 5 km of the outflow. Although temperature affects the solubility of gases (inversely related, i.e. as temperature increases solubility decreases) we did not observe any seasonal trends with respect to in-stream temperatures.

Table 3.3 Average observed nitrous oxide percent saturation and flux values found in urban-impacted aquatic riverine systems (ranges are shown in parentheses).

Site	N_2O Percent Saturation	N_2O Flux ($\mu mol\ N_2O–N\ m^{-2}\ d^{-1}$)	Reference
Ohio River, USA		10.5–534	(Beaulieu et al. 2010)
Agricultural/ Urban Canal, Mexico		141 (42.8–2100)	(Harrison et al. 2005)
Assabet River, USA	3475 (380–18364)	136 (46.3–1360)	(Hemond and Duran 1989)
Potomac River, USA	2250 (100–5000)		(McElroy et al. 1978)
South Platte River, USA		53.1 (0.33–1170)	(McMahon and Dennehy 1999)
Grand River, Canada		(-35–4200)	(Rosamond et al. 2012)
Tama River, Japan	1051 (93–6756)		(Toyoda et al. 2009)
Shanghai River Network, China	770 (103–21172)	68.5 (0.43–1860)	(Yu et al. 2013)
Tianjin River Network, China	252–3116	50.4 (2.64–125.52)	(Liu et al. 2015)
Brisbane River, Australia	140–230		(Sturm et al. 2016)
Brisbane River[†], Australia	298–3000		(Sturm et al. 2016)
River Swale-Ouse, England		33.6–2400	(Garcia-Ruiz et al. 1999)
Xin'an Tang River, China	813 (597–1370)	48.1 (35.5–75.1)	(Xia et al. 2013)
New South Wales[¥], Australia	2320 (171–13200)		(Short et al. 2014)
Red Run Watershed, USA	110–4700	182–5340	(Smith et al. 2017)
Paquequer River Basin, Brazil	100–1640	0.480–121	(Alvim et al. 2014)
Nanfei River, China	5664	203 (9.35–812)	(Yang et al. 2011)
Nanfei River[§], China	2590	166 (38.6–59.2)	(Yang et al. 2011)
Suzhou River, China	2625	11.1(69.6)	(Wang et al. 2015a)
Wascana Creek[*], Canada	26200 (125–139000)	12500 (9.78–72800)	This study
Wascana Creek Effluent, Canada	77000 (53000–101000)		This study

[†]8 km downstream of outflow; [¥]Untreated sewage; [§]Diurnal values; [*]WWTP Wascana Creek impact sites (W2–4)

3.5.2 Evidence of In-stream Production Downstream of WWTP

Comparing the results from both methods for estimating N_2O % loss (Eq. 3.9 and 3.10), showed that loss from W2 to W3 could range between 62 and 78% as seen in Figure 3.2. Because there was only a 16% difference between off-gassing estimations and measured N_2O losses from W2 to W3, it was determined that not only the majority of the N_2O in Wascana Creek originated directly from the WWTP effluent but there was a significant loss of N_2O by W3. The lower % loss of N_2O, as calculated by Eq. 3.10, could be explained by in-stream biological processes such as nitrification and denitrification, which can produce N_2O, as these are not accounted for in the estimate from Eq. 3.9. However, it should be noted that the data are highly variable over the course of a season, which also may account for the discrepancy.

At the downstream sites W4 and QA2, which lie outside the zone where effluent N_2O directly impacts emissions, elevated N_2O levels provide evidence that in-stream production of N_2O is occurring. Both sites were typically supersaturated with N_2O, although emissions were markedly lower from these sites relative to the sites directly influenced by N_2O from the effluent. In the most downstream Wascana Creek site (W4), N_2O % saturation exceeded associated measurements at the upstream control site (W1), suggesting the increased N loads associated with the WWTP stimulate in-stream production, a result further supported by correlations between concentrations of NO_3^- and denitrification activity and N_2O % saturation (section 3.5.3). Moreover, as described in Chapter 2, W4 observed elevated rates of denitrification relative to W1. The effect of the WWTP effluent was also observed ~12 km downstream of the Wascana Creek confluence at QA2, where significant upstream vs. downstream differences (QA1 vs. QA2) were observed in N_2O % saturation. This suggests that the effects of the WWTP effluent on emissions occur > 60 km downstream.

3.5.3 Controls on In-Stream Production of N_2O

In order to discover possible predictors of N_2O concentrations, a suite of physicochemical factors was measured. In downstream areas where in-stream N_2O production drove emissions (e.g. sites W4 and QA2) as well as controls sites (W1 and QA1), strong relationships were observed between NO_3^- concentration and N_2O % saturation, as well as rates of denitrification and N_2O %

saturation. This suggests that N_2O production and emissions are stimulated by increased N concentrations, as documented elsewhere (Garnier et al. 2009; Beaulieu et al. 2010; Yang et al. 2011). Also, substrate availability often controls rates of nitrification (Rysgaard et al. 1994; Kemp and Dodds 2002; Strauss et al. 2002), and denitrification (Oremland et al. 1984; Seitzinger 1988; Kemp and Dodds 2002; Bernot and Dodds 2005; Herrman et al. 2008; Silvennoinen et al. 2008; Garnier et al. 2009), and can also influence the N_2O yields of these processes. Consequently, although DO is usually negatively related with N_2O production from denitrification (Rosamond et al. 2011; Venkiteswaran et al. 2014; Burgos et al. 2015; Wang et al. 2015b), no significant correlation was observed in the study system. In systems where sites experience anoxia, strong, negative relationships between DO and N_2O have been observed (Rosamond et al. 2011); however the study system rarely experienced sustained periods of anoxia.

3.5.4 WWTP N_2O Emissions

Wastewater treatment plants are upgraded for a number of reasons including, but not limited to the following: 1) to reduce their ecological impact by increasing effluent water quality, 2) to meet new effluent regulations/ discharge standards, and 3) to increase storage and processing capacity (Zhou and Smith 2002; Holeton et al. 2011). This work suggests that the N_2O emitted directly downstream from the WWTP is significantly higher than any aquatic system and suggests that although the Regina WWTP improved water quality by reducing TAN (N. Dylla; Chapter 2) this decrease was not associated with a decrease in in-stream N_2O % saturation. It should be noted that if I included chamber measured *k* values in the determination of *k*, its inclusion would have led to an average 21% decrease in estimated fluxes. Because of the greater sample size across a wider range of seasonal and flow conditions, BASE modeled *k* values were used with (± 1 STD) to account for possible variability.

Although a growing amount of work has assessed the C footprints of WWTPs, specifically their N_2O emissions, this has tended to focus on quantifying emissions directly from their respective WWTP (Czepiel et al. 1995; Schulthess and Gujer 1996; Kimochi et al. 1998; Kampschreue et al. 2009; Law et al. 2012). Nitrous oxide was the major contributor to the WWTP's C footprint in 16 Scandinavian WWTPs; even when only direct emissions from the plant were considered (i.e. excluding downstream emissions; Gustavsson and Tumlin 2013).

Interestingly, these results contrast Intergovernmental Panel on Climate Change (IPCC) assumptions that most of the N_2O emissions are produced and indirectly emitted downstream of a WWTP (IPCC 2006). The results show that extremely high N_2O emissions are occurring downstream of the Regina WWTP, and that these extremely high N_2O concentrations are mainly the result of off-gassing from the supersaturated effluent. Results showed that not only are concentrations downstream higher than those in the literature, but also that the origin of N_2O stems mainly from the effluent and not in-stream production. Because of this finding, future C footprint WWTP focused studies, especially in effluent dominated systems, should aim to assess not only direct WWTP emissions but also indirect downstream emissions, ultimately encompassing a life-cycle focused approach (Klopffer 1997). While IPCC estimated global emissions from WWTPs (0.2 Tg N_2O-N yr^{-1}; IPCC 2007) appear to be relatively insignificant when compared to livestock emissions (1.5 Tg N_2O-N yr^{-1}; Oenema et al. 2005), the IPCC acknowledges that their indirect, downstream emission factors are based on limited data and ranged from 0.0005–0.25 kg N_2O-N kg N^{-1} with a default value of 0.005 kg N_2O-N kg N^{-1}. Therefore, global N_2O emissions could be overestimated by up to 10 times. Although more constrained, the IPCC emission factors from direct WWTPs ranged from 2–8 (g N_2O $person^{-1}$ $year^{-1}$). With such high uncertainty of emission factors, N_2O emissions from treated wastewater could be vastly underestimated.

3.5.5 Diel Cycles in Nutrient Concentrations and Nitrous Oxide Percent Saturation

During the course of the diel sampling campaign (~36 h), I observed several trends at both the upstream site W1 and the downstream site W3. TDN and urea followed a diel pattern where concentrations decreased overnight and increased during the day. Although this trend occurred at both sites, the trend for TDN was more prevalent at W3, most likely due to the WWTP effluent. Diel changes in TDN are most strongly driven by urea and NO_3^- concentrations at W3 and by DON at W1. Although a few studies have focused on diel cycling of TDN, none focused on effluent dominated systems. This trend observed in the Wascana Creek system agrees with results from a eutrophic pond in China (Yu et al. 2016), but differs from a study focused on only dissolved inorganic nitrogen (DIN; NO_2^-, NO_3^-, and TAN) in a sewage impacted system that did not observe a diel trend (Gammons et al. 2011). However, more research should be carried out to determine

patterns of these species in high-nutrient waters. This is significant as most sampling occurs during the day, which might bias results of an entire study.

Although TDN exhibited a diel pattern at both W1 and W3, this was not as apparent for NO_3^- or TAN at W1 (Figure 3.5). Wascana Creek impact site W3 seemed to exhibit an increase in NO_3^- concentrations at 08:00, which could be related to the diel cycle of humans as this follows the operational pattern of the plant when effluent is discharged to create space to accommodate incoming flow as residential water usage spikes in the morning (Atinkpahoun et al. 2018). Moreover, the effects of society/ culture have been shown to not only impact the inflow of nutrients to WWTPs but also the nutrients in the treated effluent to downstream systems (Matos et al. 2013). While treated effluent from a highly populated city may exhibit less pronounced diel cycles of flow and nutrients leaving the WWTP (i.e. smaller variation) (Gernaey et al. 2011), peaks in the morning and night are still observable (Rodríguez et al. 2013). In addition to the societal impacts on the diel cycling of WWTPs, solids residence time of sludge needed for nitrification to occur may also impact the outflow of nutrients (Bayo et al. 2016).

Un-ionized ammonia is proportional to NH_4^+, pH, and temperature—increasing ten-fold with a one unit increase in pH and two-fold with a 10° C increase in temperature (Environment Canada 1999). Since both temperature and pH increased during the day, reaching maximal values near the end of day, I used the diel data to test exceedances of the Canadian freshwater guideline for NH_3—0.019 mg L^{-1} (Canadian Council of Ministers of the Environment 2010). However, even with these increases in pH and temperature, NH_3 concentrations constantly remained below the lethal limit following the upgrade. Determining the diel pattern of TAN, pH, and temperature in other effluent dominated systems may be critical for accurately assessing NH_3 concentrations as I observed diel trends in nearly all variables.

Several studies have shown a diel pattern of N_2O concentrations (Laursen and Seitzinger 2004; Harrison et al. 2005; Clough et al. 2007; Rosamond et al. 2011; Baulch et al. 2012a; Thuss et al. 2014). The same pattern was observed in the effluent dominated system studied here, but only at the impacted site, W3. Nitrous oxide concentrations ranged from 64–190% saturation at W1 and 1.35 x 10^4–9.20 x 10^4 % saturation at W3 over the course of 36 h. The lack of a diel trend at W1 might be due the near-saturation of N_2O at that site. Nevertheless, N_2O can vary greatly over periods of several hours in an effluent dominated system, which suggests an error in flux

estimations from a single point measurement of approximately 3.0–6.8-fold within a single day (in summer). Over the course of a year, flux estimates vary greatly across sites with an approximate 6.8–310-fold range at the impacted Wascana Creek sites, with fluxes increasing from spring to summer (Figure A3.13). This could be due to lower gas solubility in the warmer months. In order for future studies to account for possible variability of N_2O on the daily scale (e.g. sampling when daily mean values occur), diel sampling should be used.

3.6 Conclusion

This study presented novel results assessing how a WWTP and its upgrade affected nutrients and N_2O concentrations and emissions in an effluent dominated system. The N_2O impact zone downstream of the WWTP, or the length of stream that it took for 95% of effluent N_2O to dissipate, was ~5 km. Although the Regina WWTP upgrade successfully reduced TAN concentrations (N. Dylla: Chapter 2), the upgrade produced no benefit in terms of mitigating N_2O emissions. This was most likely because the effluent contained supersaturated concentrations of N_2O (mean post-upgrade % saturation at W2 of 4.66×10^4), while NO_3^- remained unchanged by the upgrade. The WWTP effluent had a major impact on N_2O emissions before and after the upgrade with average N_2O emission rates at the most impacted site (W2) of 1.27×10^4 μmol N_2O–N m^{-2} d^{-1} pre-upgrade and 1.69×10^4 μmol N_2O–N m^{-2} d^{-1} post-upgrade. Moreover, the greatest emissions were observed immediately downstream of the WWTP with a maximum estimated flux rate of 4.36×10^4 μmol N_2O–N m^{-2} d^{-1}, indicative of the importance of direct release from the WWTP. The maximum and average amount of N_2O emitted from Wascana Creek impact site W2 were the highest values recorded in an urban-impacted system, to the best of my knowledge (Table 3.3). Therefore, results indicate that hotspots of N_2O emission in an effluent dominated system can occur where emissions result from injection of N_2O supersaturated effluent and at sites further downstream where in-stream production of N_2O is dominant. Future studies may look to trace effluent-originating N_2O using ^{15}N site preference as a way to not only quantify how much N_2O stems from the WWTP but also how much in-stream production of N_2O is occurring (Snider et al. 2015). This is an important consideration in the context of GHG budgets for these systems. With an increasing focus on C taxes around the world for GHG emissions, future WWTP upgrades may

want to examine possible tools for reducing both in-plant and downstream emissions (Metcalf et al. 2008; Beck et al. 2015; Molinos-Senante et al. 2015; Dong et al. 2017).

3.7 Acknowledgements

I would like to acknowledge the SaskWatChe (Saskatchewan Water Chemistry) lab group, specifically Kimberly Gilmour and Katy Nugent for their support with field expeditions, laboratory analyses, and experiments. I would like to acknowledge the National Sciences and Engineering Research Council (NSERC) of Canada's Collaborative Research and Training Experience Program for scholarship. Also, I want to acknowledge the NSERC Discovery Grant to HMB for funding, faculty start-up funding at the U of S (CJW), support of the Global Institute for Water Security, and the Centennial Enhancement Chair Program. Lastly, I would like to thank Dr. Vijay Tumber for assistance with experimental design though his past experience with the study area.

3.8 Author Contributions

Nicholas P. Dylla performed the bulk of the field work as well as the laboratory and statistical analyses for this manuscript. NPD was lead author on manuscript, with editing and commenting of thesis chapters provided by CJW and HMB. CJW and HMB also obtained funding for the research as well as provided knowledge for project design.

Chapter 4: GENERAL CONCLUSION

4.0 Summary

Anthropogenic nutrient loading to water bodies can have major impacts on ecosystems and greenhouse gas (GHG) emissions (Rapport et al. 1998; Deemer et al. 2016). While the agriculture sector introduces significant amounts of phosphorus (0.56 Tg yr^{-1}) and nitrogen (~6.1 Tg N_2O-N yr^{-1}) into freshwater systems and the atmosphere, treated sewage can be a significant source of N_2O and nutrients (Mosier et al. 1998; Mekonnen and Hoekstra 2018). The advancement of wastewater treatment plants (WWTPs) offer a way to reduce nutrient loading to receiving water bodies. In efforts to further reduce nutrients from their effluent, WWTPs can upgrade their processing trains from primary to advanced levels (IPCC 2006; Meals et al. 2010). This thesis aimed to determine how a WWTP and its upgrade can directly impact an effluent dominated system—Wascana Creek and the larger Qu'Appelle River. Chapter 2 assessed the change in nutrient chemistry and denitrification rates before, during, and after the Regina WWTP upgrade, while Chapter 3 determined how the upgrade impacted GHG emissions by measuring nitrous oxide (N_2O) in the same time span. Chapter 3 also illustrated the diel cycle of nutrients, physical parameters, and N_2O concentrations.

With an increasing global and urban population, water demand and usage is expected to intensify which may lead to the increased volume of wastewater (Matos et al. 2013; Hernández-Chover et al. 2018). For example, in a study researching the impact of population growth in two developing cities in Africa, researchers found that not only did the amount of households connected to the sewer system increased by up to 37.8%, but also that the inflow of sewage to WWTPs increased by upwards of 45% (Teklehaimanot et al. 2015). Therefore, with global population constantly rising WWTPs will have to process more human excreta, which, in the absence of improved treatment, can cause an increase in nutrients such as nitrate (NO_3^-), total ammonia nitrogen (TAN; $NH_4^+ + NH_3$), total dissolved nitrogen (TDN), urea and dissolved organic carbon (DOC) in treated effluent. In the previously mentioned case study investigating population impact on WWTPs, the rapid growth and demand on wastewater treatment caused existing WWTPs to become inefficient resulting in poor effluent water quality (Teklehaimanot et al. 2015). Cities may build more WWTPs as they grow or build WWTPs to handle a larger influent

capacity, however increasing the number of WWTPs is costly (e.g. construction costs, more employees per plant, training, etc.) and scaling WWTPs to economies while maintaining efficiency is often difficult (Hernández-Chover et al. 2018). Therefore, the increased nutrient loading can then cause the formation of eutrophic conditions and ultimately hypoxic waters as seen in Wascana Creek (W3) where concentrations varied from oxygenated during the day to hypoxic overnight. These dramatic shifts in DO concentrations may be just as important to ecosystem health now and in the future.

Denitrification can remove overlying NO_3^- by converting it to inert N_2, thus providing an ecosystem service (Burgin and Hamilton 2007). However, NO_3^- saturation, which is considered a negative indicator of ecosystem health can occur, limiting the capacity of sediment to process excess NO_3^- due to limitations in other substrates or conditions (Udy et al. 2006). It was concluded that the Regina WWTP significantly increased denitrification rates downstream while the upgrade had no observable effect on denitrification rates. NO_3^- saturation occurred throughout the study (before and after the upgrade) at sites downstream of the WWTP on Wascana Creek, suggesting significant impacts on ecosystem services persist. Given high NO_3^- loads that remain in this system, and many other wastewater impacted systems, WWTPs may want to optimize their downstream ecosystems to further process nutrients in their effluent. For example, if denitrification (a biological nutrient removal process) becomes NO_3^--saturated, WWTPs might allow for higher concentrations of C in their effluent in order to increase these downstream rates, ultimately further reducing NO_3^- from the water if adequate oxygenation can be maintained for aquatic health. Alternately, they may re-engineer waterways to increase residence time and increase sediment-water contact. With regards to changes in nutrients before, during, and after the Regina WWTP upgrade, the only significant change in water chemistry was a decrease in TAN; however, this was localized to the most immediate downstream sites, W2 and W3. The change in NH_3 is significant as the concentrations decreased from above the Canadian freshwater guideline to well below it (Canadian Council of Ministers of the Environment 2010).

The results from Chapter 2 showed that Wascana Creek is an extremely impacted system where a total WWTP upgrade had no significant impact on an important, in-stream biological nutrient removal process—denitrification—based on comparing denitrification rates across the pre- and post-upgrade periods. Although Wascana Creek is a smaller receiving water body than

most effluent-impacted systems, increasing global populations, particularly in developing countries, may begin to deposit treated waste into smaller and decreasing volumes of water (Rosegrant et al. 2003). Therefore, Chapter 2 provides significant information about a WWTP and its upgrade on possible scenarios where water shortages may be more common (Murray et al. 2012).

Since areas downstream of WWTPs can form hot zones and hot periods of biogeochemical processes, and ultimately emissions of gases (McClain et al. 2003), Chapter 3 aimed to address the magnitude of N_2O concentrations downstream of the Regina WWTP and assessed the impact of the upgrade on N_2O concentrations. Dissolved N_2O concentrations were collected throughout the upgrade using the headspace equilibration technique (Kampbell et al. 1989). These findings show that the WWTP effluent contains extremely high, supersaturated concentrations of N_2O that eventually dissipate from the system (95% within ~5 km downstream) and that the upgrade had no significant impact on N_2O concentrations or emissions. These results offer insight into how a point-source, such as a WWTP, could be assessed in a life-cycle analysis. Since most studies to date have focused on direct N_2O emissions from the plant during the treatment process (Czepiel et al. 1995; Schulthess and Gujer 1996; Kimochi et al. 1998; Kampschreue et al. 2009; Law et al. 2012), a facility's C footprint might be vastly underestimated. The N_2O concentrations and rates of flux downstream of the Regina WWTP were greater than those published in the literature (Hasegawa et al. 2000; Outram and Hiscock 2012; Yu et al. 2013). Chapter 3 also illustrated the diel cycling of nutrients and physical parameters in an effluent dominated system. Results showed that many variables changed significantly throughout the course of a day. For future studies, when assessing nutrients downstream, we should design monitoring programs that account for possible diel changes.

Overall, it has been shown how a WWTP significantly impacted biological processes, water quality, and GHG emissions from an effluent dominated system. While the upgrade did not impact denitrification rates, it is possible that there may be observable differences in the future since activity in biological processes can be delayed due to the legacy of nutrients in the system (Meals et al. 2010; Van Meter et al. 2016). Both chapters also showed that a WWTP upgrade significantly reduced nutrients such as TAN. Overall, the Regina WWTP had a major impact on

its downstream ecosystem throughout the study; however, the upgrade appears to have increased the health of Wascana Creek by reducing concentrations of TAN.

4.1 Limitations and Future Research

Although this research provided new insight as to the impact of a WWTP and its upgrade in a novel riverine system, more work needs to be done in order to fully assess the effects of the upgrade. For instance, Chapter 2 showed that denitrification rates remained NO_3^--saturated post-upgrade, but results suggest that there might be a trend towards possible NO_3^- limitation. In order to determine how fast the system can respond to the upgrade, denitrification experiments should be carried out into the future while pairing column water and porewater sampling to best characterize the denitrification/ nutrient relationship as NO_3^- concentrations in the water column did not significantly change throughout the upgrade process. A preliminary reason for the lack of change in NO_3^- concentrations is that the newly employed biological nutrient removal (BNR) process more effectively converted NH_4^+ to NO_3^- while also providing less seasonal variation in NO_3^- concentrations, ultimately resulting in no observed significant changes in NO_3^- concentrations (Kayla Gallant, personal communication, November 20, 2018). Moreover, NO_3^- concentrations did not change significantly post-upgrade, yet denitrification rates remained NO_3^--saturated; thus it is worth pursuing the effect of increasing concentrations of DOC on denitrification rates in laboratory or mesocosm experiments. Because increasing DOC concentrations have been shown to increase rates of denitrification, it might provide a useful in-stream treatment option for WWTPs (Van Kessel 1978; Caffrey et al. 1993) however it may lead to concurrent issues of O_2 depletion (due to increased BOD). A possible solution to increasing DOC and ultimately BOD may be to construct a riffle-pool design in the stream which may help increase DO concentrations due to induced up-welling of waters (Naranjo et al. 2015).

Even though N_2O samples were collected using a well-documented headspace equilibration method (Kampbell et al. 1989; Robbins et al. 1993), sample volumes were limited to a 1 L bottle. Sampling campaigns also occurred bi-weekly, typically during daytime hours, contributing to error in temporal extrapolation, along with limited spatial coverage. Future studies could employ continual data measurements through the use of Fourier-transform infrared spectroscopy (FTIR) and the build-up of gases in a static flux chamber. However, the operation

and price of an FTIR device is extremely costly, especially when compared to the headspace technique, which could limit the number of sites at which it can be simultaneously situated (Rapson and Dacres 2014). Also, although Chapter 3 covered a wide range of flow, temperature, and even some winter conditions, winter sampling, especially under-ice, was not carried-out. While ice cover is a barrier to gas exchange, ice cover was not complete, and full emissions budgets would require research during this period. In addition, future cold weather studies could aim to monitor N_2O concentrations under ice throughout winter as these concentrations are rarely studied (Baulch et al. 2011, 2012b; Cavaliere and Baulch 2018). This would offer insight into potential pulses of emissions during ice-off in spring, and emissions from ice-free areas during winter.

Overall, this thesis provided a basis for future studies involving the impact of WWTPs on both nutrients, N cycling, and N_2O emissions. Wastewater treatment plants could implement new ways to manage their effluent and their impact on the ecosystem. With respect to estimating the C footprint of a WWTP, regulating authorities might institute methods to adequately encompass all WWTP effects, both direct and indirect. Moreover, the results from this thesis could also provide insight for the development of new frameworks aiming to quantify emissions from a WWTP. Although this thesis provided novel results on the N cycle and N_2O, more research must be performed to quantify other GHGs known to be important downstream of WWTPs—carbon dioxide (CO_2) and methane (CH_4). To fully assess the impact that a WWTP has on its receiving water body, other major biological processes such methanogenesis (biological CH_4 production), respiration (in-stream—CO_2), and nitrification (N_2O) could be explored. Moreover, the use of isotopes may also provide a possible way to constrain global N_2O production/ emissions (Wada and Ueda 1996; Thuss et al. 2014). Lastly, quantifying both downstream CO_2 and CH_4 emissions as well as direct WWTP GHG emissions (mainly CO_2, CH_4, and N_2O) would aid in better understanding the respective amounts of GHG emissions from both the plant and downstream ecosystem.

REFERENCES

Allan, R. J., and M. Roy. 1980. Lake Water Nutrient Chemistry and Chlorophyll a in Pasqua, Echo, Mission, Katepwa, Crooked and Round Lakes on the Qu'Appelle River, Saskatchewan, National W. Environment Canada.

Alvim, R. B., W. Zamboni de Mello, C. S. Silveira, D. C. Kligerman, and R. P. Ribeiro. 2014. Nitrous Oxide Emissions from Unpolluted and Polluted Rivers of the Paquequer River Basin (Teresopolis, Rio de Janeiro). Sanit. Environ. Eng. **19**.

Andersen, B. C., G. P. Lewis, and K. A. Sargent. 2004. Influence of Wastewater-treatment Effluent on Concentrations and Fluxes of Solutes in the Bush River, South Carolina, during Extreme Drought Conditions. Environ. Geosci. **11**: 28–41. doi:10.1306/eg.10200303017

Anderson, I. C., and J. S. Levine. 1986. Relative Rates of Nitric Oxide and Nitrous Oxide Production by Nitrifiers, Denitrifiers, and Nitrate Respirers. Appleid Environ. Microbiol. **51**: 938–945.

Antoniou, P., J. Hamilton, B. Koopman, R. Jain, B. Holloway, G. Lyberatos, and S. A. Svoronos. 1990. Effect of Temperature and ph on the Effective Maximum Specific Growth Rate of Nitrifying Bacteria. Water Res. **24**: 97–101. doi:10.1016/0043-1354(90)90070-M

Arango, C. P., and J. L. Tank. 2008. Land Use Influences the Spatiotemporal Controls on Nitrification and Denitrification in Headwater Streams. J. North Am. Benthol. Soc. **27**: 90–107. doi:10.1899/07-024.1

Arbabi, M., J. Elzinga, and C. ReVelle. 1974. The Oxygen Sag Equation: New Properties and a Linear Equation for the Critical Deficit. Water Resour. Res. **10**: 921–929.

ASTM International. 2016. Standard Test Method (D8083-16) for Total Nitrogen, and Total Kjeldahl Nitrogen (TKN) by Calculation, in Water by High Temperature Catalytic Combustion and Chemiluminescence Detection.

ASTM International. 2018. Standard Test Method (D7573-18) for Total Carbon and Organic Carbon in Water by High Temperature Catalytic Combustion and Infrared Detection.

Atinkpahoun, C. N. H., N. D. Le, S. Pontvianne, H. Poirot, J. P. Leclerc, M. N. Pons, and H. H. Soclo. 2018. Population Mobility and Urban Wastewater Dynamics. Sci. Total Environ. **622–623**: 1431–1437. doi:10.1016/j.scitotenv.2017.12.087

Audet, J., M. B. Wallin, K. Kyllmar, S. Andersson, and K. Bishop. 2017. Nitrous Oxide

Emissions from Streams in a Swedish Agricultural Catchment. Agric. Ecosyst. Environ. **236**: 295–303. doi:10.1016/j.agee.2016.12.012

Avanzino, R. J., and V. C. Kennedy. 1993. Long-Term Frozen Storage of Stream Water Samples for Dissolved Orthophosphate, Nitrate plus Nitrite, and Ammonia Analysis. Water Resour. Res. **29**: 3357–3362. doi:10.1029/93WR01684

Bartsch, A. F. 1948. Biological Aspects of Stream Pollution. Sewage Work. J. **20**: 292–302.

Baulch, H. M. 2009. Nitrous Oxide Emissions from Streams. Trent University.

Baulch, H. M., P. J. Dillon, R. Maranger, J. J. Venkiteswaran, H. F. Wilson, and S. L. Schiff. 2012a. Night and Day: Short-Term Variation in Nitrogen Chemistry and Nitrous Oxide Emissions from Streams. Freshw. Biol. **57**: 509–525. doi:10.1111/j.1365-2427.2011.02720.x

Baulch, H. M., S. L. Schiff, R. Maranger, and P. J. Dillon. 2011. Nitrogen Enrichment and the Emission of Nitrous Oxide from Streams. Global Biogeochem. Cycles **25**: 1–15. doi:10.1029/2011GB004047

Baulch, H. M., S. L. Schiff, R. Maranger, and P. J. Dillon. 2012b. Testing Models of Aquatic N_2O Flux for Inland Waters. Can. J. Fish. Aquat. Sci. **69**: 145–160. doi:10.1139/f2011-144

Bayo, J., J. López-Castellanos, and J. Puerta. 2016. Operational and Environmental Conditions for Efficient Biological Nutrient Removal in an Urban Wastewater Treatment Plant. Clean Soil, Air, Water **44**: 1123–1130. doi:10.1002/clen.201500972

Beaulieu, J. J., C. P. Arango, S. K. Hamilton, and J. L. Tank. 2008. The Production and Emission of Nitrous Oxide from Headwater Streams in the Midwestern United States. Glob. Chang. Biol. **14**: 878–894. doi:10.1111/j.1365-2486.2007.01485.x

Beaulieu, J. J., W. D. Shuster, and J. A. Rebholz. 2010. Nitrous Oxide Emissions from a Large, Impounded River: The Ohio River. Environ. Sci. Technol. **44**: 7527–7533. doi:10.1021/es1016735

Beck, M., N. Rivers, R. Wigle, and H. Yonezawa. 2015. Carbon Tax and Revenue Recycling: Impacts on Households in British Columbia. Resour. Energy Econ. **41**: 40–69. doi:10.1016/j.reseneeco.2015.04.005

Bernot, M. J., and W. K. Dodds. 2005. Nitrogen Retention, Removal, and Saturation in Lotic Ecosystems. Ecosystems **8**: 442–453. doi:10.1007/s10021-003-0143-y

Bernstein, B. B., and J. Zalinski. 1983. An Optimum Sampling Design and Power Tests for Environmental Biologists. J. Environ. Manage. **16**: 35–43.

Betlach, M. R., and J. M. Tiedje. 1981. Kinetic Explanation for Accumulation of Nitrite, Nitric Oxide, and Nitrous Oxide during Bacterial Denitrification. Appl. Environ. Microbiol. **42**: 1074–1084. doi:Article

Box, G. E. P., and D. R. Cox. 1964. An Analysis of Transformations. J. R. Stat. Soc. Ser. B **26**: 211–252.

Bradley, P. M., P. B. McMahon, and F. H. Chapelle. 1995. Effects of Carbon and Nitrate on Denitrification in Bottom Sediments of an Effluent Dominated River. Water Resour. Res. **31**: 1063–1068.

Brin, L. D., A. E. Giblin, and J. J. Rich. 2017. Similar Temperature Responses Suggest Future Climate Warning Will Not Alter Partitioning between Denitrification and Anammox in Temperate Marine Sediments. Glob. Chang. Biol. **23**: 331–340.

Broecker, W. S., and T. H. Peng. 1974. Gas Exchange Rates between Air and Sea. Tellus **1**–**2**: 21–35. doi:10.3402/tellusa.v26i1-2.9733

Burgin, A. J., and S. K. Hamilton. 2007. Have We Overemphasized the Role of Denitrification in Aquatic Ecosystems? A Review of Nitrate Removal Pathways. Front. Ecol. Environ. **5**: 89–96.

Burgos, M., A. Sierra, T. Ortega, and J. M. Forja. 2015. Anthropogenic Effects on Greenhouse Gas (CH_4 and N_2O) Emissions in the Guadalete River Estuary (SW Spain). Sci. Total Environ. **503**–**504**: 179–189. doi:10.1016/j.scitotenv.2014.06.038

Caffrey, J. M., N. P. Sloth, H. F. Kaspar, and T. H. Blackburn. 1993. Effect of Organic Loading on Nitrification and Denitrification in a Marine Sediment Microcosm. FEMS Microbiol. Ecol. **12**: 159–167. doi:http://dx.doi.org/

Camargo, J. A., and Á. Alonso. 2006. Ecological and Toxicological Effects of Inorganic Nitrogen Pollution in Aquatic Ecosystems: A Global Assessment. Environ. Int. **32**: 831–849. doi:10.1016/j.envint.2006.05.002

Canadian Council of Ministers of the Environment. 2010. Canadian Water Quality Guidelines for the Protection of Aquatic Life: Ammonia.

Canfield, D. E., A. N. Glazer, and P. G. Falkowski. 2010. The Evolution and Future of Earth's

Nitrogen Cycle. Science (80-.). **330**: 192–196. doi:10.1126/science.1186120

Carey, R. O., and K. W. Migliaccio. 2009. Contribution of Wastewater Treatment Plant Effluents to Nutrient Dynamics in Aquatic Systems: A Review. Environ. Manage. **44**: 205–217. doi:10.1007/s00267-009-9309-5

Cavaliere, E., and H. M. Baulch. 2018. Denitrification Under Lake Ice. Biogeochem. Lett. doi:10.1007/s10533-018-0419-0

Cavari, B. Z., and G. Phelps. 1977. Denitrification in Lake Kinneret in the Presence of Oxygen. Freshw. Biol. **7**: 385–391. doi:10.1111/j.1365-2427.1977.tb01686.x

Cavigelli, M. A., and P. G. Robertson. 2000. The Functional Significance of Denitrifier Community Composition in a Terrestrial Ecosystem. Ecol. Soc. Am. **81**: 1402–1414.

Chambers, P. A., G. J. Scrimgeour, and A. Pietroniro. 1997. Winter Oxygen Conditions in Ice-Covered Rivers: The Impact of Pulp Mill and Municipal Effluents. Popul. (English Ed. **2806**: 2796–2806. doi:10.1139/cjfas-54-12-2796

Chapra, S. C., and D. M. Di Toro. 1991. Delta Method for Estimating Primary Production, Respiration, and Reaeration in Streams. J. Environ. Eng. **117**: 640–655.

Chen, N., J. Wu, X. Zhou, Z. Chen, and T. Lu. 2015. Riverine N_2O Production, Emissions and Export from a Region Dominated by Agriculture in Southeast Asia (Jiulong River). Agric. Ecosyst. Environ. **208**: 37–47. doi:10.1016/j.agee.2015.04.024

Cherry, K. A., M. Shepherd, P. J. A. Withers, and S. J. Mooney. 2008. Assessing the Effectiveness of Actions to Mitigate Nutrient Loss from Agriculture: A Review of Methods. Sci. Total Environ. **406**: 1–23. doi:10.1016/j.scitotenv.2008.07.015

Christensen, P. B., and J. Serrensen. 1988. Denitrification in Sediment of Lowland Streams: Regional and Seasonal Variation in Gelbaek and Rabis Baek, Denmark. FEMS Microbiol. Ecol. **53**: 335–344.

Churchill, M. A., H. L. Elmore, and R. A. Buchingham. 1962. The Prediction of Stream Reaeration Rates. J. Sanit. Eng. Div. Am. Soc. Eng. **88**: 1–46.

Van Cleemput, O., and W. H. Patrick. 1974. Nitrate and Nitrite Reduction in Flooded Gamma-Irradiated Soil Under Controlled pH and Redox Potential Conditions. Soil Biol. Biochem. **6**: 85–88. doi:10.1016/0038-0717(74)90064-9

Clough, T. J., L. E. Buckthought, F. M. Kelliher, and R. R. Sherlock. 2007. Diurnal Fluctuations

of Dissolved Nitrous Oxide (N2O) Concentrations and Estimates of N2O Emissions from a Spring-fed River: Implications for IPCC Methodology. Glob. Chang. Biol. **13**: 1016–1027. doi:10.1111/j.1365-2486.2007.01337.x

Cnaan, A., N. Laird, and P. Slasor. 1997. Using the General Linear Mixed Model to Analyse Unbalanced Repeated Measures and Longitudinal Data. Stat. Med. **16**: 2349–2380. doi:10.1002/(SICI)1097-0258(19971030)16:20<2349::AID-SIM667>3.0.CO;2-E [pii]

Cole, J. I., and N. F. Caraco. 1998. Atmospheric Exchange of Carbon Dioxide in a Low-Wind Oligotrophic Lake Measured by the Addition of SF_6. Limnol. Oceanogr. **43**: 647–656.

Cooke, J. G., and R. E. White. 1987. Spatial Distribution of Denitrification Activity in a Stream Draining an Agricultural Catchment. Freshw. Biol. **18**: 509–519.

Cornwell, J. C., M. W. Kemp, and T. M. Kana. 1999. Denitrification in Coastal Ecosystems: Methods, Environmental Controls, and Ecosystem Level Controls, A Review. Aquat. Ecol. **33**: 41–54. doi:10.1023/A

Correll, D. L. 1998. The Role of Phosphorus in the Eutrophication of Receiving Waters: A Review. J. Environ. Qual. **27**: 261. doi:10.2134/jeq1998.00472425002700020004x

Czepiel, P., P. Crill, and R. Harriss. 1995. Nitrous Oxide Emissions from Municipal Wastewater Treatment. Environ. Sci. Technol. **29**: 2352–2356. doi:10.1021/es00009a030

Daims, H., E. V. Lebedeva, P. Pjevac, and others. 2015. Complete Nitrification by Nitrospira Bacteria. Nature **528**: 504–509. doi:10.1038/nature16461

Dalsgaard, T., B. Thamdrup, and D. E. Canfield. 2005. Anaerobic Ammonium Oxidation (Anammox) in the Marine Environment. Res. Microbiol. **156**: 457–464. doi:10.1016/j.resmic.2005.01.011

David, A., J.-L. Perrin, D. Rosain, and others. 2011. Implication of Two In-stream Processes in the Fate of Nutrients Discharged by Sewage System into a Temporary River. Environ. Monit. Assess. **181**: 491–507. doi:10.1007/s10661-010-1844-2

Davies, T. R., and W. A. Pretorius. 1975. Denitrification with a Bacterial Disc Unit. Water Res. **9**: 459–463. doi:10.1016/0043-1354(75)90193-1

Deemer, B. R., J. A. Harrison, S. Li, and others. 2016. Greenhouse Gas Emissions from Reservoir Water Surfaces: A New Global Synthesis Manuscript. Bioscience **66**: 949–964. doi:10.1093/biosci/biw117

Demars, B. O. L., J. Thompson, and J. R. Manson. 2015. Stream Metabolism and the Open Diel Oxygen Method: Principles, Practice, and Perspectives. Limnol. Oceanogr. Methods **13**: 356–374. doi:10.1002/lom3.10030

Dodds, W. K. K., and E. B. Welch. 2000. Establishing Nutrient Criteria in Streams. Source J. North Am. Benthol. Soc. J. N. Am. Benthol. Soc **19**: 186–196.

Dong, H., H. Dai, Y. Geng, and others. 2017. Exploring Impact of Carbon Tax on China's CO_2 Reductions and Provincial Disparities. Renew. Sustain. Energy Rev. **77**: 596–603. doi:10.1016/j.rser.2017.04.044

Duchemin, E., M. Lucotte, and R. Canuel. 1998. Comparison of Static Chamber and Thin Boundary Layer Equation Methods for Measuring Greenhouse Gas Emissions from Large Water Bodies. Environ. Sci. Technol. **33**: 350–357. doi:10.1021/es9800840

Eberhardt, L. L. 1976. Quatitative Ecology and Impact Assessment. J. Environ. Manage. **4**: 27–70.

Ekka, S. A., B. E. Haggard, M. D. Matlock, and I. Chaubey. 2006. Dissolved Phosphorus Concentrations and Sediment Interactions in Effluent–Dominated Ozark Streams. Ecol. Eng. **26**: 375–391. doi:10.1016/j.ecoleng.2006.01.002

Emerson, K., R. C. Russo, R. E. Lund, and R. V. Thurston. 1975. Aqueous Ammonia Equilibrium Calculations: Effect of pH and Temperature. J. Fish. Res. Board Canada **32**: 2379–2383.

Emmet, R. T. 1969. Spectrophotometric Determination of Urea and Ammonia in Natural Waters with Hypochlorite and Phenol. Anal. Chem. **41**: 1648–1652. doi:10.1021/ac60281a007

Environment Canada. 1999. Canadian Environmental Protection Act, 1999 - Priority Substances List Assessment Report.

Environment Canada. 2017a. Real-Time Hydrometric Data Graph for Wascana Creek Near Lumsden (05JF005)[SK]. Real-Time Data.

Environment Canada. 2017b. Real-Time Hydrometric Graph for Qu'Appelle River Near Lumsden (05JF001)[SK]. Real-Time Data.

Environment Canada. 2018. Canadian Climate Normals 1981-2010 Station Data. Clim. Norm. Averages.

Environmental Protection Agency. 2013. Aquatic Life Ambient Water Quality Criteria for

Ammonia – Freshwater. 255.

Evrard, V., R. N. Glud, and P. L. M. Cook. 2013. The Kinetics of Denitrification in Permeable Sediments. Biogeochemistry **113**: 563–572. doi:10.1007/s10533-012-9789-x

Fair, G. M. 1939. The Dissolved Oxygen Sag: An Analysis. Sewage Work. J. **11**: 445–461.

Figueroa-Nieves, D., W. H. Mcdowell, J. D. Potter, and G. Martínez. 2016. Limited Uptake of Nutrient Input from Sewage Effluent in a Tropical Landscape. Soc. Freshw. Sci. **35**: 12–24. doi:10.1086/684992

Firestone, M. K., and E. A. Davidson. 1989. Microbiological Basis of NO and N_2O Production and Consumption in Soil. Exch. Trace Gases between Terr. Ecosyst. Atmos. 7–21.

Flather, D. H., and E. G. Beauchamp. 1992. Inhibition of the Fermentation Process in Soil by Acetylene. Soil Biol. Biochem. **24**: 905–911. doi:10.1016/0038-0717(92)90013-N

Foley, J., D. de Haas, Z. Yuan, and P. Lant. 2009. Nitrous Oxide Generation in Full-Scale Biological Nutrient Removal Wastewater Treatment Plants. Water Res. **44**: 831–844. doi:10.1016/j.watres.2009.10.033

Fowler, D., M. Coyle, U. Skiba, and others. 2013. The Global Nitrogen Cycle in the Twenty-First Century. Philos. Trans. R. Soc. B Biol. Sci. **368**: 1–13. doi:http://dx.doi.org/10.1098/rstb.2013.0164

Fox, J., and S. Weisberg. 2011. An R Companion to Applied Regression, Second.

Galloway, J. N., J. D. Aber, J. W. Erisman, S. P. Seitzinger, R. W. Howarth, E. B. Cowling, and J. B. Cosby. 2003. The Nitrogen Cascade. Bioscience **53**: 341–356.

Galloway, J. N., F. J. Dentener, D. G. Capone, and others. 2004. Nitrogen Cycles: Past, Present, and Future. Biogeochemistry **70**: 153–226.

Galloway, J. N., W. H. Schlesinger, H. Levy II, A. Michaels, and J. L. Schnoor. 1995. Nitrogen Fixation: Anthropogenic Enhancement-Environmental Repsonse. Global Biogeochem. Cycles **9**: 235–252.

Gammons, C. H., J. N. Babcock, S. R. Parker, and S. R. Poulson. 2011. Diel Cycling and Stable Isotopes of Dissolved Oxygen, Dissolved Inorganic Carbon, and Nitrogenous Species in a Stream Receiving Treated Municipal Sewage. Chem. Geol.

Garcia-Ruiz, R., S. N. Pattinson, and B. A. Whitton. 1998. Kinetic Parameters of Denitrification in a River Continuum. Appl. Environ. Microbiol. **64**: 2533–2538.

Garcia-Ruiz, R., S. N. Pattinson, and B. A. Whitton. 1999. Nitrous Oxide Production in the River Swale-Ouse, North-East England. Water Res. **33**: 1231–1237.

Garnier, J., G. Billen, G. Vilain, A. Martinez, M. Silvestre, E. Mounier, and F. Toche. 2009. Nitrous oxide (N_2O) in the Seine River and Basin: Observations and Budgets. Agric. Ecosyst. Environ. **133**: 223–233. doi:10.1016/j.agee.2009.04.024

Gejlsbjerg, B., L. Frette, and P. Westermann. 1998. Dynamics of N_2O Production from Activated Sludge. Water Res. **32**: 2113–2121.

Gernaey, K. V., X. Flores-Alsina, C. Rosen, L. Benedetti, and U. Jeppsson. 2011. Dynamic Influent Pollutant Disturbance Scenario Generation Using a Phenomenological Modelling Approach. Environ. Model. Softw. **26**: 1255–1267. doi:10.1016/j.envsoft.2011.06.001

Giling, D., R. Mac Nally, N. Bond, and M. Grace. 2018. User Guide for Package 'BASEmetab.' 1–11.

Gooding, R. M., and H. M. Baulch. 2017. Small Reservoirs as a Beneficial Management Practice for Nitrogen Removal. J. Environ. Qual. **46**: 96–104. doi:10.2134/jeq2016.07.0252

Goreau, T. J., W. A. Kaplan, and S. C. Wofsy. 1980. Production of NO_2^- and N_2O by Nitrifying Bacteria at Reduced Concentrations of Oxygen. Appl. Environ. Microbiol. **40**: 526–532.

Government of Canada. 2017. Canadian Climate Normals 1981-2010.

Government of Canada, and Agriculture and Agri-Food Canada. 2018. Land Use 2010.

Government of Canada, and Natural Resources Canada. 2018. National Hydro Network - NHN - GeoBase Series.

Grace, M. R., D. P. Giling, S. Hladyz, V. Caron, R. M. Thompson, and R. Mac Nally. 2015. Fast Processing of Diel Oxygen Curves: Estimating Stream Metabolism with BASE (BAyesian Single-station Estimation). Limnol. Oceanogr. Methods **13**: 103–114. doi:10.1002/lom.10011

Grantz, E. M., A. Kogo, and J. Thad Scott. 2012. Partitioning Whole-lake Denitrification using In Situ Dinitrogen Gas Accumulation and Intact Sediment Core Experiments. Limnol. Oceanogr. **57**: 925–935. doi:10.4319/lo.2012.57.4.0925

Groffman, P. M., M. A. Altabet, J. K. Bohlke, and others. 2006. Methods for Measuring Denitrification: Diverse Approaches to a Difficult Problem. Ecol. Appl. **16**: 2091–2122. doi:10.1890/1051-0761

Groffman, P. M., E. A. Holland, D. D. Myrold, G. P. Robertson, and X. Zou. 1999. Denitrification, p. 273–288. *In* G.P. Robertson, C.S. Bledsoe, D.C. Coleman, and P. Sollins [eds.], Standard Soil Methods for Long-Term Ecological Research. Oxford University Press.

Gustavsson, D. J. I., and S. Tumlin. 2013. Carbon Footprints of Scandinavian Wastewater Treatment Plants. Water Sci. Technol. **68**: 887–893.

Hamersley, M. R., D. Woebken, B. Boehrer, M. Schultze, G. Lavik, and M. M. M. Kuypers. 2009. Water Column Anammox and Denitrification in a Temperate Permanently Stratified Lake (Lake Rassnitzer, Germany). Syst. Appl. Microbiol. **32**: 571–582. doi:10.1016/j.syapm.2009.07.009

Hammer, U. T. 1971. Limnological Studies of the Lakes and Streams of the Upper Qu'Appelle River System, Saskatchewan, Canada. Hydrobiologia **37**: 473–507. doi:10.1007/BF00018815

Harrison, J. A., P. A. Matson, and S. E. Fendorf. 2005. Effects of a Diel Oxygen Cycle on Nitrogen Transformations and Greenhouse Gas Emissions in a Eutrophied Subtropical Stream. Aquat. Sci. **67**: 308–315. doi:10.1007/s00027-005-0776-3

Harrison, J., and P. Matson. 2003. Patterns and Controls of Nitrous Oxide Emissions from Waters Draining a Subtropical Agricultural Valley. Global Biogeochem. Cycles **17**: 1–13. doi:10.1029/2002GB001991

Hasegawa, K., K. Hanaki, T. Matsuo, and S. Hidaka. 2000. Nitrous Oxide from the Agricultural Water System Contaminated with High Nitrogen. Chemosph. - Glob. Chang. Sci. **2**: 335–345. doi:10.1016/S1465-9972(00)00009-X

Hemond, H. F., and A. P. Duran. 1989. Fluxes of N_2O at the Sediment-Water and Water-Atmosphere Boundaries of a Nitrogen-Rich River. Water Resour. Res. **25**: 839–846.

Hernández-Chover, V., Á. Bellver-Domingo, and F. Hernández-Sancho. 2018. Efficiency of Wastewater Treatment Facilities: The Influence of Scale Economies. J. Environ. Manage. **228**: 77–84. doi:10.1016/j.jenvman.2018.09.014

Herrman, K. S., V. Bouchard, and R. H. Moore. 2008. Factors Affecting Denitrification in Agricultural Headwater Streams in Northeast Ohio, USA. Hydrobiologia **598**: 305–314. doi:10.1007/s10750-007-9164-4

Hershey, A. E., A. J. Ulseth, and K. Fortino. 2004. Use of Stable Isotopes to Trace Sewage Effluent through a Forested Mid-order Stream in the Vicinity of Greensboro, N.C. *Proceedings of the 77th Annual Water Environment Federation Technical Exhibition and Conference*. Water Environment Federation.

Holeton, C., P. A. Chambers, L. Grace, and K. Kidd. 2011. Wastewater Release and Its Impacts on Canadian Waters. Can. J. Fish. Aquat. Sci. **68**: 1836–1859. doi:10.1139/f2011-096

Holmes, R. M., J. B. Jones, S. G. Fisher, and N. B. Grimm. 1996. Denitrification in a Nitrogen-Limited Stream Ecosystem. Biogeochemistry **33**: 125–146. doi:10.1007/BF02181035

Hothorn, T., F. Bretz, and P. Westfall. 2008. Simultaneous Inference in General Parametric Models. Biometrical J. **50**: 346–363.

Hu, B. L., L. D. Shen, P. Zheng, A. hui Hu, T. T. Chen, C. Cai, S. Liu, and L. P. Lou. 2012. Distribution and Diversity of Anaerobic Ammonium-Oxidizing Bacteria in the Sediments of the Qiantang River. Environ. Microbiol. Rep. **4**: 540–547. doi:10.1111/j.1758-2229.2012.00360.x

Inwood, S. E., J. L. Tank, and M. J. Bernot. 2005. Patterns of Denitrification Associated with Land Use in 9 Midwestern Headwater Streams. J. North Am. Benthol. Soc. **24**: 227–245. doi:10.1899/04-032.1

IPCC. 2001. Atmospheric Chemistry and Greenhouse Gases.

IPCC. 2006. Chapter 6: Wastewater Treatment and Discharge, p. 1–28. *In* Volume 5: Waste.

IPCC. 2007. Couplings Between Changes in the Climate System and Biogeochemistry.

IPCC. 2013. Carbon and other Biogeochemical Cycles.

IPCC. 2014. Climate Change 2014: Synthesis Report.

Jähne, B., and H. Haußecker. 1998. Air-Water Gas Exchange. Annu. Rev. Fluid Mech. **30**: 443–468.

Jähne, B., G. Heinz, and W. Dietrich. 1987. Measurement of the Diffusion Coefficients of Sparingly Soluble Gases in Water. J. Geophys. Res. Ocean. **92**: 10767–10776. doi:10.1029/JC092iC10p10767

Jetten, M. S. M., M. Strous, K. T. van de Pas-Schoonen, and others. 1999. The Anaerobic Oxidation of Ammonium. FEMS Microbiol. Rev. **22**: 421–437. doi:10.1111/j.1574-6976.1998.tb00379.x

Ji, Q., A. R. Babbin, A. Jayakumar, S. Oleynik, and B. B. Ward. 2015. Nitrous Oxide Production by Nitrification and Denitrification in the Eastern Tropical South Pacific Oxygen Minimum Zone. Geophys. Res. Lett. **10**: 755–764. doi:10.1002/2015GL066853

Jiang, Q.-Q., and L. R. Bakken. 1999. Nitrous Oxide Production and Methane Oxidation by Different Ammonia-Oxidizing Bacteria. Appl. Environ. Microbiol. **65**: 2679–2684.

Jofre, M. B., and W. H. Karasov. 1999. Direct Effect of Ammonia on Three Species of North American Anuran Amphibians. Environ. Toxicol. Chem. **18**: 1806–1812. doi:10.1002/etc.5620180829

Johnston, C. A., N. E. Detenbeck, and G. J. Niemi. 1990. The Cumulative Effect of Wetlands on Stream Water Quality and Quantity. A Landscape Approach. Biogeochemistry **10**: 105–141.

Jørgensen, K. S., H. B. Jensen, and J. Sørensen. 1984. Nitrous Oxide Production from Nitrification and Denitrification in Marine Sediment at Low Oxygen Concentrations. Can. J. Microbiol. **30**: 1073–1078.

Kampbell, D. H., J. T. Wilson, and S. A. Vandegrift. 1989. Dissolved Oxygen and Methane in Water by a GC Headspace Equilibration Technique. Int. J. Environ. Anal. Chem. **36**: 249–257. doi:10.1080/03067318908026878

Kampschreue, M. J., H. Temmink, R. Kleerebezem, M. S. M. Jetten, and M. C. M. van Loosdrecht. 2009. Nitrous Oxide Emission during Wastewater Treatment. Water Res. **43**: 4093–4103. doi:10.1016/j.watres.2009.03.001

Kanter, D., D. L. Mauzerall, A. R. Ravishankara, J. S. Daniel, R. W. Portmann, P. M. Grabiel, W. R. Moomaw, and J. N. Galloway. 2013. A Post-Kyoto Partner: Considering the Stratospheric Ozone Regime as a Tool to Manage Nitrous Oxide. Proc. Natl. Acad. Sci. U. S. A. **110**: 4451–4457. doi:10.1073/pnas.1222231110

Kartal, B., W. J. Maalcke, N. M. De Almeida, and others. 2011. Molecular Mechanism of Anaerobic Ammonium Oxidation. Nature **479**: 127–130. doi:10.1038/nature10453

Kaspar, H. F. 1982. Dentrification in Marine Sediment: Measurement of Capacity and Estimate of In Situ Rate. Appl. Environ. Microbiol. **43**: 522–527.

Kassambara, A. 2018. ggpubr: “ggplot2” Based Publication Ready Plots. R Packag. version 0.1.7.

Kayla Gallant personal communication. 2018. Regina Wastewater Treatment Plant.

Kemp, M. J., and W. K. Dodds. 2002. The Influence of Ammonium, Nitrate, and Dissolved Oxygen Concentrations on Uptake, Nitrification, and Denitrification Rates associated with Prairie Stream Substrata. Limnol. Oceanogr. **47**: 1380–1393. doi:10.4319/lo.2002.47.5.1380

Van Kessel, J. F. 1978. Gas Production in Aquatic Sediments in the Presence and Absence of Nitrate. Water Res. **12**: 291–297. doi:10.1016/0043-1354(78)90115-X

Kessel, M. A. H. J. Van, D. R. Speth, M. Albertsen, P. H. Nielsen, and J. M. Huub. 2016. Complete Nitrification by a Single Microorganism. Nature **528**: 555–559. doi:10.1038/nature16459.Complete

Khalil, K., B. Mary, and P. Renault. 2004. Nitrous Oxide Production by Nitrification and Denitrification in Soil Aggregates as Affected by O_2 Concentration. Soil Biol. Biochem. **36**: 687–699. doi:10.1016/j.soilbio.2004.01.004

Khalil, M. A. K., and R. A. Rasmussen. 1992. The Global Sources of Nitrous Oxide. J. Geophys. Res. **97**: 14651–14660. doi:10.1029/92JD01222

Kim, H. 2014. Factors Controlling Sediment Denitrification Rates in Grassland and Forest Streams. Terr. Atmos. Ocean. Sci. **25**: 463–470. doi:10.3319/TAO.2014.01.09.01(Hy)

Kimochi, Y., Y. Inamori, M. Mizuochi, K.-Q. Xu, and M. Matsumura4. 1998. Nitrogen Removal and N_2O Emission in a Full-Scale Domestic Wastewater Treatment Plant with Intermittent Aeration. J. Ferment. Bioeng. **86**: 202–206.

Klopffer, W. 1997. Life Cycle Assessment From the Beginning to the Current State. Environ. Sci. Pollut. Res. **4**: 223–228.

Knowles, R. 1982. Denitrification. Microbiol. Rev. **46**: 43–70.

Knowles, R., and T. Yoshinari. 1976. Acetylene Inhibition of Nitrous Oxide Reduction by Denitrifying Bacteria. Biocehmical Biophys. Res. Commun. **69**: 705–710.

Köppen, W., and R. Geiger. 1936. Handbook of Climatology,.

Korom, S. F. 1992. Natural Denitrification in the Saturated Zone: A Review. Water Resour. Res. **28**: 1657–1668. doi:10.1029/92WR00252

Kremer, J. N., S. W. Nixon, B. Buckley, and P. Roques. 2003. Technical Note : Conditions for Using the Floating Chamber Method to Estimate Air-Water Gas Exchange Background. Estuaries **26**: 985–990. doi:10.1007/BF02803357

Kroeze, C., E. Dumont, and S. Seitzinger. 2010. New Estimates of Global Emissions of N_2O from Rivers and Estuaries. J. Integr. Environ. Sci. **2**: 159–165. doi:10.1080/1943815X.2010.496789

Kuznetsova, A., P. B. Brockhoff, and R. H. B. Christensen. 2017. lmerTest Package: Tests in Linear Mixed Effects Models. J. Stat. Softw. **82**: 1–26. doi:10.18637/jss.v082.i13

Lambert, M., and J. L. Fréchette. 2005. Analytical Techniques for Measuring Fluxes of CO_2 and CH_4 from Hydroelectric Reservoirs and Natural Water Bodies, p. 37–60. *In* A. Tremblay, L. Varfalvy, C. Roehm, and M. Garneau [eds.], Greenhouse Gas Emissions—Fluxes and Processes. Springer Berlin Heidelberg.

Laursen, A. E., and S. P. Seitzinger. 2004. Diurnal Patterns of Denitrification, Oxygen Consumption and Nitrous Oxide Production in Rivers Measured at the Whole-reach Scale. Freshw. Biol. **49**: 1448–1458. doi:10.1111/j.1365-2427.2004.01280.x

Laursen, A., and S. Seitzinger. 2005. Limitations to Measuring Riverine Denitrification at the Whole Reach Scale: Effects of Channel Geometry, Wind Velocity, Sampling Interval, and Temperature Inputs of N_2-Enriched Groundwater. Hydrobiologia **545**: 225–236. doi:10.1007/s10750-005-2743-3

Law, Y., L. Ye, Y. Pan, and Z. Yuan. 2012. Nitrous Oxide Emissions from Wastewater Treatment Processes. Philos. Trans. Biol. Sci. **367**: 1265–1277. doi:10.1098/rstb.2011.0317

Leavitt, P. R., C. S. Brock, C. Ebel, and A. Patoine. 2006. Landscape-scale effects of urban nitrogen on a chain of freshwater lakes in central North America. Limnol. Oceanogr. **51**: 2262–2277.

Liao, M., G. Yu, and Y. Guo. 2017. Eutrophication in Poyang Lake (Eastern China) Over the Last 300 Years in Response to Changes in Climate and Lake Biomass. PLoS One **12**: 1–22. doi:10.1371/journal.pone.0169319

Lindstrom, M. J., and D. M. Bates. 1990. Nonlinear Mixed Effects Models for Repeated Measures Data. Int. Biometric Soc. **46**: 673–687.

Liss, P. S., and P. G. Slater. 1974. Flux of Gases across the Air-Sea Interface. Nature **247**: 181–184. doi:10.1038/247181a0

Liu, X.-L., L. Bai, Z.-L. Wang, J. Li, F.-J. Yue, and S.-L. Li. 2015. Nitrous Oxide Emissions from River Network with Variable Nitrogen Loading in Tianjin, China. J. Geochemical

Explor. **157**: 153–161. doi:10.1016/j.gexplo.2015.06.009

Liu, X. L., C. Q. Liu, S. L. Li, F. S. Wang, B. L. Wang, and Z. L. Wang. 2011. Spatiotemporal Variations of Nitrous Oxide (N_2O) Emissions from Two Reservoirs in SW China. Atmos. Environ. **45**: 5458–5468. doi:10.1016/j.atmosenv.2011.06.074

Lofton, D. D., A. E. Hershey, and S. C. Whalen. 2007. Evaluation of Denitrification in an Urban Stream Receiving Wastewater Effluent. Biogeochemistry **86**: 77–90. doi:10.1007/s10533-007-9146-7

Lohmann, U., R. Sausen, L. Bengtsson, U. Cubasch, J. Perlwitz, and E. Roeckner. 1993. The Koppen Climate Classification as a Diagnostic Tool for General Circulation Models. Clim. Res. **3**: 177–193. doi:10.3354/cr003177

Lorke, A., P. Bodmer, C. Noss, and others. 2015. Technical Note: Drifting Versus Anchored Flux Chambers for Measuring Greenhouse Gas Emissions from Running Waters. Biogeosciences **12**: 7013–7024. doi:10.5194/bg-12-7013-2015

Van Luijn, F., P. C. M. Boers, L. Lijklema, and J.-P. R. A. Sweerts. 1999. Nitrogen Fluxes and Processes in Sandy and Muddy Sediments from a Shallow Eutrophic Lake. Water Res. **33**: 33–42. doi:10.1016/S0043-1354(98)00201-2

Maag, M., and F. P. Vinther. 1996. Nitrous Oxide Emission by Nitrification and Denitrification in Different Soil Types and at Different Soil Moisture Contents and Temperatures. Appl. Soil Ecol. **4**: 5–14. doi:10.1016/0929-1393(96)00106-0

Martikainen, P. J. 1985. Nitrous Oxide Emission Associated with Autotrophic Ammonium Oxidation in Acid Coniferous Forest Soil. Appl. Environ. Microbiol. **50**: 1519–25.

Martin, L. A., P. J. Mulholland, J. R. Webster, and H. M. Valett. 2001. Denitrification Potential in Sediments of Headwater Streams in the Southern Appalachian. J. North Am. Benthol. Soc. **20**: 505–519.

Matos, C., C. A. Teixeira, A. A. L. S. Duarte, and I. Bentes. 2013. Domestic Water Uses: Characterization of Daily Cycles in the North Region of Portugal. Sci. Total Environ. **458–460**: 444–450. doi:10.1016/j.scitotenv.2013.04.018

McBride, G. B., and S. C. Chapra. 2005. Rapid Calculation of Oxygen in Streams: Approximate Delta Method. J. Environ. Eng. **131**: 336–343.

McClain, M. E., E. W. Boyer, C. L. Dent, and others. 2003. Biogeochemical Hot Spots and Hot

Moments at the Interface of Terrestrial and Aquatic Ecosystems. Ecosystems **6**: 301–312. doi:10.1007/s10021-003-0161-9

McElroy, M. B., W. Elkins, S. C. Wofsy, C. E. Kolb, A. P. Dura, and W. A. Kaplan. 1978. Production and release of N_2O from the Potomac Estuary. Limnol. Oceanogr. **23**: 1168–1182.

McMahon, P. B., and K. F. Dennehy. 1999. N_2O Emission from a Nitrogen-Enriched River. Environ. Sci. Technol. **33**: 21–25.

Meals, D. W., S. A. Dressing, and T. E. Davenport. 2010. Lag Time in Water Quality Response to Best Management Practices: A Review. J. Environ. Qual. **39**: 85–96. doi:10.2134/jeq2009.0108

Mekonnen, M. M., and A. Y. Hoekstra. 2018. Global Anthropogenic Phosphorus Loads to Freshwater and Associated Grey Water Footprints and Water Pollution Levels: A High-Resolution Global Study. Water Resour. Res. **54**: 345–358. doi:10.1002/2017WR020448

Metcalf, G. E., S. Paltsev, J. M. Reilly, and others. 2008. MIT Joint Program on the Science and Policy of Global Change Analysis of U.S. Greenhouse Gas Tax Proposals Analysis of U.S. Greenhouse Gas Tax Proposals.

Van Meter, K. J., N. B. Basu, J. J. Veenstra, and C. . . Burras. 2016. The Nitrogen Legacy: Emerging Evidence of Nitrogen Accumulation in Anthropogenic Landscapes. Environ. Res. Lett. **11**: 1–24.

Migliaccio, K. W., B. E. Haggard, I. Chaubey, and M. D. Matlock. 2007. Linking Watershed Subbasin Characteristics to Water Quality Parameters in War Eagle Creek Watershed. Trans. ASABE **50**: 2007–2016.

Ministry of the Environment. 2001. The Determination of Ammonium Nitrogen and Nitrate Plus Nitrite Nitrogen in Water and Precipitation by Colorimetry, *In* Ministry of Environment Laboratory Services Branch Quality Management Unit.

Molinos-Senante, M., N. Hanley, and R. Sala-Garrido. 2015. Measuring the CO_2 Shadow Price for Wastewater Treatment: A Directional Distance Function Approach. Appl. Energy **144**: 241–249. doi:10.1016/j.apenergy.2015.02.034

Moore, T. A., Y. Xing, B. Lazenby, and others. 2011. Prevalence of Anaerobic Ammonium-Oxidizing Bacteria in Contaminated Groundwater. Environ. Sci. Technol. **45**: 7217–7225.

doi:10.1021/es201243t

Mortimer, C. H. 1941. The Exchange of Dissolved Substances Between Mud and Water in Lakes. J. Ecol. **29**: 280–329.

Mosier, A., C. Kroeze, C. Nevison, O. Oenema, and S. Seitzinger. 1998. Closing the Global N_2O Budget : Nitrous Oxide Emissions Through the Agricultural Nitrogen Cycle Inventory Methodology. Nutr. Cycl. Agroecosystems **52**: 225–248. doi:10.1023/A:1009740530221

Mulholland, P. J., R. O. Hall, D. J. Sobota, and others. 2009. Nitrate Removal in Stream Ecosystems Measured by $^{N}15$ Addition Experiments: Denitrification. Limnol. Oceanogr. **54**: 653–665. doi:10.4319/lo.2009.54.3.0653

Mulholland, P. J., A. M. Helton, G. C. Poole, and others. 2008. Stream Denitrification across Biomes and its Response to Anthropogenic Nitrate Loading. Nature **452**: 202–206. doi:10.1038/nature06686

Müller, M. M., V. Sundman, and J. Skujins. 1980. Denitrification in Low pH Spodosols and Peats Determined with the Acetylene Inhibition Method. Appl. Environ. Microbiol. **40**: 235–239.

Munodawafa, T. P., and A. Chitata. 2012. Assessment of Human Impact on Water Quality along Manyame River. Int. J. Dev. Sustain. **1**: 754–765.

Murray, S. J., P. N. Foster, and I. C. Prentice. 2012. Future Global Water Resources with Respect to Climate Change and Water Withdrawals as Estimated by a Dynamic Global Vegetation Model. J. Hydrol. **448**–**449**: 14–29. doi:10.1016/j.jhydrol.2012.02.044

Nakagawa, S., and H. Schielzeth. 2010. Repeatability for Gaussian and Non-Gaussian Data: A Practical Guide for Biologists. Biol. Rev. **85**: 935–956. doi:10.1111/j.1469-185X.2010.00141.x

Naranjo, R. C., R. G. Niswonger, and C. J. Davis. 2015. Mixing Effects on Nitrogen and Oxygen Concentrations and the Relationship to Mean Residence Time in a Hyporheic Zone of a Riffle-pool Sequence. Water Resour. Res. **51**: 5974–5997. doi:10.1002/2014WR015608

NOAA, and ESRL. 2018. Nitrous Oxide Data from the NOAA/ESRL Halocarbons in situ Program.

O'Connor, D. 1967. The Temporal and Spatial Distribution of Dissolved Oxygen in Streams. Water Res. **3**: 65–79.

O'Connor, D. J., and W. E. Dobbins. 1958. Mechanism of Reaeration in Natural Streams. Am. Soc. Civ. Eng. Trans. **123**: 641–684.

Oenema, O., N. Wrage, G. L. Velthof, J. W. Van Groenigen, and P. J. Kuikman. 2005. Trends in Global Nitrous Oxide Emissions from Animal Production Systems. Nutr. Cycl. Agroecosystems **72**: 51–65. doi:10.1007/s10705-004-7354-2

Oremland, R. S., C. Umberger, C. W. Culbertson, and R. L. Smith. 1984. Denitrification in San Francisco Bay Intertidal Sediments. Appl. Environ. Microbiol. **47**: 1106–1112.

Oren, A., and T. H. Blackburn. 1979. Estimation of Sediment Denitrification Rates at In Situ Nitrate Concentrations. Appl. Environ. Microbiol. **37**: 174–176.

Orihel, D. M., H. M. Baulch, N. J. Casson, R. L. North, C. T. Parsons, D. C. M. Seckar, and J. J. Venkiteswaran. 2017. Internal Phosphorus Loading in Canadian Fresh Waters: A Critical Review and Data Analysis. Can. J. Fish. Aquat. Sci. **2029**: 1–25. doi:10.1139/cjfas-2016-0500

Outram, F. N., and K. M. Hiscock. 2012. Indirect Nitrous Oxide Emissions from Surface Water Bodies in A Lowland Arable Catchment: A Significant Contribution to Agricultural Greenhouse Gas Budgets? Environ. Sci. Technol. **46**: 8156–8163. doi:10.1021/es3012244

Owens, M., R. W. Edwards, and J. W. Gibbs. 1964. Some Reaeration Studies in Streams. Int. J. Air Water Pollut. **8**: 469–486.

Park, K. Y., Y. Inamori, M. Mizuochi, and K. Hong Ahn. 2000. Emission and Control of Nitrous Oxide from a Biological Wastewater Treatment System with Intermittent Aeration. J. Biosci. Bioeng. **90**: 247–252.

Perrin, D. D. 1982. Ionization Constants of Inorganic Acids and Bases in Aqueous Solution, Second. Pergamon.

Popova, Y. A., V. G. Keyworth, B. E. Haggard, and D. E. Storm. 2006. Stream Nutrient Limitation and Sediment Interactions in the Eucha-Spavinaw Basin. Soil Water **61**: 105–115.

Poth, M., and D. D. Focht. 1985. ^{15}N Kinetic Analysis of N_2O Production by Nitrosomonas Examination of Nitrifier Denitrification. Appl. Environ. Microbiol. **49**: 1134–1141.

R Core Team. 2018. R: A Language and Environment for Statistical Computing. R Found. Stat. Comput. doi:10.1007/978-3-540-74686-7

Rabalais, N. N., E. R. Turner, and W. J. Wiseman Jr. 2002. Gulf of Mexico Hypoxia, A.K.A. The Dead Zone. Annu. Rev. Ecol. Syst. **33**: 235–263.

Ramalho, R. S. 1977. Introduction, p. 1–25. *In* Introduction to Wastewater Treatment Processes. Academic Press, Inc.

Rapport, D. J., R. Costanza, and A. J. McMichael. 1998. Assessing Ecosystem Health. Trends Ecol. Evol. **13**.

Rapson, T. D., and H. Dacres. 2014. Analytical Techniques for Measuring Nitrous Oxide. Trends Anal. Chem. **54**: 65–74. doi:10.1016/j.trac.2013.11.004

Ravishankara, A. R., J. S. Daniel, and R. W. Portmann. 2009. Nitrous Oxide (N_2O): The Dominant Ozone-Depleting Substance Emitted in the 21st Century. Science (80-.). **326**: 123–125. doi:10.1126/science.1176985

Raymond, P. A., and J. J. Cole. 2001. Gas Exchange in Rivers and Estuaries: Choosing a Gas Transfer Velocity. Estuaries **24**: 312–317. doi:10.2307/1352954

Reay, D. S., E. a. Davidson, K. a. Smith, P. Smith, J. M. Melillo, F. Dentener, and P. J. Crutzen. 2012. Global agriculture and nitrous oxide emissions. Nat. Clim. Chang. **2**: 410–416. doi:10.1038/nclimate1458

Ribot, M., S. Bernal, M. Nikolakopoulou, and others. 2017. Enhancement of Carbon and Nitrogen Removal by Helophytes along Subsurface Water Flowpaths Receiving Treated Wastewater. Sci. Total Environ. **599–600**: 1667–1676. doi:10.1016/j.scitotenv.2017.05.114

Ritchie, G. A. F., and D. J. Nicholas. 1972. Identification of the Sources of Nitrous Oxide Produced by Oxidative and Reductive Processes in Nitrosomonas europaea. Biochem. J. **126**: 1181–1191.

Ritz, C., F. Baty, J. C. Streibig, and D. Gerhard. 2015. Dose-Response Analysis Using R. PLoS One **10**.

Robbins, G. A., S. Wang, and J. D. Stuart. 1993. Using the Static Headspace Method To Determine Henry ' s Law Constants. **10**: 3113–3118.

Rodríguez, J. P., N. McIntyre, M. Díaz-Granados, S. Achleitner, M. Hochedlinger, and Č. Maksimović. 2013. Generating Time-series of Dry Weather Loads to Sewers. Environ. Model. Softw. **43**: 133–143. doi:10.1016/j.envsoft.2013.02.007

Rosamond, M. S., S. J. Thuss, and S. L. Schiff. 2012. Dependence of Riverine Nitrous Oxide

Emissions on Dissolved Oxygen Levels. Nat. Geosci. **5**: 715–718. doi:10.1038/NGEO1556

Rosamond, M. S., S. J. Thuss, S. L. Schiff, and R. J. Elgood. 2011. Coupled Cycles of Dissolved Oxygen and Nitrous Oxide in Rivers along a Trophic Gradient in Southern Ontario, Canada. J. Environ. Qual. **40**: 256–270. doi:10.2134/jeq2010.0009

Rosegrant, M. W., X. Cai, and S. A. Cline. 2003. Will the World Run Dry? Global Water and Food Security. Environment **45**: 1–13.

Rudolfs, W., L. L. Falk, and R. A. Ragotzkie. 1986. Interactions of Temperature, pH, and Biomass on the Nitrification Process. Water Pollut. Control Fed. **58**: 52–59. doi:10.1016/S0262-1762(99)80122-9

Rysgaard, S., N. Risgaard-Petersen, N. P. Sloth, K. Jensen, L. P. Nielsen, and P. Nielsen. 1994. Oxygen Regulation of Nitrification and Denitrification in Sediments. Limnol. Oceanogr. **39**: 1643–1652. doi:10.4319/lo.1994.39.7.1643

Sabba, F., A. Terada, G. Wells, B. F. Smets, and R. Nerenberg. 2018. Nitrous Oxide Emissions from Biofilm Processes for Wastewater Treatment. Environ. Biotechnol. **102**: 9815–9829. doi:10.1007/s00253-018-9332-7

Santoro, A. E., C. Buchwald, M. R. McIlvin, and K. L. Casciotti. 2011. Isotopic Signature of N_2O Produced by Marine Ammonia-Oxidizing Archaea. Science (80-.). **333**: 1282–1285. doi:10.1126/science.1208386

Schaller, J. L., T. V Royer, M. B. David, and J. L. Tank. 2004. Denitrification Associated with Plants and Sediments in an Agricultural Stream. J. North Am. Benthol. Soc. **23**: 667–676. doi:10.1899/0887-3593(2004)023<0667:DAWPAS>2.0.CO;2

Schindler, D. W. 1974. Eutrophication and Recovery in Experimental Lakes: Implications for Lake Management. Science (80-.). **184**: 897–899. doi:10.1126/science.184.4139.897

Schubert, C. J., E. Durisch-kaiser, B. Wehrli, B. Thamdrup, P. Lam, and M. M. M. Kuypers. 2006. Anaerobic Ammonium Oxidation in a Tropical Freshwater System (Lake Tanganyika). Environ. Microbiol. **8**: 1857–1863. doi:10.1111/j.1462-2920.2006.001074.x

Schulthess, R. V., and W. Gujer. 1996. Release of Nitrous Oxide (N_2O) from Denitrifying Activated Sludge: Verification and Application of a Mathematical Model. Water Res. **30**: 521–530.

Schumacher, B. A. 2002. Methods for the Determination of Total Organic Carbon (TOC) in

Soils and Sediments.

Seitzinger, S. P. 1985. Eutrophication and the Rate of Denitrification and N_2O Production in Coastal Marine Sediments. Limnol. Oceanogr. **30**: 1332–1339. doi:10.4319/lo.1985.30.6.1332

Seitzinger, S. P. 1988. Denitrification in Freshwater and Coastal Marine Ecosystems: Ecological and Geochemical Significance. Limnol. Oceanogr. **33**: 702–724. doi:10.4319/lo.1988.33.4_part_2.0702

Seitzinger, S. P., and C. Kroeze. 1998. Global Distribution of Nitrous Oxide Production and N imputs in Freshwater and Coastal Marine Ecosystems. Global Biogeochem. Cycles **12**: 93–113. doi:10.1029/97GB03657

Sharpley, A., B. Foy, and P. Withers. 2000. Practical and Innovative Measures for the Control of Agricultural Phosphorus Losses to Water: An Overview. J. Environ. Qual. **29**: 1. doi:10.2134/jeq2000.00472425002900010001x

Sharpley, A., H. P. Jarvie, A. Buda, L. May, B. Spears, and P. Kleinman. 2013. Phosphorus Legacy: Overcoming the Effects of Past Management Practices to Mitigate Future Water Quality Impairment. J. Environ. Qual. **42**: 1308–1326. doi:10.2134/jeq2013.03.0098

Short, M. D., A. Daikeler, G. M. Peters, K. Mann, N. J. Ashbolt, R. M. Stuetz, and W. L. Peirson. 2014. Municipal GravitySewers: An Unrecognised Source of Nitrous Oxide. Sci. Total Environ. **468–469**: 211–218. doi:10.1016/j.scitotenv.2013.08.051

Silvennoinen, H., A. Liikanen, J. Torssonen, C. F. Stange, and P. J. Martikainen. 2008. Denitrification and Nitrous Oxide Effluxes in Boreal, Eutrophic River Sediments under Increasing Nitrate Load: A laboratory Microcosm Study. Biogeochemistry **91**: 105–116. doi:10.1007/s10533-008-9262-z

Smith, E. P. 2002. BACI Design. Encycl. Environmetrics **Volume 1**: 141?148. doi:10.1002/9780470057339.vab001.pub2

Smith, M. S., and J. M. Tiedje. 1979. Phases of Denitrification Following Oxygen Depletion in Soil. Soil Biol. Biochem. **11**: 261–267. doi:10.1016/0038-0717(79)90071-3

Smith, R. M., S. S. Kaushal, J. J. Beaulieu, M. J. Pennino, and C. Welty. 2017. Influence of Infrastructure on Water Quality and Greenhouse Gas Dynamics in Urban Streams. Biogeosciences **14**: 2831–2849. doi:10.5194/bg-2016-380

Smith, V. H., G. D. Tilman, and J. C. Nekola. 1998. Eutrophication: Impacts of Excess Nutrient Inputs on Freshwater, Marine, and Terrestrial Ecosystems. Environ. Pollut. **100**: 179–196. doi:10.1016/S0269-7491(99)00091-3

Snider, D. M., J. J. Venkiteswaran, S. L. Schiff, and J. Spoelstra. 2015. From the Ground Up: Global Nitrous Oxide Sources are Constrained by Stable Isotope Values. PLoS One **10**: 1–19. doi:10.1371/journal.pone.0118954

Sonune, A., and R. Ghate. 2004. Developments in Wastewater Treatment Methods. Desalination **167**: 55–63. doi:10.1016/j.desal.2004.06.113

Sosiak, A. 2002. Long-term Response of Periphyton and Macrophytes to Reduced Municipal Nutrient Loading to the Bow River (Alberta, Canada). Can. J. Fish. Aquat. Sci. **59**: 987–1001. doi:10.1139/f02-071

Starry, O. S., H. M. Valett, and M. E. Schreiber. 2005. Nitrification Rates in a Headwater Stream: Influences of Seasonal Variation in C and N Supply. J. North Am. Benthol. Soc. **24**: 753–768. doi:10.1899/05-015.1

Statistics Canada. 2016. 2016 Census Profile.

Stevens, R. J., R. J. Laughlin, and J. P. Malone. 1998. Soil pH Affects the Processes Reducing Nitrate to Nitrous Oxide and Di-Nitrogen. Soil Biol. Biochem. **30**: 1119–1126. doi:10.1016/S0038-0717(97)00227-7

Stewart-Oaten, A., W. W. Murdoch, and K. R. Parker. 1986. Environmental Impact Assessment: "Pseudoreplication" in Time? Ecology **67**: 929–940.

Strauss, E. A., N. L. Mitchell, and G. A. Lamberti. 2002. Factors Regulating Nitrification in Aquatic Sediments: Effects of Organic Carbon, Nitrogen Availability, and pH. Can. J. Fish. Aquat. Sci. **59**: 554–563. doi:10.1139/f02-032

Sturm, K., A. Grinham, U. Werner, and Z. Yuan. 2016. Sources and Sinks of Methane and Nitrous Oxide in the Subtropical Brisbane River Estuary, South East Queensland, Australia. Estuar. Coast. Shelf Sci. **168**: 10–21. doi:10.1016/j.ecss.2015.11.002

Teixeira, C., C. Magalhães, R. A. R. Boaventura, and A. A. Bordalo. 2010. Potential Rates and Environmental Controls of Denitrification and Nitrous Oxide Production in a Temperate Urbanized Estuary. Mar. Environ. Res. **70**: 336–342. doi:10.1016/j.marenvres.2010.07.001

Teklehaimanot, G. Z., I. Kamika, M. A. A. Coetzee, and M. N. B. Momba. 2015. Population

Growth and Its Impact on the Design Capacity and Performance of the Wastewater Treatment Plants in Sedibeng and Soshanguve, South Africa. Environ. Manage. **56**: 984–997. doi:10.1007/s00267-015-0564-3

Thuan, N. C., K. Koba, M. Yano, and others. 2017. N_2O Production by Denitrification in an Urban River: Evidence from Isotopes, Functional Genes, and Dissolved Organic Matter. Limnology **19**: 1–12. doi:10.1007/s10201-017-0524-0

Thuss, S. J., J. J. Venkiteswaran, and S. L. Schiff. 2014. Proper Interpretation of Dissolved Nitrous Oxide Isotopes, Production Pathways, and Emissions Requires a Modelling Approach. PLoS One **9**: 1–15. doi:10.1371/journal.pone.0090641

Toyoda, S., H. Iwai, K. Koba, and N. Yoshida. 2009. Isotopomeric Analysis of N_2O Dissolved in a River in the Tokyo Metropolitan Area. Rapid Commun. Mass Spectrom. **23**: 809–821. doi:10.1002/rcm

Udy, J. W., C. S. Fellows, M. E. Bartkow, S. E. Bunn, J. E. Clapcott, and B. D. Harch. 2006. Measures of Nutrient Processes as Indicators of Stream Ecosystem Health. Hydrobiologia **572**: 89–102. doi:10.1007/s10750-005-9006-1

United Nations Environment Program. 2010. Sick Water? The Central Role of Wastewater Management in Sustainable Development, E. Corcoran, C. Nelleman, E. Baker, R. Bos, D. Osborn, and H. Savelli [eds.].

Unity Scientific SmartChem. 2011a. 170/200 Method NO3-002-A Nitrate/Nitrite by Cadmium Reduction SM 4500 NO_3^- E. Revision May 2011.

Unity Scientific SmartChem. 2011b. 200 Method AMM-002-A Ammonia - Standard Methods 4500-NH_3 G. Revision May 2011.

Venables, W. N., and B. D. Ripley. 2002. Modern Applied Statistics with S, Fourth. Springer.

Venkiteswaran, J. J., M. S. Rosamond, and S. L. Schiff. 2014. Nonlinear Response of Riverine N2O Fluxes to Oxygen and Temperature. Environ. Sci. Technol. **48**: 1566–1573. doi:10.1111/j.1365-2389.2010.01265.x

Venkiteswaran, J. J., S. L. Schiff, and W. D. Taylor. 2015. Linking Aquatic Metabolism, Gas Exchange, and Hypoxia to Impacts along the 300-km Grand River, Canada. Freshw. Sci. **34**: 1216–1232. doi:10.1086/683241

Veraart, A. J., J. J. M. de Klein, and M. Scheffer. 2011. Warming Can Boost Denitrification

Disproportionately Due to Altered Oxygen Dynamics. PLoS One **6**: 1–6. doi:10.1371/journal.pone.0018508

Vitousek, P. M., H. a Mooney, J. Lubchenco, and J. M. Melillo. 1997. Human Domination of Earth's Ecosystems. Science (80-.). **277**: 494–499. doi:10.1126/science.277.5325.494

Wada, E., and S. Ueda. 1996. Carbon Nitrogen and Oxygen Isotope Ratios of CH_4 and N_2O on Soil Ecosystems, p. 177–204. *In* T.W. Boutton and S.I. Yamasaki [eds.], Mass Spectrometry of Soils. Marcel Dekker.

Waiser, M. J., D. Humphries, V. Tumber, and J. Holm. 2011a. Effluent-dominated streams. Part 2: Presence and Possible Effects of Pharmaceuticals and Personal Care Products in Wascana Creek, Saskatchewan, Canada. Environ. Toxicol. Chem. **30**: 508–519. doi:10.1002/etc.398

Waiser, M. J., V. Tumber, and J. Holm. 2011b. Effluent-dominated Streams. Part 1: Presence and Effects of Excess Nitrogen and Phosphorus in Wascana Creek, Saskatchewan, Canada. Environ. Toxicol. Chem. **30**: 496–507. doi:10.1002/etc.399

Wang, D., Y. Tan, Z. Yu, Y. Li, S. Chang, H. Deng, B. Hu, and Z. Chen. 2015a. Nitrous Oxide Production in River Sediment of Highly Urbanized Area and the Effects of Water Quality. Wetlands **35**: 1213–1223. doi:10.1007/s13157-015-0708-5

Wang, J., N. Chen, W. Yan, B. Wang, and L. Yang. 2015b. Effect of Dissolved Oxygen and Nitrogen on Emission of N_2O from Rivers in China. Atmos. Environ. **103**: 347–356. doi:10.1016/j.atmosenv.2014.12.054

Wanninkhof, R. 1992. Relationship Between Wind Speed and Gas Exchange. J. Geophys. Res. **97**: 7373–7382. doi:10.1029/92JC00188

Warwick, J. J. 1986. Diel Variation of In-Stream Nitrification. Water Res. **20**: 1325–1332. doi:10.1016/0043-1354(86)90165-X

Weiss, R. F., and B. A. Price. 1980. Nitrous Oxide Solubility In Water And Seawater. Mar. Chem. **8**: 347–359.

Wetzel, R. G., and G. E. Likens. 1991. Limological Analyses, Second. Springer-Verlag.

Willer, J., and C. C. Delwiche. 1954. Investigations on the Denitrification Process in Soil. Plant Soil **5**: 155–169.

Wrage, N., G. L. Velthof, M. L. van Beusichem, and O. Oenema. 2001. Role of Nitrifier Denitrication in the Production of Nitrous Oxide. Soil Biol. Biochem. **33**: 1723–1732.

Wu, Q., and R. Knowles. 1995. Effect of Chloramphenicol on Denitrification in Flexibacter canadensis and "'Pseudomonas denitrificans.'" Appl. Environ. Microbiol. **61**: 434–437.

Xia, Y., Y. Li, X. Li, M. Guo, D. She, and X. Yan. 2013. Diurnal Pattern in Nitrous Oxide Emissions from a Sewage-enriched River. Chemosphere **92**: 421–428. doi:10.1016/j.chemosphere.2013.01.038

Yang, L., W. Yan, P. Ma, and J. Wang. 2011. Seasonal and Diurnal Variations in N_2O Concentrations and Fluxes from Three Eutrophic Rivers in Southeast China. J. Geogr. Sci. **21**: 820–832. doi:10.1007/s11442-011-0882-1

Yu, Z., H. Deng, D. Wang, M. Ye, Y. Tan, Y. Li, Z. Chen, and S. Xu. 2013. Nitrous Oxide Emissions in the Shanghai River Network: Implications for the effects of Urban Sewage and IPCC Methodology. Glob. Chang. Biol. **19**: 2999–3010. doi:10.1111/gcb.12290

Yu, Z., H. Deng, D. Wang, M. Ye, Y. Tan, Y. Li, Z. Chen, and S. Xu. 2016. Seasonal and Diurnal Dynamics of Physicochemical Parameters and Gas Production in Vertical Water Column of a Eutrophic Pond. Ecol. Eng. **87**: 313–323.

Zhou, H., and D. W. Smith. 2002. Advanced Technologies in Water and Wastewater Treatment. J. Environ. Eng. Sci. **1**: 247–264. doi:10.1139/S02-020

APPENDIX

Supplemental Information Chapter 2: The Effect of a Wastewater Treatment Plant Upgrade on In-Stream Denitrification

The supplemental information for Chapter 2 contains figures that describe the diel flow (Figure A2.1), NO_3^- and TAN effluent concentrations via the personal communication of Kayla Gallant (Regina WWTP; Figure A2.2), as well as periods of anoxia in Wascana Creek (Figure A2.3). This section also describes NH_3 concentrations pre-vs post upgrade (Figure A2.4), pH values pre-upgrade and post-upgrade at sites W2 and W3 (Figure A2.5), denitrification rates versus NO_3^- and temperature (Figure A2.6), as well as correlation plots for denitrification rates versus NO_3^-, DO, pH, SOC, water temperature, DOC, and TDN (Figures A2.7–12). The last figure in this section shows pH as a function of distance from the WWTP/ confluence (Figure A2.13). Statistical analyses for Chapter 2, using the R programming language, can be found on GitHub (https://github.com/nickdylla/Masters-Thesis).

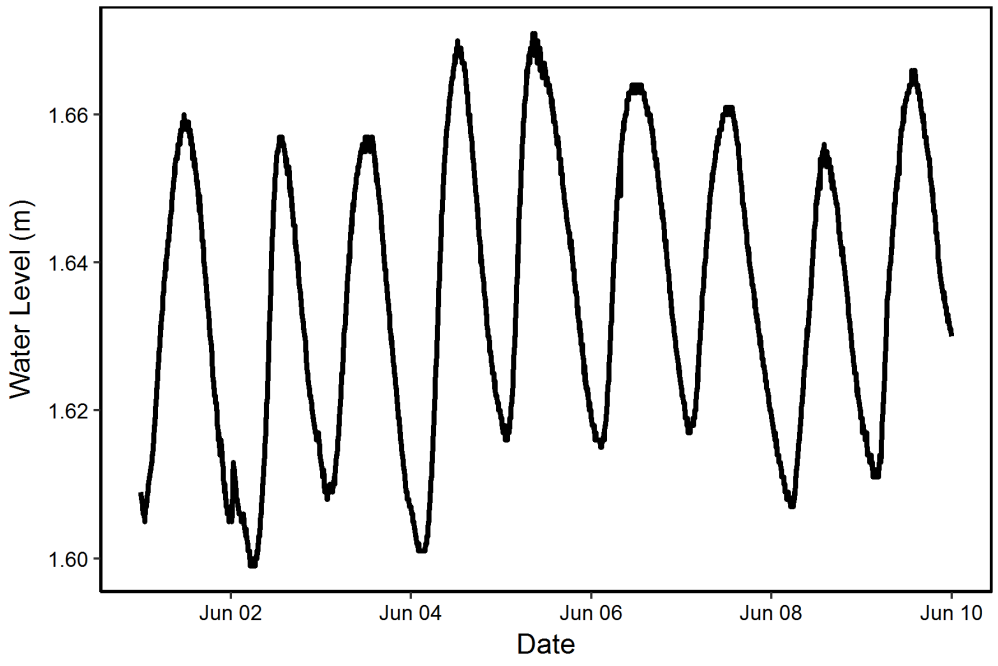

Figure A2.1 Example of the diel cycle of the Wascana Creek flow level during low-flow conditions in 2016. Data obtained from Environment Canada Hydrometric Gauging Station at Wascana Creek (Station ID Number: 05JF005).

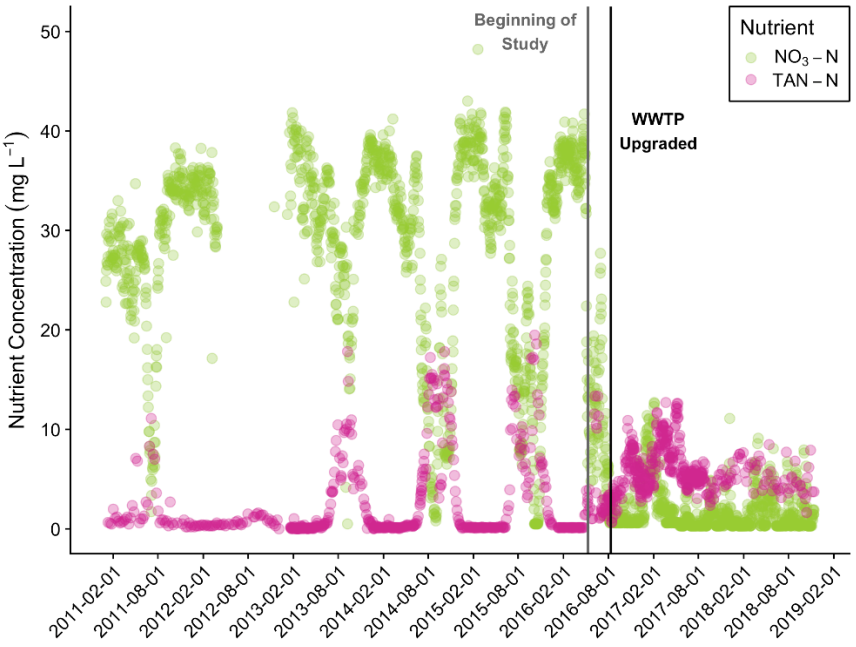

Figure A2.2 Regina wastewater treatment plant final effluent concentrations of nitrate (green points) and total ammonia nitrogen (purple points). The gray vertical line on May 10th, 2016 signifies when this study began and the black vertical line signifies when the Regina WWTP was substantially upgraded. Data were provided by Kayla Gallant as a personal communication from the Regina WWTP.

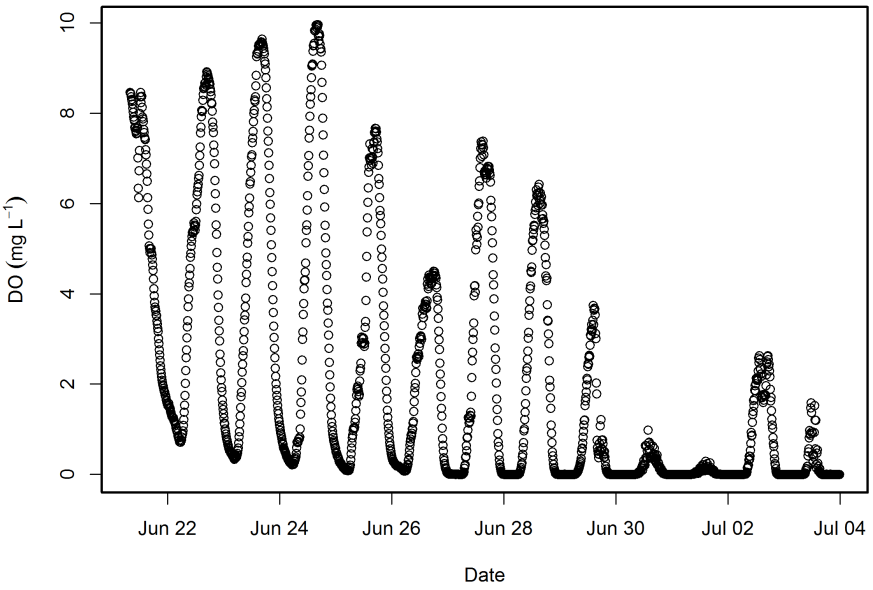

Figure A2.3 Dissolved oxygen concentration (mg O_2 L^{-1}) during the summer of 2016 at Wascana Creek site W3 where several periods of hypoxia (< 4 mg L^{-1}) were observed.

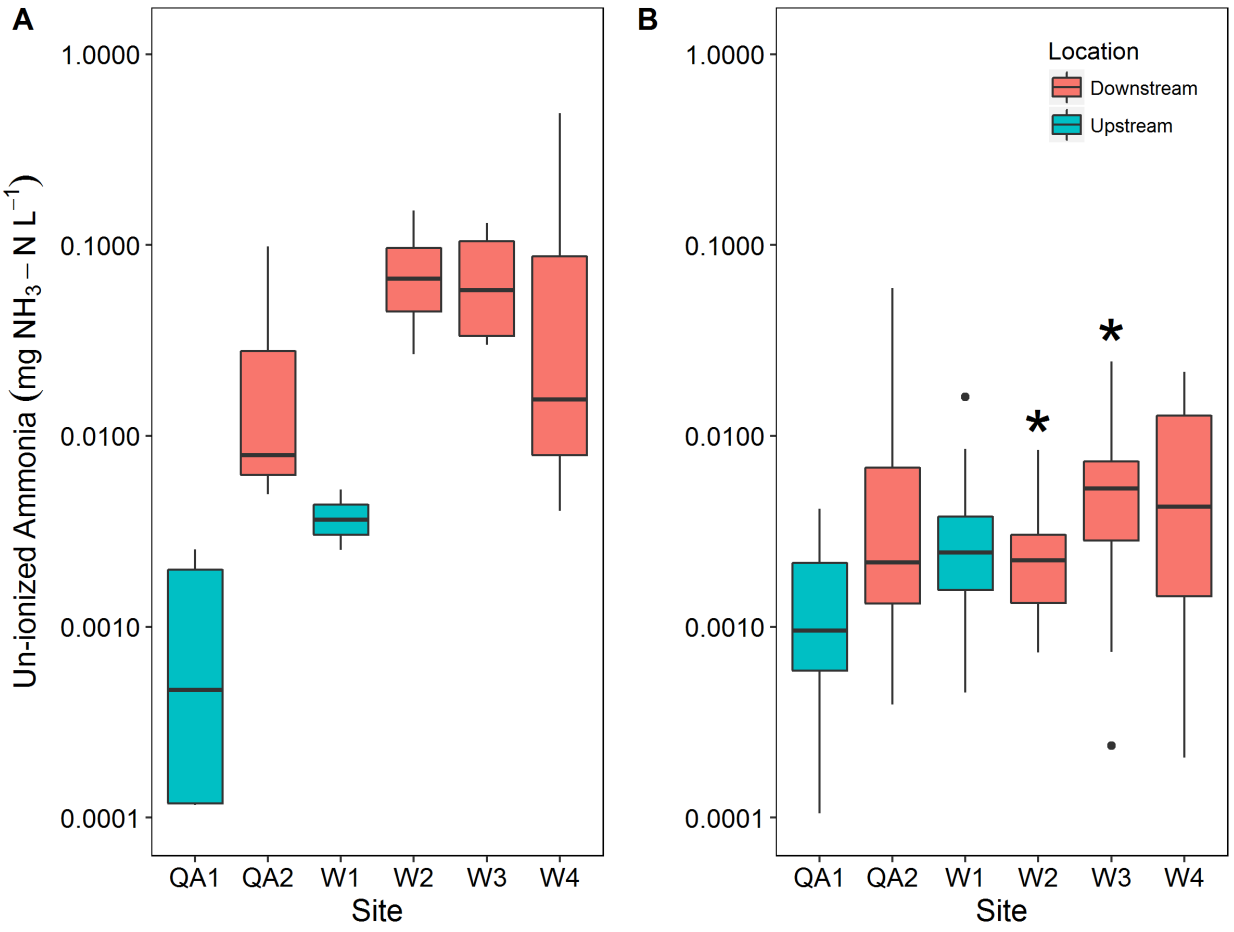

Figure A2.4 Un-ionized ammonia (NH_3) concentrations (mg NH_3–N L^{-1}) pre-upgrade (panel A) and post-upgrade (panel B). Upstream sites are indicated by blue boxplots while downstream sites are orange boxplots. Significant differences of NH_3 concentrations with-in each site (i.e. W1 pre-upgrade vs W1 post-upgrade) are indicated with an asterisk (*; ANOVA $F(11,33) = 4.43$, $p < 0.001$; TukeyHSD $p < 0.05$). The boxplot and whiskers encompass 95% of the data observed where the outliers are represented as dots, inside the box are the first and third quartiles with the median represented as the center line.

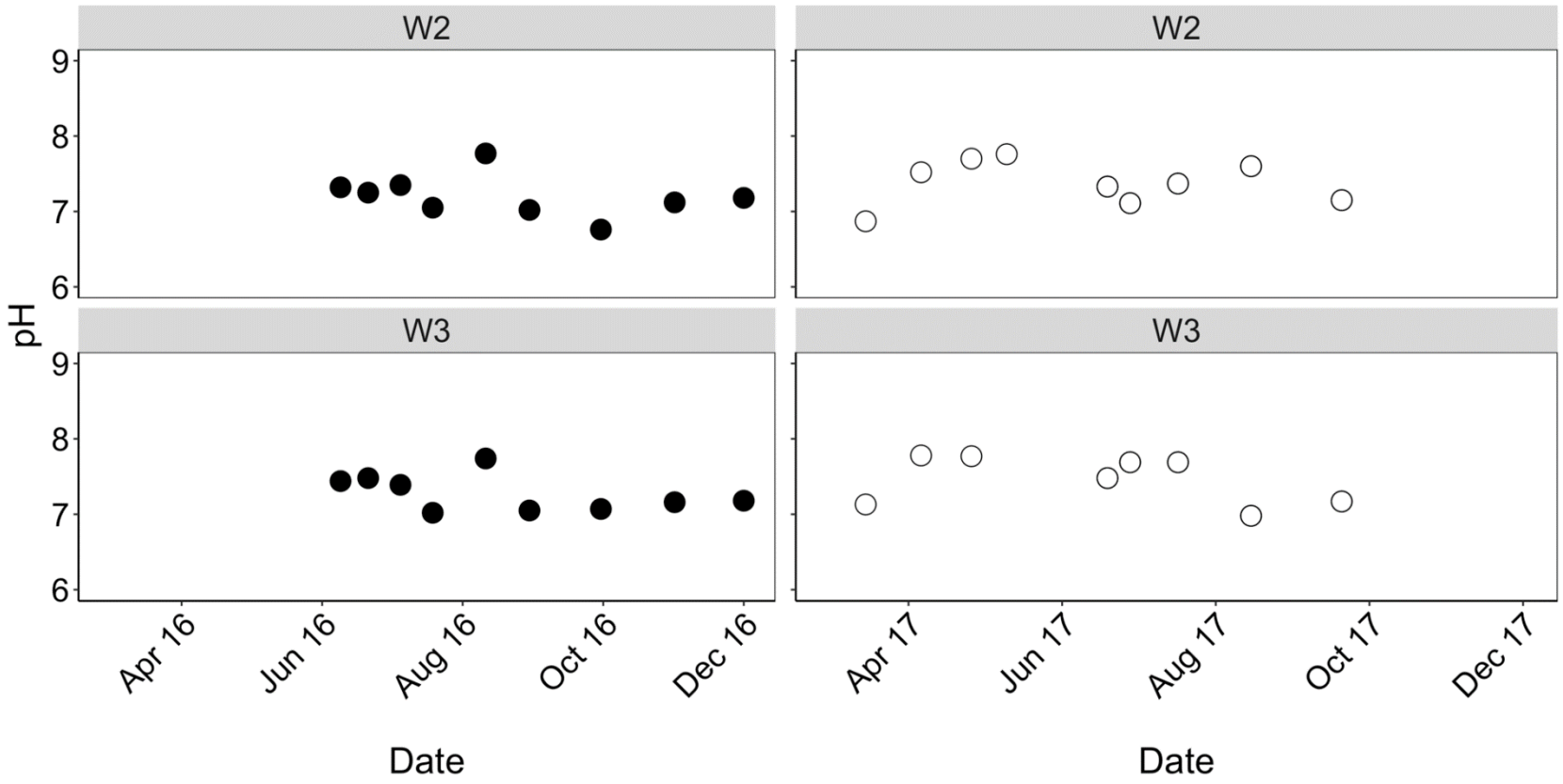

Figure A2.5 Observed pH values at Wascana Creek impact sites (W2 and W3) during pre-upgrade period (solid points) and post-upgrade period (hollow points).

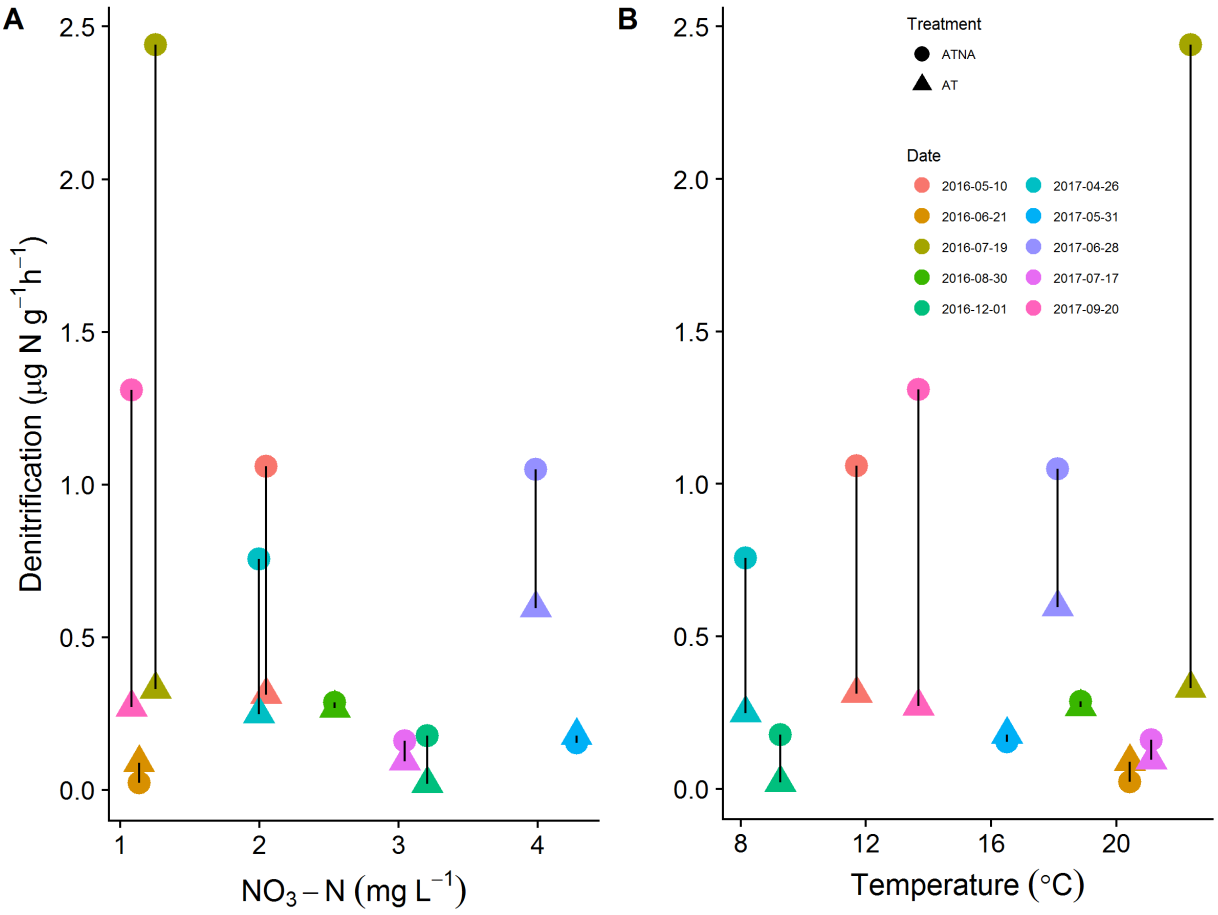

Figure A2.6 Denitrification rates (AT; µg N g^{-1} h^{-1}) versus NO_3^- concentrations (NO_3-N mg L^{-1}; Panel A) and temperature (°C; Panel B) at Wascana Creek impact site W3 throughout the study.

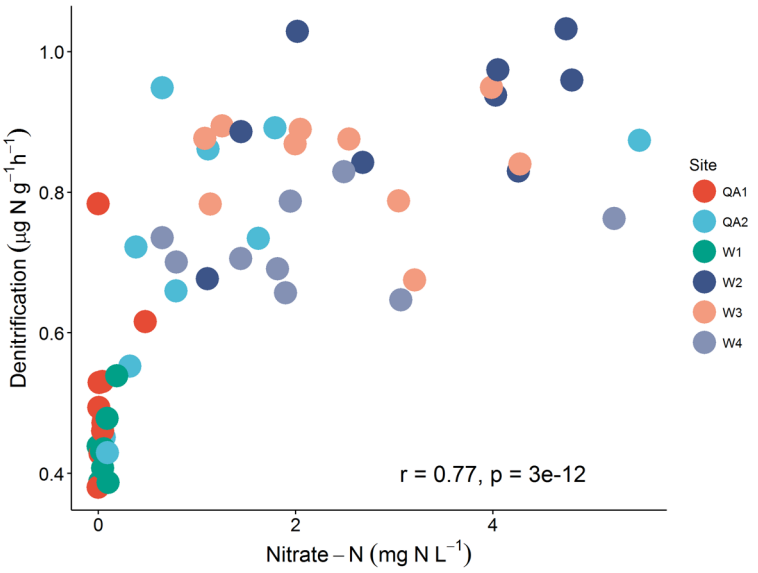

Figure A2.7 Correlation plot for nitrate concentrations (NO_3-N mg L^{-1}) and denitrification rates (AT; µg N g^{-1} h^{-1}). The reported correlation value and significant level were determined from the Spearman rank correlation test. I acknowledge that although some sites approach saturation points (e.g. W3, W4, and QA2), the overall data maintain a monotnic relationship (i.e. the denitrification rates increase with NO_3^- concentrations even though the relationship begins to slow/plateau under higher NO_3^- concentrations).

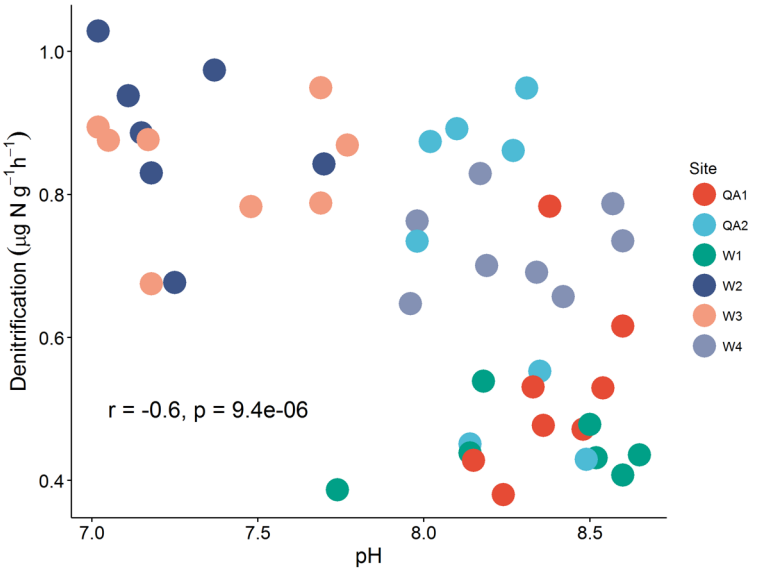

Figure A2.8 Correlation plot for pH and denitrification rates (AT; µg N g^{-1} h^{-1}). The reported correlation value and significance level were determined from the Spearman rank correlation test.

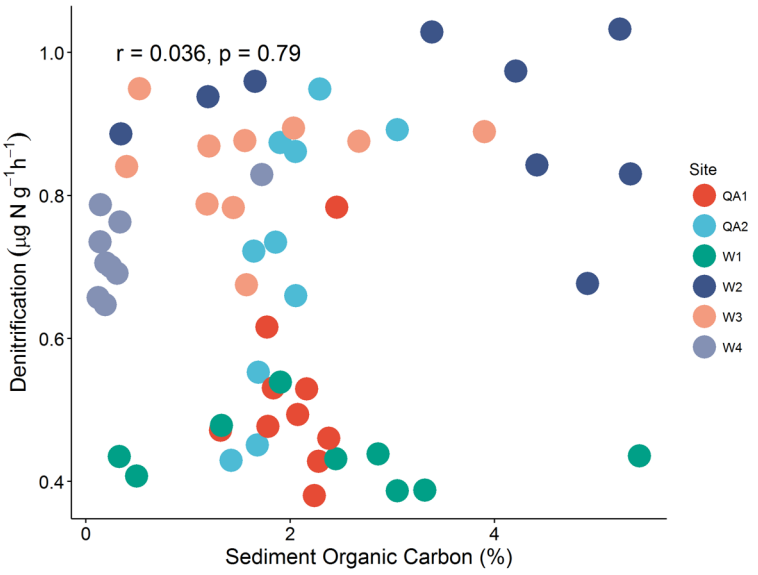

Figure A2.9 Correlation plot for sediment organic carbon (%) and denitrification rates (AT; µg N g^{-1} h^{-1}). The reported correlation value and significance level were determined from the Spearman rank correlation test.

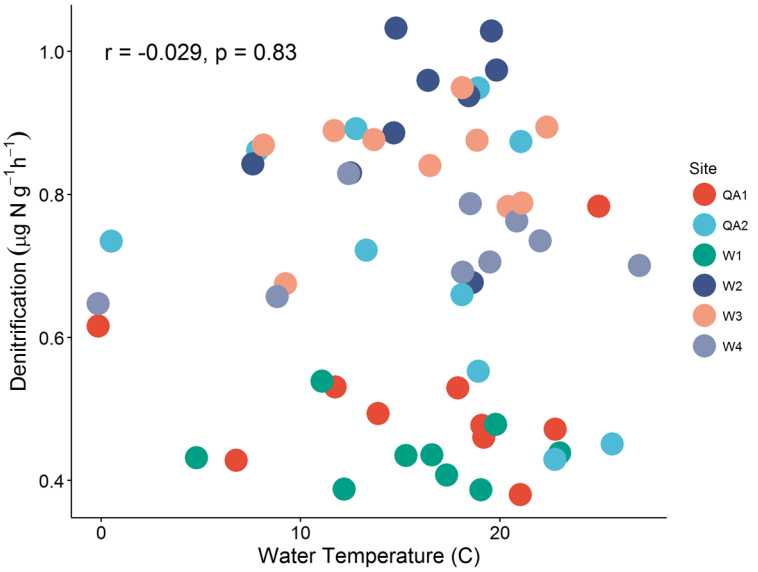

Figure A2.10 Correlation plot for lab water temperature (°C) and denitrification rates (AT; µg N g^{-1} h^{-1}). Lab water temperature was kept within ± 2 °C of sampled water temperature. The reported correlation value and significant level were determined from the Spearman rank correlation test.

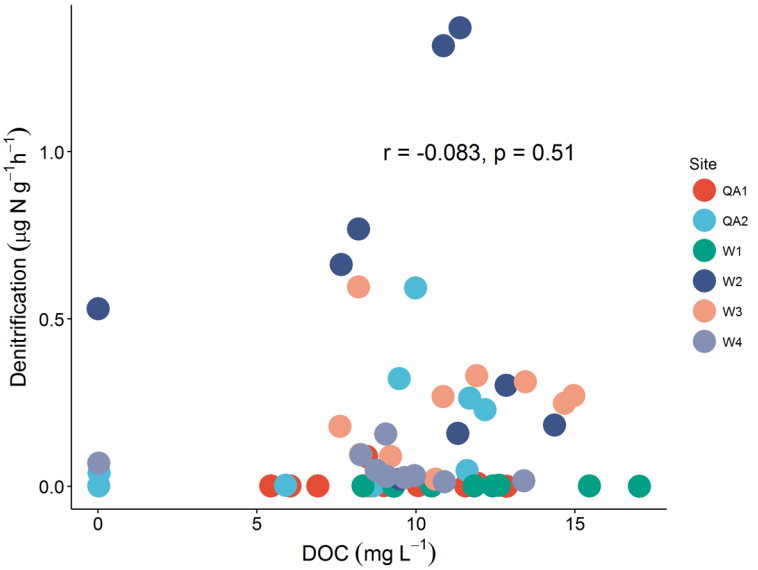

Figure A2.11 Correlation plot for dissolved organic carbon (mg L^{-1}) and denitrification rates (AT; μg N g^{-1} h^{-1}). The reported correlation value and significant level were determined from the Spearman rank correlation test.

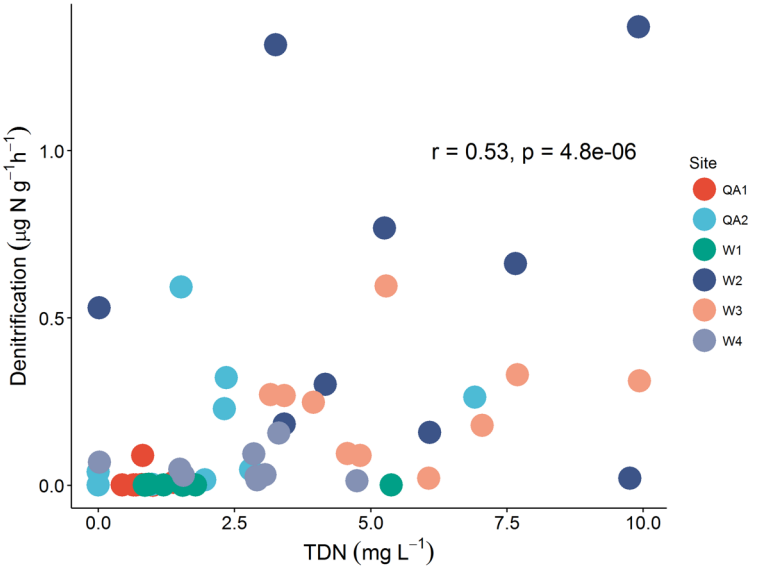

Figure A2.12 Correlation plot for total dissolved nitrogen (mg L^{-1}) and denitrification rates (AT; μg N g^{-1} h^{-1}). The reported correlation value and significant level were determined from the Spearman rank correlation test.

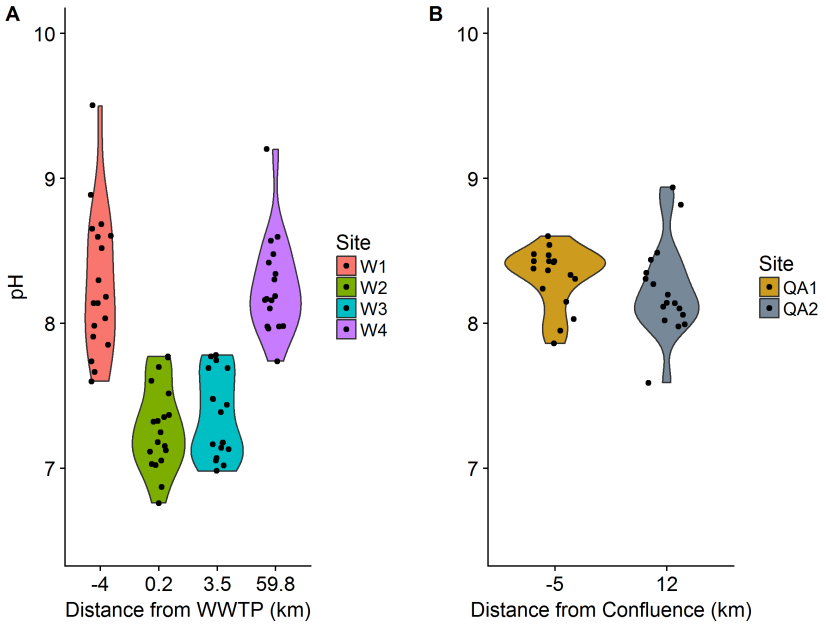

Figure A2.13 pH as a function of distance (km) from the WWTP for Wascana Creek (Panel A) and Qu'Appelle River (Panel B).

Supplemental Information Chapter 3: The Downstream Effect of a Wastewater Treatment Plant Upgrade on Nitrous Oxide

The supplemental information for Chapter 3 contains figures that show the sampling points of DO using HOBO sensors (Figure A3.1) and an example of the BASE model output (Figure A3.2). This section also contains figures that show the design of the "flying" flux chamber (Lorke et al. 2015; Figure A3.3), the range of values when comparing DO modeled *k* values and flux chamber calculated *k* values (Figure A3.4), the range of flux chamber derived *k* values across all sites (Figure A3.5) as well as DO modeled *k* values versus semi-empirical modeled *k* values (Figure A3.6). Nitrous oxide % saturation variability (Figure A3.7) and water temperature were described for all sites (Figure A3.8). Discharge values, paired with sampling dates, were show for both the Qu'Appelle River and Wascana Creek for 2016–17 (Figure A3.9). Diel NH_3 concentrations (Figure A3.10), Wascana Creek flow (Figure A3.11), and TDN, DIN, DON, and urea concentrations (Figure A3.12) were visualized. Lastly, seasonal N_2O flux values were shown for all sites across the entire study (Figure A3.13). Statistical analyses for Chapter 2, using the R programming language, can be found on GitHub (https://github.com/nickdylla/Masters-Thesis).

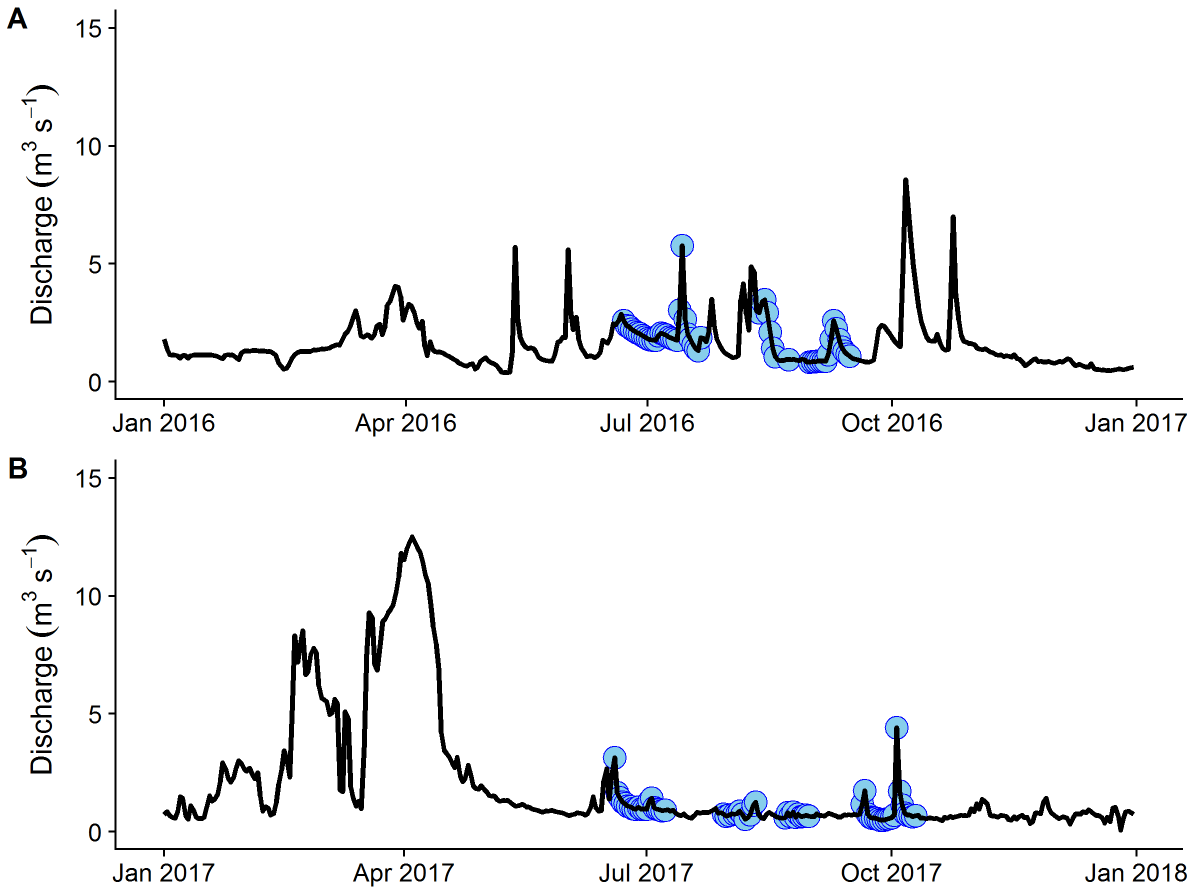

Figure A3.1 Date (blue circles) and discharge condition corresponding to dissolved oxygen measurements from HOBO sensors that were used to estimate *k* in Wascana Creek in 2016 (Panel A) and 2017 (Panel B). In total, 133 days were measured for DO across sites W1, W2, and W3.

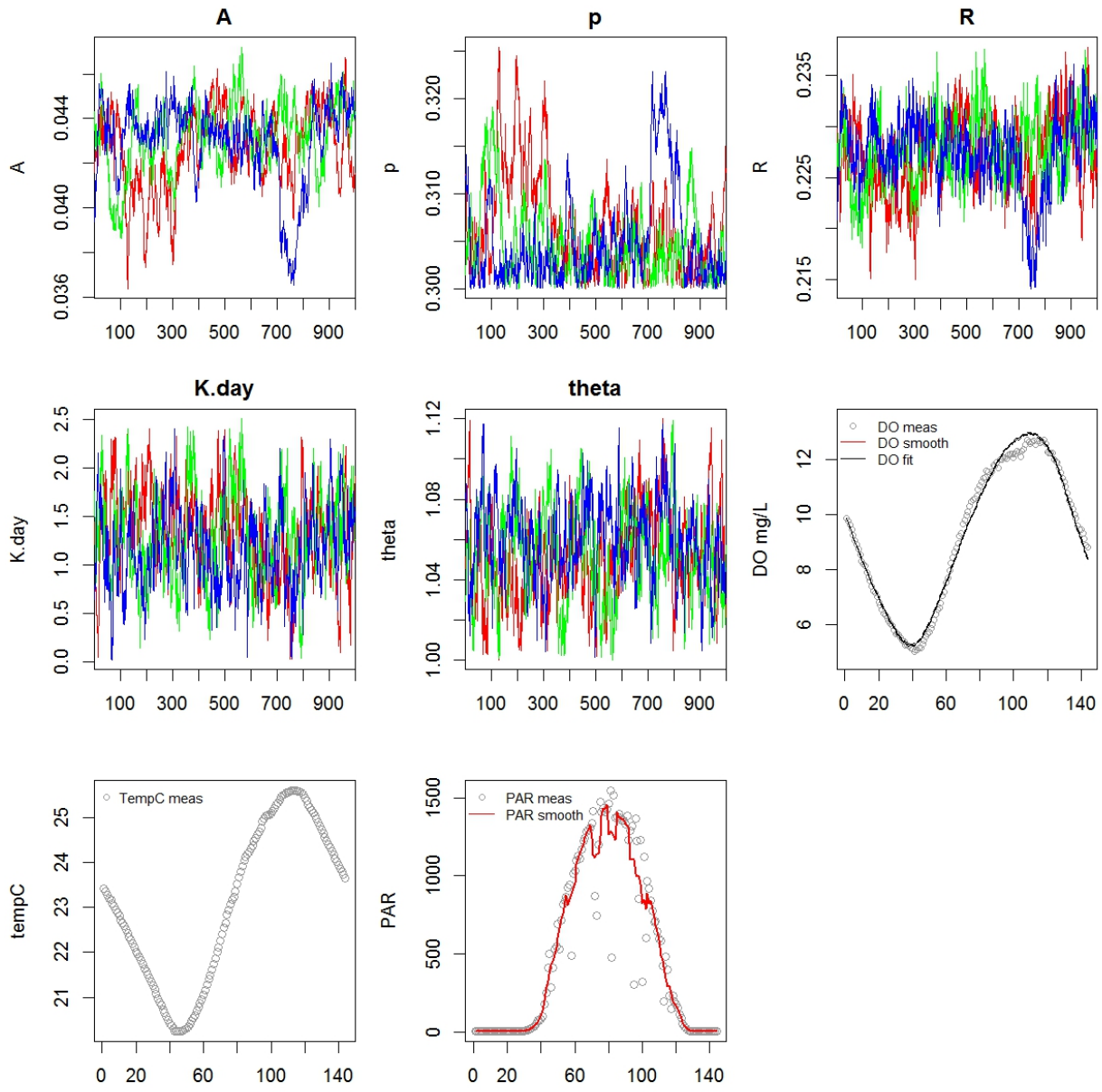

Figure A3.2 Example of BASE model output. The three colors (blue, red, and green) represent each convergence of three-chains used in the model for parameters A, p, R, K, and θ. The x-axis for these variables refers to the number of MCMC iterations used to estimate the aforementioned variables. Dissolved oxygen is shown as the sixth panel with the fitted curve overlaying the data points. Temperature is shown as the seventh panel as well as PAR (smoothed as shown by the red line) as the eighth panel. Dissolved oxygen, temperature, and PAR are shown over the diel period. The x-axis for these parameters refers to the number of time-steps used in the model, since I used 10 min intervals, there were 144 per day (1440 mins d^{-1}).

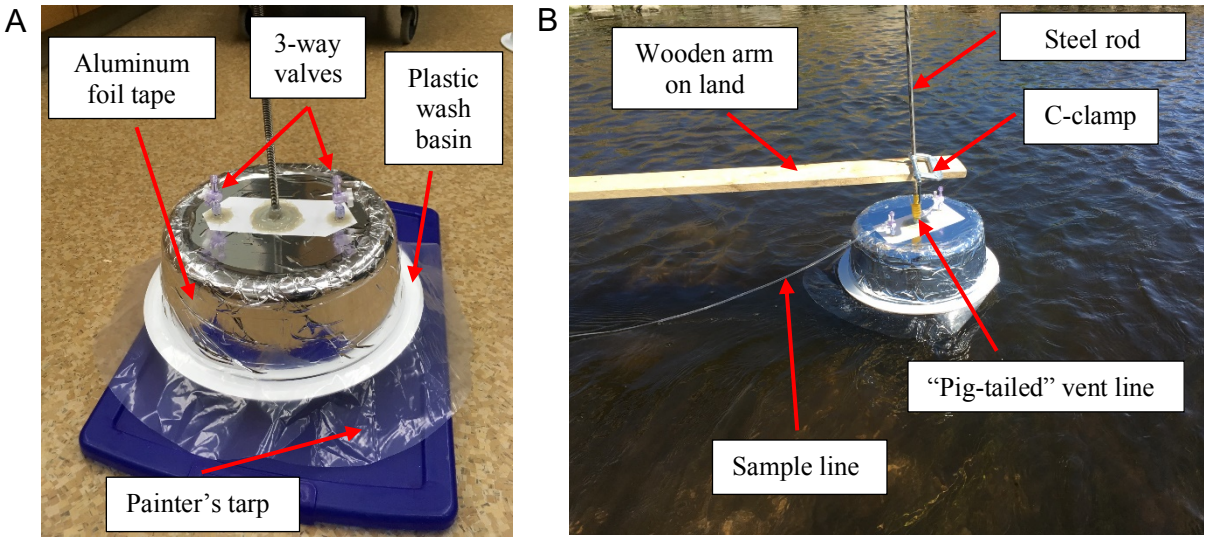

Figure A3.3 Flying flux chamber design as designed from Lorke et al. 2015. Picture A shows the flying flux chamber in the lab after construction and Picture B shows the flying flux chamber in the field. Both pictures describe all parts needed in the construction of flying chamber.

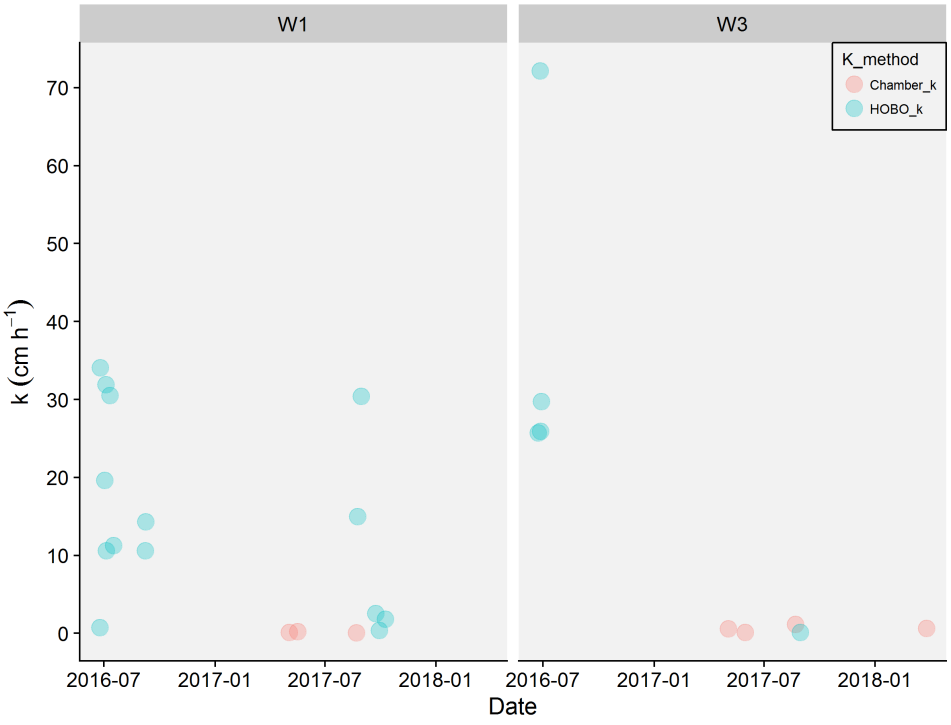

Figure A3.4 Static flux chamber *k* values (red point) compared to HOBO dissolved oxygen derived, BASE modeled *k* values (blue point) over time at sites W1 and W3.

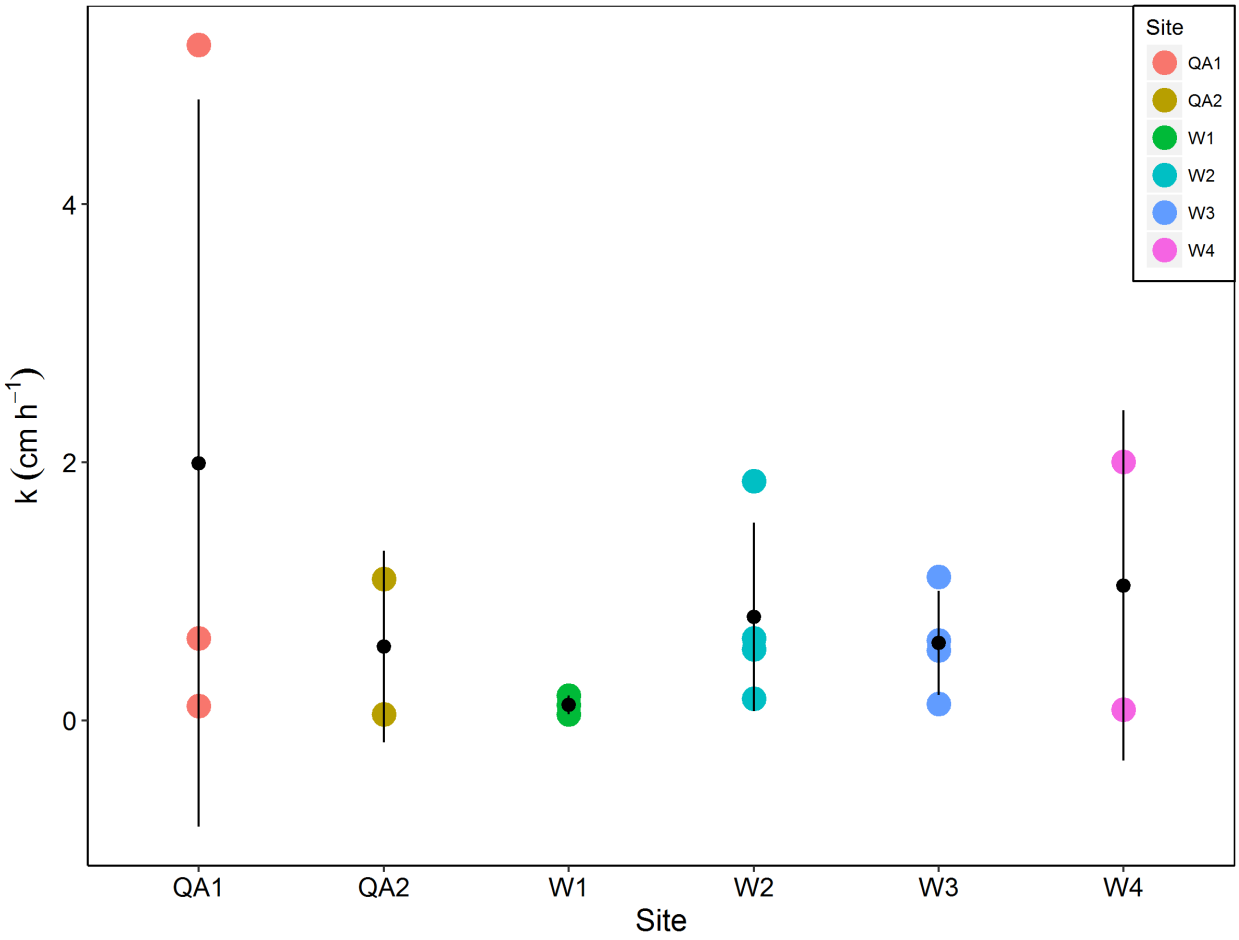

Figure A3.5 Range of static flux chamber-measured *k* values for each site.

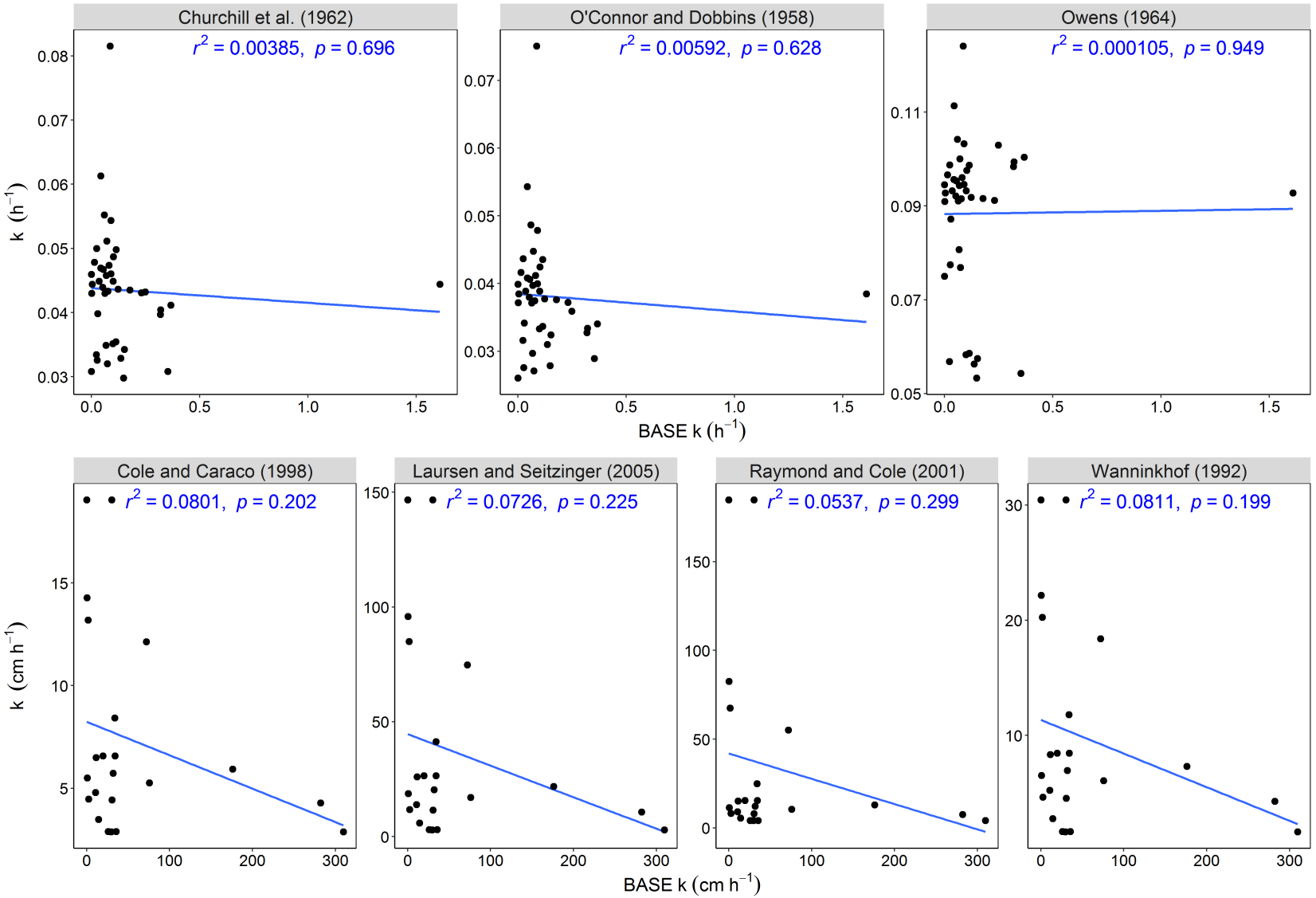

Figure A3.6 BASE modeled k values compared to semi-empirical benthic models (h^{-1}, Top Row) and wind models (cm h^{-1}, Bottom Row). Displayed are individual linear regressions with their respective coefficients of determination (R^2) and *p*-value.

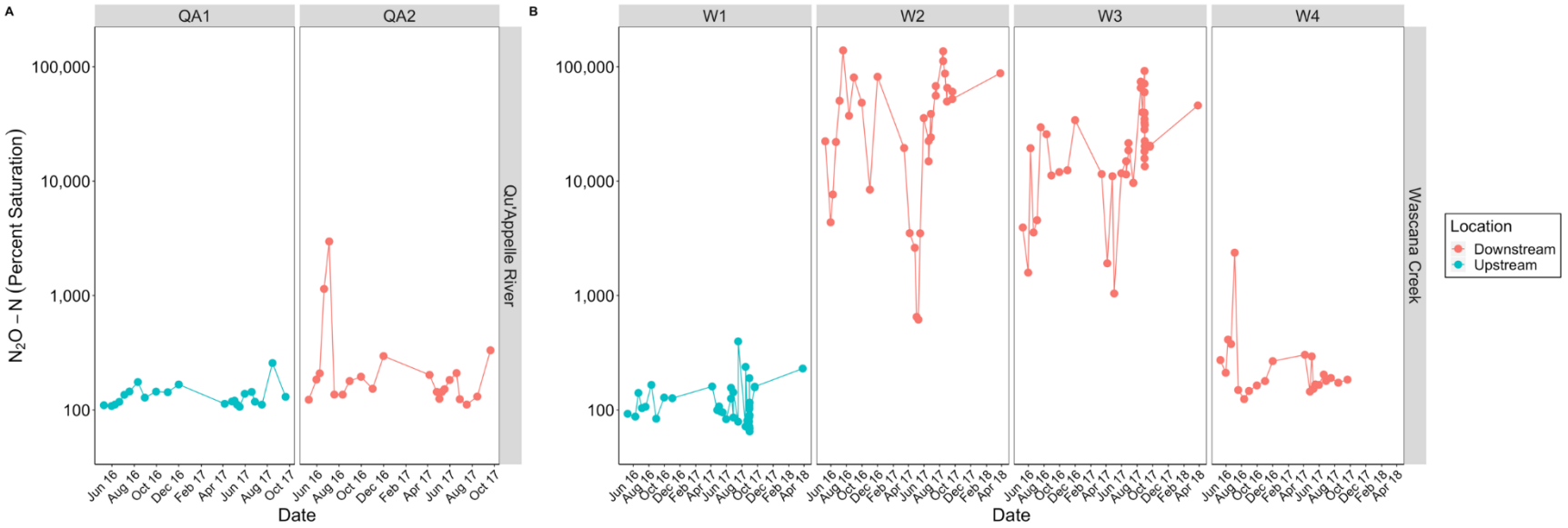

Figure A3.7 Variability of nitrous oxide percent saturations over time for all sites. Note, a base-10 log scale was used for the y-axis. Upstream sites are distinguished by blue points/lines and downstream sites are distinguished orange points/lines.

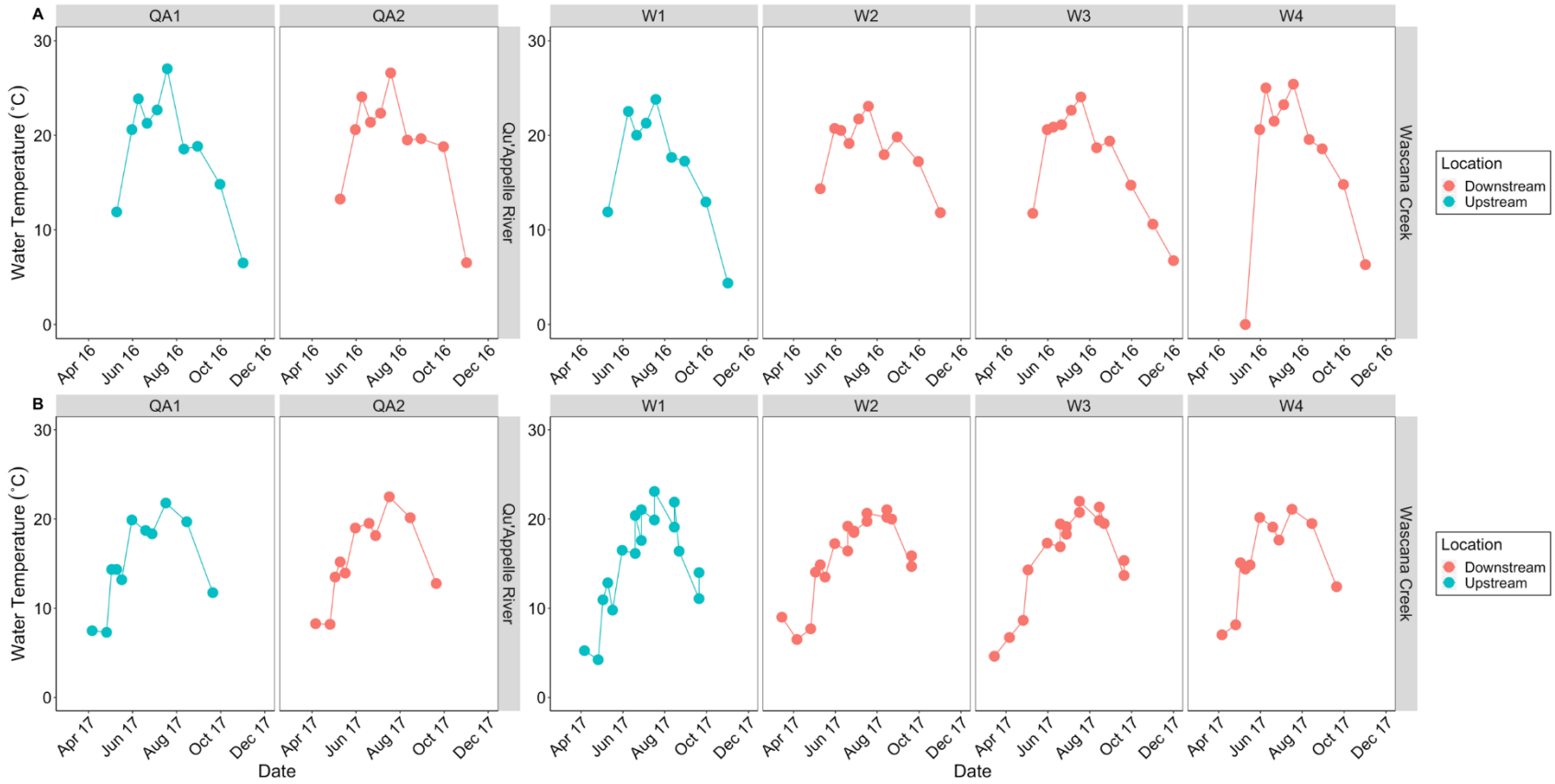

Figure A3.8 Directly measured water temperature (˚C) across all study sites for 2016 (Row A) and 2017 (Row B). Upstream sites are distinguished by blue points/lines and downstream sites are distinguished orange points/lines.

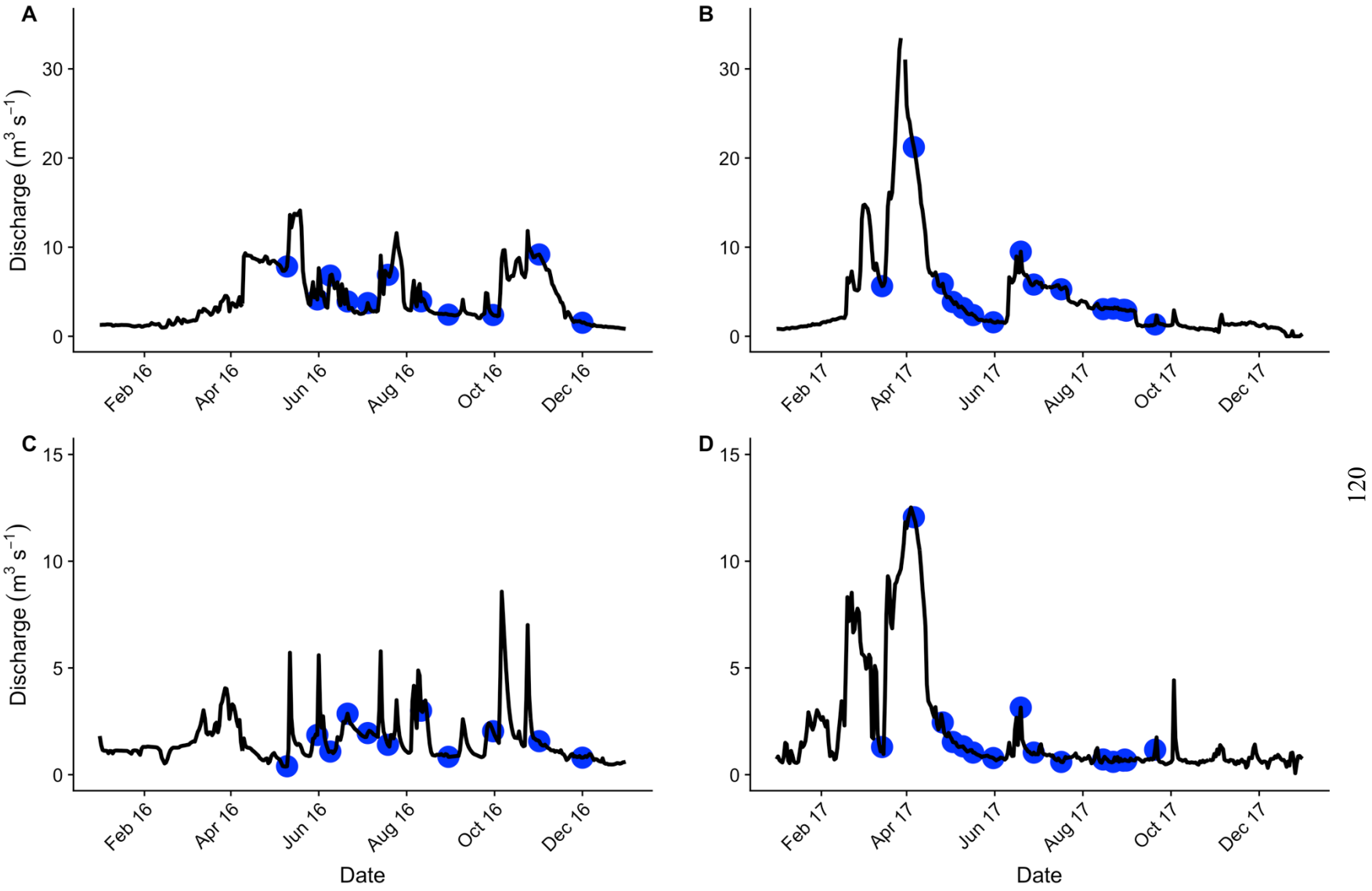

Figure A3.9 Discharge (m^3 s^{-1}) at Qu'Appelle River gauging site QA1 during 2016 (Panel A) and 2017 (Panel B) as well as discharge at Wascana Creek gauging site W4 during 2016 (Panel C) and 2017 (Panel D). Blue circles denote the dates and flow conditions at which samples were taken.

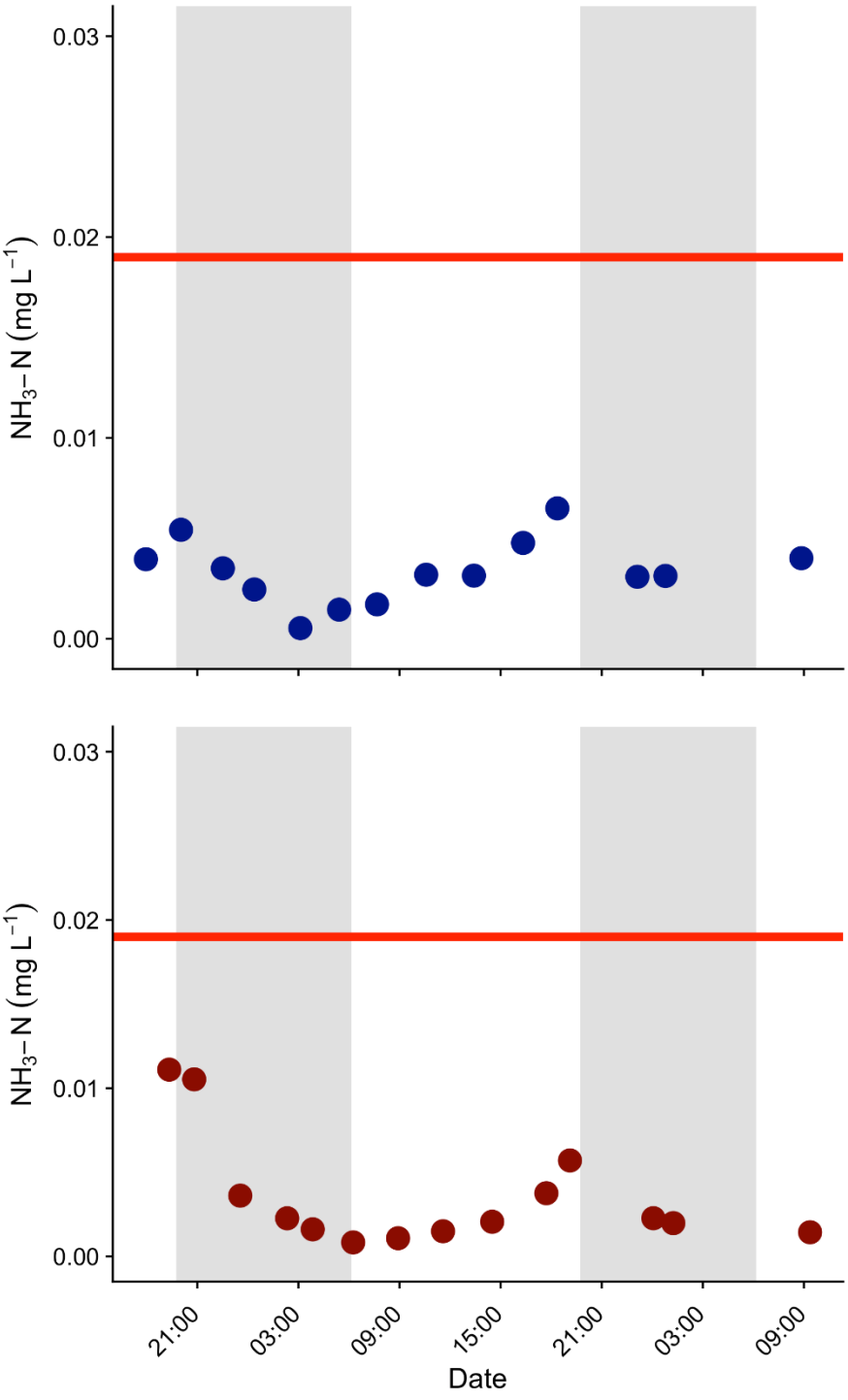

Figure A3.10 Un-ionized ammonia (NH_3) concentrations over the diel sampling campaign that occurred August 29th–August 31st, 2016 at Wascana Creek sites W1 (Top Panel, blue points) and W3 (Bottom Panel, red points). The red horizontal line indicates the freshwater guideline limit of NH_3–N (0.019 mg L^{-1}) in water bodies.

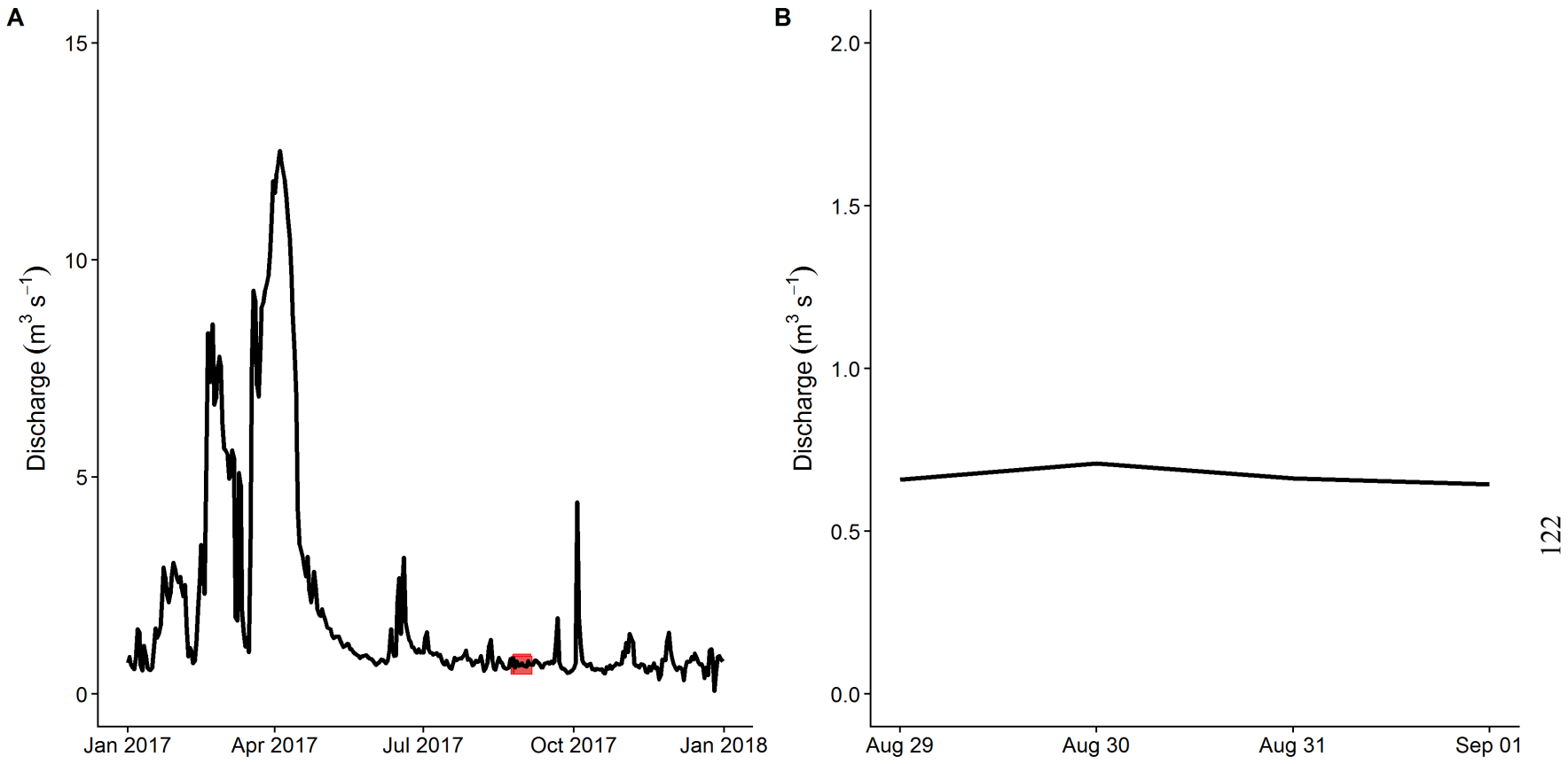

Figure A3.11 Wascana flow during 2017 (Panel A) and the diel sampling campaign (August 30th–31st, 2017; Panel B).

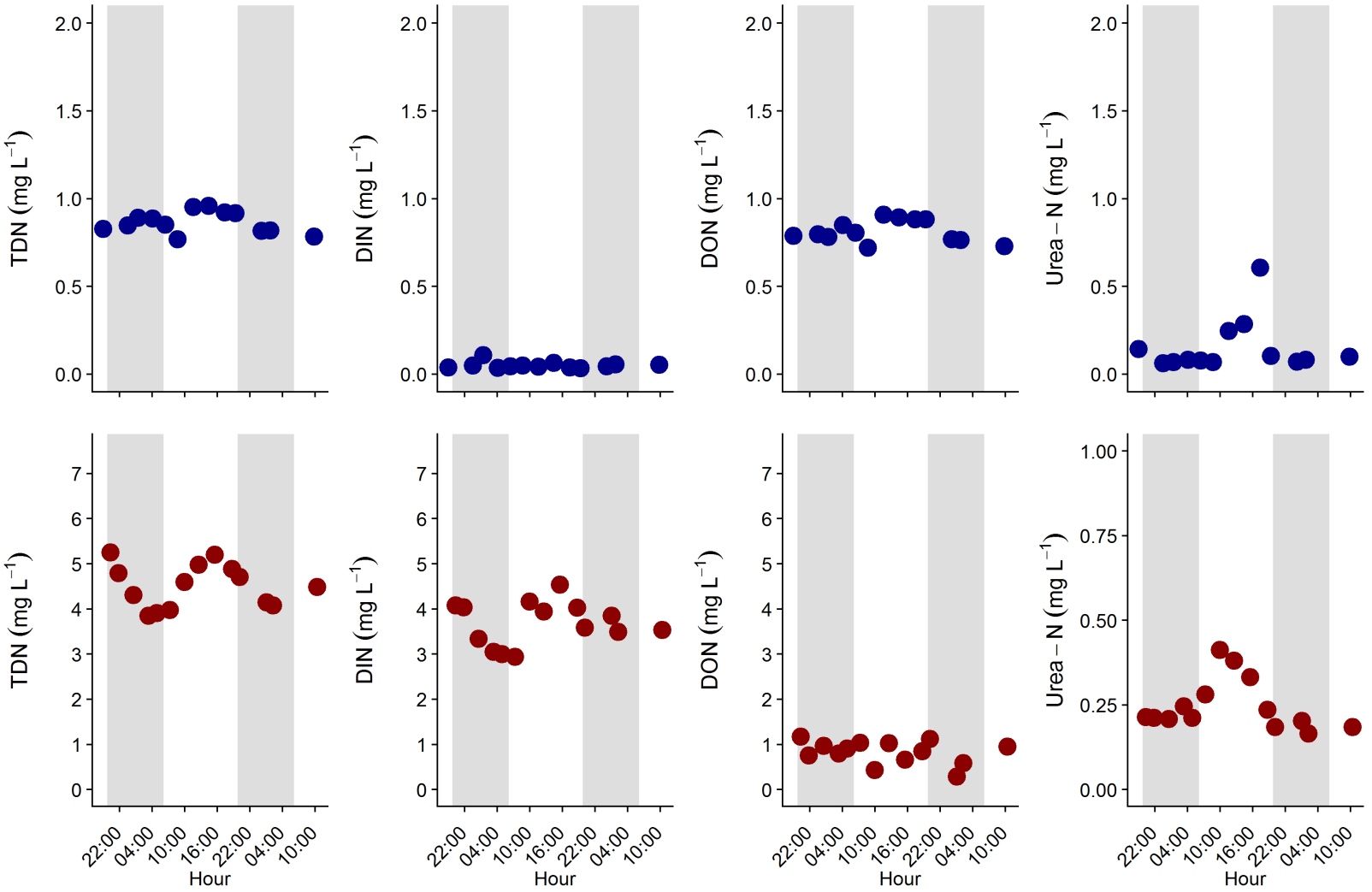

Figure A3.12 TDN, DIN, DON, and urea concentrations over the diel sampling campaign that occurred August 29th–August 31st, 2016 for the upstream Wascana Creek site W1 (Top Row, blue points) and the downstream Wascana Creek site W3 (Bottom Row, red points). The y-axis range was reduced in order to display the diel cycle of urea at both W1 and W3.

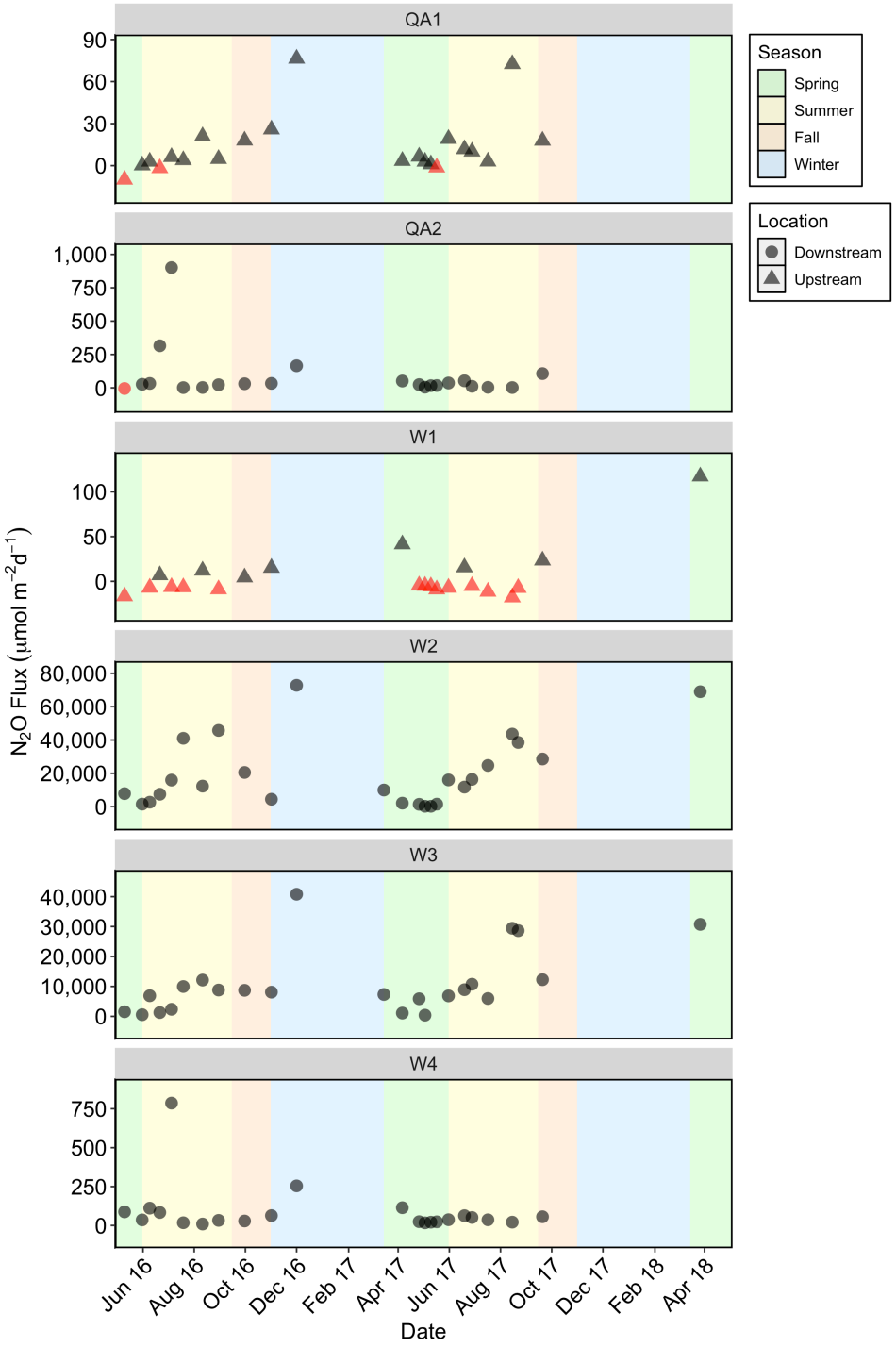

Figure A3.13 Seasonal N_2O flux (µmol N_2O–N m^{-2} d^{-1}) across all study sites. Seasons are shown as vertical rectangles as spring (green), summer (yellow), fall (orange), and winter (blue). The y-axes are independent for each site in order to adequately show seasonal variation across sites. Triangles represent sites upstream of the WWTP/ confluence and circles represent sites downstream of the WWTP/ confluence. Black points indicate flux values > 0 µmol N_2O–N m^{-2} d^{-1} (N_2O source) and red points indicate flux values < 0 µmol N_2O–N m^{-2} d^{-1} (N_2O sink). Note that the points are made 65 % transparent to account for visual overlap.